New York Science Journal

ISSN 1554-0200

Volume 1 - Number 1 (Cumulated No. 1), January 1, 2008

Marsland Press

http://www.sciencepub.org editor@sciencepub.net

New York Science Journal

The ***New York Science Journal*** is an international journal with a purpose to enhance our natural and scientific knowledge dissemination in the world under the free publication principle. Any valuable papers that describe natural phenomena and existence or any reports that convey scientific research and pursuit are welcome, including both natural and social sciences. Papers submitted could be reviews, objective descriptions, research reports, opinions/debates, news, letters, and other types of writings that are nature and science related. The journal is calling for papers and seeking co-operators and editors as well.

Introductions to Authors

1. General Information

(1) Goals: As an international journal published both in print and on internet, *The New York Science Journal* is dedicated to the dissemination of fundamental knowledge in all areas of nature and science. The main purpose of *The New York Science Journal* is to enhance our knowledge spreading in the world under the free publication principle. It publishes full-length papers (original contributions), reviews, rapid communications, and any debates and opinions in all the fields of nature and science.

(2) What to Do: *The New York Science Journal* provides a place for discussion of scientific news, research, theory, philosophy, profession and technology - that will drive scientific progress. Research reports and regular manuscripts that contain new and significant information of general interest are welcome.

(3) Who: All people are welcome to submit manuscripts in any fields of nature and science.

(4) Distributions: The Journal is published in the both printed version and online version. The abstracts of all the articles in this journal are free accessed publicly online, and the full text will be charged to the readers for US$10/article. The authors will get 30% of the article selling and the other 70% of the article selling will be used to cover the publication cost. If the authors or others need hard copy of the journal, it will be charged for US$60/issue to cover the printing and mailing fee. For the subscription of other readers please contact with: sciencepub@gmail.com or editor@sciencepub.net.

.

(5) Advertisements: The price will be calculated as US$400/page, i.e. US$200/a half page, US$100/a quarter page, etc. Any size of the advertisement is welcome.

2. Manuscripts Submission

(1) Submission Methods: Electronic submission through email is encouraged and hard copies plus an IBM formatted computer diskette would also be accepted.

(2) Software: The Microsoft Word file will be preferred.

(3) Font: Normal, Times New Roman, 10 pt, single space.

(4) Indent: Type 4 spaces in the beginning of each new paragraph.

(5) Manuscript: Don't use "Footnote" or "Header and Footer".

(6) Cover Page: Put detail information of authors and a short title in the cover page.

(7) Title: Use Title Case in the title and subtitles, e.g. "**Debt and Agency Costs".**

(8) Figures and Tables: Use full word of figure and table, e.g. **"Figure 1.** Annul Income of Different Groups**", Table 1. Annual Increase of Investment".**

(9) References: Cite references by "last name, year", e.g. "(Smith, 2003)". References should include all the authors' last names and initials, title, journal, year, volume, issue, and pages etc.

Reference Examples:

Journal Article: Hacker J, Hentschel U, Dobrindt U. Prokaryotic chromosomes and disease. Science 2003;301(34):790-3.

Book: Berkowitz BA, Katzung BG. Basic and clinical evaluation of new drugs. In: Katzung BG, ed. Basic and clinical pharmacology. Appleton & Lance Publisher. Norwalk, Connecticut, USA. 1995:60-9.

(10) Submission Address: Marsland Company, 525 Rockaway PKWY, #B44, Brooklyn, New York 11212, The United States; Telephone: (347) 321-7172; Email: editor@sciencepub.net,

.

(11) Reviewers: Authors are encouraged to suggest 2-8 competent reviewers with their name and email.

2. Manuscript Preparation

Each manuscript is suggested to include the following components but authors can do their own ways:

(1) Title page: including the complete article title; each author's full name; institution(s) with which each author is affiliated, with city, state/province, zip code, and country; and the name, complete mailing address, telephone number, facsimile number (if available), and e-mail address for all correspondence.

(2) Abstract: including Background, Materials and Methods, Results, and Discussions.

(3) Key Words.

(4) Introduction.

(**5) Materials and Methods**.

(**6) Results**.

(**7) Discussions**.

(**8) References**.

(**9) Acknowledgments**.

Journal Address:

Marsland Press
525 Rockaway PKWY, #B44
Brooklyn, New York 11212
The United States
Telephone: (347) 321-7172
E-mail: sciencepub@gmail.com;
editor@sciencepub.net
Websites: http://www.sciencepub.org

New York Science Journal

Volume 1 - Number 1 (Cumulated No. 1), January 1, 2008; ISSN 1554-0200

Contents

Marsland Press, 525 Rockaway PKWY, Brooklyn, New York 11212, The United States; (347) 321-7172; editor@sciencepub.net,

http://www.sciencepub.org editor@sciencepub.net

Nodulation and Nitrogen Fixation by Landrace Legumes in Yam/Cassava Based Cropping Systems of the tropical rainforest

Ibeawuchi I.I., Obiefuna J. C., Nwufo, M. I. and Ofoh, M.C.
Department of Crop Science and Technology
Federal University of Technology
P.M.B. 1526, Owerri Nigeria
ii_ibeawuchi@yahoo.co.uk

Abstract: The study assessed the nodulation / nitrogen fixation of landrace legumes: the velvet bean *(Mucuna pruriens Var. utilis)*. African yam bean *(Sphenostylis sternocarpa)* and lime bean *(Phaseolus lunatus)* for increased yield in yam/ cassava based cropping systems of the tropical rainforest of Southeastern Nigeria. In both sole cropping and formed systems the landrace legumes formed nodules within 4 WAP. Dry nodule weight was higher in sole legumes than in yam/cassava based crop mixtures and further decreased with increasing number of crops in the mixture. Mucuna pruriens fixed significantly more N, had higher symbiotic dependence ranging from 57.02% in yam/maize/cassava/mucuna to 57.62 in sole cropping than the other legumes used.the experiment. African yam bean had significantly more efficient nodules than mucuna and lima bean either in sole cropping or intercropping. Also, there were significant differences in the dry matter per plant between cropping systems and within the landrace legume species and Mucuna had the highest (8.8 g) in sole cropping system. [New York Science Journal. 2008;1(1):1-12]. (ISSN: 1554-0200).

Keywords: Nodulation and Nitrogen Fixation, Landrace Legumes, Yam/Cassava Based Cropping Systems, Tropical Rain Forest

Introduction:

The agro-ecological zones of the world are made up of different cultures practicing different cropping systems for the sustenance of their environment. In many parts of the developing countries of the world, there is an increasing deficit of nitrogen. It is estimated that between 20 and 70 kg N ha^{-1} yr^{-1} may be imported every year by developing countries in sub-Saharan Africa and Latin America (Giller2001) Nitrogen is lost mainly through leaching, volatilization and denitrification, and to the atmosphere through burning. These loses must be replaced if agricultural productivity is to be sustained.

In agricultural production systems, adequate levels of nitrogen (N) are essential for proper plant growth as it is useful for chlorophyll, enzymes as well as for the amino acids and proteins used for building plant tissues and cell organelles (Brady, 1990). In many tropical agricultural systems, the importance of nitrogen is second only to water and the N content of most surface mineral soils is about 0.02 – 0.5%(Webster and Wilson, 1998). However, most of the soil N is in Organic form associated with humus and silicate clays and only about 2-3% of this is mineralized each year (Brady 1990). Amongst the soil nutrient elements, nitrogen (N) is so important to plants that after photosynthesis, biological nitrogen fixation is probably the second most important biological process on earth (Brady 1990). Biological nitrogen fixation through legumes has a great potential to contribute to the productivity and sustainability of the tropical agricultural systems by substituting for fertilizer inputs (Boddey et al 1997). The southeastern Nigeria agro ecological zone is characterized by varying seasonal temperatures, rainfall, humidity, low soil pH and organic matter levels, poor soil fertility status particularly Nitrogen. There is minimal external input use by small-scale farmers, practicing mostly yam and or cassava based cropping systems with maize, legumes and some vegetables, predominating the zone. This farming system had received limited attention from the research communities as early efforts were focused on fertilizer trials instead of exploiting the landrace legumes to improve our farming systems, as practiced by traditional smallholder farmers. The contemporary research efforts to improve soil fertility is directed towards the introduction of edible and non-edible leguminous species into our farming systems to harness fertility potentials with yam and or cassava as the base crops.

The Velvet bean, *Mucuna pruriens* is a leguminous plant indigenous to Southeastern Nigeria. It is called “Agbiri” (Igbo) because of the itching nature of the pod trichomes when in contact with the human skin. It is a vigorously growing and twining annual plant and has a number of species and hybrids. (Qudhia, 2001a). *Mucuna pruriens* apart from having some medical properties fixes nitrogen and serve as a green

manure and cover crop (Oudhia 2001b). Providing support to the plant helps to increase the yield by 25% and reduces pest infestation (Oudhia and Tripathi 2001) and yield of 500kg ha^{-1} have been obtained from well, managed irrigated farms (Singh *et al* 1995, Farooqi *et al* 1999)

The lima bean *Phaseolus lunatus* L is a warm season crop belonging to the family legumenoseae. It is propagated by seed (Van der Maeseen and Sadikin 1989, Darbie *et al* 1999). There are three culti-groups of the lima bean, sieve, potato and the big Lima. However the fourth culti- group called sieve big Lima type exists (Liol *et al* 1991). Lower yield of 200 – 300 $kgha^{-1}$ has been reported in India while in Western Nigeria under experimental condition yield of over 300 $kgha^{-1}$ have been reported indicating potentials of the crop in the humid tropics (Daisy 1979). It is often planted along with yam and the beans, using the same stakes as the yam for support (Ibeawuchi and Ofoh 2000)

The African yam bean *Sphenostylis sternocarpa* is a vigorous growing herbaceous plant that climbs and twines to height of over 3m and requires staking. Small-scale cultivation is practiced throughout Southeastern Nigeria where the plant is adapted for low land conditions. The African yam bean has trifoliate leaves and flowers profusely in 100-150 days after planting (IPGRL FAO 2001) .Its management is the same as employed traditionally by farmers in Africa where it is always found in mixed culture and scattered in small plots (NAS 1979).).

Yam, *Dioscorea species* is a monocot and it is wide spread in West Africa of which Nigeria is the center of production (Onwueme- and Sinha 1991. Lothar 1983). Over 59% of yams and 75% of maize grown in Nigeria are intercropped (Okigbo and Greenland 1975). In the soils of the rain forest zone of Nigeria, yam / maize /melon and yam/maize/cassava are the must dominant yam based crop combinations (Agboola 1979, Ezeilo *et al* 1975). In most traditions practicing yam based farming systems, yam is usually the first or one of the first crops to be planted after the land is cleared from bush fallow (Degrass 1993).

Cassava, *Manihot esculenta* (L) Crantz is a dicotyledonous plant growing 1-3m high. It belongs to the family Euphorbiceae (Pierre 1989, Howard 1988) Cassava based cropping systems are found mainly on poor sandy soils of the coastal belt where food crops other than cassava hardly give satisfactory yield except coconut or oil palm. Cassava is the predominant staple food crop in southeastern Nigeria replacing especially cocoyam, potato and even yam to some extents.

The yam/cassava based cropping systems with landrace legume is expected to be a good crop combination for soil improvement. This cropping system may help in biological nitrogen fixation and availability to the companion or a subsequent crop. Legumes apart from serving as food has a variety of other uses including their ability to harbour nitrogen fixing bacteria (rhizobia) and serve as green manure crop to improve soil fertility and soil organic matter content. The potentials of legumes to fix nitrogen in the soils of low land humid environment have not fully been exploited especially using the landrace legumes of the rainforest belt of Nigeria. The Nitrogen benefit from leguminous plant in an intercropping system will depend on the active symbiotic activity under such a system. The relevance of yam and or cassava intercropping with landrace legumes such as *Mucuna pruriens*, *Sphenostylis sternocarpa* and *Phaseolus lunatus* in Southeastern Nigeria agro ecological zone lack scientific information.

This work therefore, was designed to develop farming technologies using such edible and non-edible landrace legumes to assess their potentials in nodulation/ Nitrogen fixation in a yam/cassava based cropping systems in Southeastern Nigeria.

Materials and Methods

The experiment was conducted at the Teaching and Research farm of the School of Agricultural Technology, Federal University of Technology Owerri. Nigeria, located between latitude 5^0 $23^/$ $8.7^{//}$ N and longitude 6^0. $59^/$ 39. $4^{//}$ E., which is in the tropical rainforest zone of Southeastern Nigeria. The areas have a minimum and maximum annual ambient temperature of 20 C and 32 C, respectively and mean annual rainfall of 2500mm (Nwosu and Adeniyi 1980).

The soils have been developed from deep unconsolidated marine sediments of Pleistocene age, often known as coasted plain sands (Ofomata 1975) and classified as Ultisols with low mineral reserve and are therefore low in fertility (Eshett 1993). The experimental site was under fallow for 2 years and it was previously cropped with cassava and maize to which NP K fertilizer was applied. Thesoil physical properties showed 84% sand,10.5% silt and 6.5% clay while the chemical analysis revealed that the soil had 0.05% Total N,10.9 ppm P, and available cations K, Ca and Mg of 0.76,0.47 and 0.70Cmol/kg respectively. The soil reaction (pH in water) was 4.56.

Planting materials

Three land race legumes were used namely: African yam bean – *Sphenostylis sternocarpa*; Lima bean – *Phaseolus lunatus*; and the velvet bean-*Mucuna pruriens* var. utilis. Mucuna grows in the wild but the black seed were collected from the SAAT gene bank while lima bean and African yam bean were bought from the rural markets in Owerri agricultural zone. Other planting materials: cassava - (TMS 30555); Seed yams (white) obiaeturugo– local cultivar; TZSR yellow, Cassava cuttings and maize were bought from the Imo Agricultural Development Project Headquarters Okigwe Road, **Owerri.**. For the repeat of the experiment, seeds of the land race legumes, maize seeds, seed yams and cassava cuttings harvest were got from the previous plantings

Land preparation

For the two years of the research work, land preparation was done manually with machetes, spades and rakes since minimum tillage was used. The dry trash was later packed and removed from the site. The field was thereafter marked out for planting. The experiment was laid out in a randomized complete block design replicated 3 times. Each plot measured 3 x 4 m with 1 m between plots and 2 m between blocks and 1 m experimental guard areas. The treatments included sole crops each component crop and their combinations as follows:

Yam/ maize-Based:
1. Yam/maize/mucuna (y/m/mp)
2. Yam/maize/lima (y/m/l).
3. Yam/maize/African yam bean (y/m/Ayb)
4. Yam/maize, (y/m).

Cassava/ maize - based

5. Cassava/maize/mucuna (c/m/mp)
6. Cassava/maize/lima (c/m/l)
7. Cassava/maize/African yam bean (c/m/Ayb)
8. Cassava/maize (c/m).

Yam/ maize cassava-based
9. Yam/maize/mucuna (y/m/ cassava mp).
10. Yam/maize/cassava/lima (y/m/c/l)
11. Yam/maize/cassava/African yam bean (y/m/c/Ayb)
12. Yam/maize/cassava (y/m/c)

Sole Cropping

13. Yam (y)
14. Cassava (c)
15. Maize (m)
16. Mucuna (Mp)
17. Lima bean (L)
18. African yam bean (Ayb

Planting and spacing

Two seeds of each landrace legume were planted 2-3cm deep and spaced 50 x 50 cm. These were later thinned down to 1 plant per hole after emergence giving 20,000 plants per hectare for sole and intercropped plots of each legume.

Two maize seeds were planted per hole at a depth of 2-5cm at 1 x 1m spacing. This was later thinned down after germination and emergence to 1 plant per stand giving 10,000 plants per hectare.

Yam*: Dioscorea rotundata* (white) obiaeturugo, seed yams weighing 200-300 g were planted in holes measuring 30 x 30 x 30 cm at a spacing of 1 x 1m on flat. This gave a plant population of 10,000 plants per hectare.

Cassava: (TMS 30555). Cassava cuttings measuring 20cm long were planted on flat at 1 x 1 m spacing giving a plant population of 10,000 plants/ha.

Soil samples

At the beginning of the experiment, soil samples were randomly collected with soil auger at a plough layer of 0 – 20 cm from different spots of the experimental field. The soil samples were bulked and analysed. Also, at the end of each experiment soil samples were collected with soil auger from each plot and samples from plots carrying the same treatments were bulked and analyzed.

Soil pH was determined in distilled water at 1:2.5 soil: water solution ratios using the Beckman zeromatic pH meter.

Organic matter (OM) was determined by the chromic acid oxidation method (Walkley and Black, 1934).

Nitrogen (N) was determined by the micro-kjeldahl digestion method (Bremner, 1965).

Available phosphorus (P) and exchangeable potassium (K) were determined by the Bray II (and the flame photometry, respectively. Atomic Absorption Spectrophotometry (AAS) determined calcium (Ca) and Magnesium (Mg).

Plant and Soil Sampling.

Two plants each of Mucuna pruriens var. utilis (Mucuna Black seed utilis), *Phaseolus lunatus* (Lima bean) and *Sphenostylis sternocarpa* (African yam bean) were sampled from each plot at 2 weekly intervals starting from 4-12 weeks after planting and at harvest.

At each sampling, nodule number, nodule weight, and total dry matter yield were assessed. Also, nodule colour was determined in the field using colour chart. The legume samples were dried to a constant weight at an oven temperature of 60^{o}C for 48 hours.

At each sampling time, the residual soil N and plant N accumulation were determined thus:

N -accretion = Total N in the system at harvest minus net change in soil N + seed N.

N in the system at harvest = Sum of soil N + total plant N.

Net change in soil N = Soil N after harvest – soil N before planting.

N accretion = Gradual addition of N in nature (soil).

In yam, maize, cassava intercropping with the three legumes, soil samples were taken at harvest and analyzed

Nodule counts

Two legume plants in each plot were sampled each time by digging up the entire plant and immersing the root into a bucket full of water to clear roots of soil. Thereafter, the number of nodules per plant were counted and recorded. Subsequently, the nodules were scratched to note the colour.

Dry matter.

The sampled legume plants from the plots were oven dried at 60^{o}C for 48 hours to a constant weight and recorded. At harvest, the samples (plant and grain) were also oven dried analysed and recorded .All samples were oven dried to a constant weight and recorded.

Plant analysis

At each sampling, the oven-dried materials were analyzed for plant N.

Harvesting was done at the maturity of each crop.

Data analysis

The data collected were collated and statistically analyzed using the Megastat, developed by Orris (2000) and Microsoft Excel (2000) packages. Simple linear regression equation as detailed by Koutsoyiannis (1996) was fitted into the data collected for evaluation of total dry matter and nodule weight. Wahua (1999) was used for data analysis and interpretation.

Results

Table 1 shows the mean nodule dry weight, (mg/plant) nodule number and total dry matter/plant (g/plant) for yam, cassava, and yam/cassava-based cropping systems and the sole cropping of the three-landrace legumes. The sole cropped landrace legumes had significantly higher number of nodules per plant

than the other cropping system Nodule number decline with increased number of crops per crop combination, with the least nodule number of 25/plant from yam/maize/cassava/ mucuna. There were significant differences in nodule dry weight within and between the different yam and cassava-based cropping systems. In yam-based cropping system, *Mucuna pruriens* had significantly higher nodule dry weight than lima bean (*Phaseolus lunatus*) but, similar to that *Sphenostylis sternocarpa* (the African yam bean). In Cassava and yam/cassava-based cropping system no significant differences existed among the cropping systems. However, the sole cropping of the landraces showed significantly higher number of nodule dry weight per plant for *Mucuna pruriens than Phaseolus lunatus* and *Sphenostylis sternocarpa.*

Furthermore, there were differences in the quantity of dry matter produced per plant between cropping systems and within the land race species. The highest was got from *Mucuna pruriens* under sole cropping (8.8g/plant) and it was significantly ($P \geq 0.05$) higher than those of others in the crop mixtures and the sole cropping of *Phaseolus lunatus* and *Sphenostylis sternocarpa*. The results also show a change in the dry matter of Mucuna, which was reduced by 22.72% when planted in association with yam and maize, or by 28.98% when planted in association with cassava and maize or by 26.14% when in association with yam/maize/cassava. The dry matter of lima bean was reduced by 25.22 % when associated with yam/maize, by 11.30% and 28% in cassava/maize and yam/maize/cassava, respectively. African yam bean dry matter was depressed by 25% when in association with yam/maize, by 11.21% in association with cassava/maize and by 29.83% in yam/maize/cassava association.

Figure 1 shows the relationship between mean dry nodule weight and nodule numbers for tuber-based cropping mixture. A relationship exists between them and that dry nodule weight increased with increasing number of nodules indicating that the relationship will enhance the fixation potentials of the landrace legumes.

Table 2 shows regression analysis of impact of total dry matter on mean nodule weight for tuber–based cropping systems and sole cropping of the three-landrace legumes. The results of the regression analysis are shown in the equation;

$$Y = 53.78 + 19.10X_1 \text{ ---------- (1)}$$

Where y = mean nodule dry weight (mg/plant) and

X_1 = Total dry matter (g/plant).

Test carried on this regression estimate showed that a significant relationship existed between the mean nodule dry weight and total dry matter. The empirical relationships between these two variables (nodule dry weight and total dry matter) show that each mg nodule weight requires 19.1g dry matter to form. From the same equation 59.7% (R^2 = coefficient of determination) of the variation in the nodule weight was explained by the total dry matter per plant. It showed that the t-ratio, which is coefficient/standard error, was significant at ($P \leq 0.01$) indicating a strong relationship between total dry matter and nodule dry weight.

Figure 2 shows a significant relationship between nodule dry weight and fixed nitrogen. Fixed nitrogen increased with increase nodule dry weight, which was significantly different ($P \leq 0.05$) in sole planted Mucuna.

Total fixed –N, and symbiotic dependence (SD).

Table 4, shows that among the three landrace legumes *Mucuna pruriens* fixed significantly ($P \geq 0.05$) more nitrogen than the other legumes either as sole or when intercropped. *Mucuna* also had the highest symbiotic dependence (SD) in all the cropping systems, In Mucuna SD ranged from 57.02% in yam/maize/cassava/Mucuna to 57.62 in sole cropping. In lima bean SD ranged from 45.15% in yam/maize/cassava Lima to 45.63% in sole cropping while African yam bean had 50.05% in yam/maize/African yam bean to 56.47%under sole cropping.

Nodulation Efficiency and Specific Nodule Activity.

Nodulation efficiency (NE) shows that *Sphenostylis sternocarpa* (African yam bean). had significantly ($P \geq 0.05$) more efficient nodules than the other legumes either in sole cropping or in intercropping (Table 5). The results show that there is high specific activity of nodules in the yam/cassava-based cropping system 0.38 and 0.36 for Mucuna and African yam bean, respectively, which they were significantly ($P \geq 0.05$) different from those of other legumes in the cropping system.

Table 1. Mean nodule weight (mg/plant); Fixed N (mg/plant); nodule no/plant, and total dry matter, (g/plant) for yam/cassava- based cropping system and sole cropping of the three-landrace legumes.

Treatments/Cropping System	Dry Nodule weight (mg/plant)	Total Dry Matter (g/plant)	Nodule No./ plant	Fixed N (mg/plant)
yam/maize/mucuna	168.8	6.8	38	57.1
yam/maize/lima	146.2	4.3	31	39.5
yam/maize/African yam bean	159.9	4.35	35	45.2
Cassava/maize/mucuna	156.6	6.25	36	58.3
Cassava/maize/lima	138.64	5.1	31	41.2
Cassava/maize/African yam bean	138.8	5.15	31	47.7
yam/maize/cassava/Mucuna	139.9	6.5	25	52.8
yam/maize/cassava/lima	124.35	4.14	28	38.3
yam/maize/cassava/ayb	124.36	4.07	28	44.2
Mucuna pruriens	240.2	8.8	66	65.8
lima beans	187.8	5.75	56	47.5
African yam bean	199.9	5.8	57	54.2
LSD(0.05):	18.65	1.78	12.5	10.8

Table 2. Regression Analysis showing the relationship between dry matter and nodule weight for yam/ cassava-based cropping system & sole cropping of the three-landrace legumes.

0.597	R^2
0.773	R
22.820	Std. Error of estimate
12	Observations
1	Predictor variable
(mg/plant)	Dependent variable

Regression equation: $Y = 53.78 + 19.10X_1$
Standard error of coefficient ----- (4.96)
The t-ratio (coeff./std.error)--------3.85***
Y = Mean Nodule Weight (mg/plant);
X_1 = Total Dry Matter (g/plant);

Table3. Nodulation count, Nodule Weight, Plant Dry matter, Soil N and Plant N at 4 WAP

Cropping System	Nodule Number	Nodule wt (mg)	Plant total Dry matter(g)	Soil N. mg/100g	Plant N mg/100g
Yam-based					
Yam/Maize/Mucuna	2.0	0.28	0.18	7.0	8.7
Yam/Maize/Lima	1.0	0.09	0.08	7.0	7.2
Yam/Maize/African Yam bean	1.5	0.11	0.16	7.0	6.5
Cassava-based					
Cassava/Maize/Mucuna	1.0	0.20	0.18	7.0	8.6
Cassava/Maize/Lima	1.0	0.07	0.17	7.0	7.2
Cassava/Maize/African yam bean	1.0	0.05	0.17	7.0	6.5
Yam/Cassava-based.					
Yam/Maize/Cassava/ Mucuna	2.0	0.03	0.17	7.0	8.7
Yam/Maize/Cassava/ Lima	2.0	0.19	0.16	7.0	7.2
Yam/Maize/Cassava/ African yam bean	2.0	0.22	0.16	7.0	6.5
Sole Cropping					
Mucuna pruriens	2.5	0.03	0.19	7.0	8.7
Lima bean	2.0	0.120	0.17	7.0	7.2
African yam bean.	2.0	0.22	0.18	7.0	6.5
LSD(0.05)	0.25	NS	NS	NS	NS

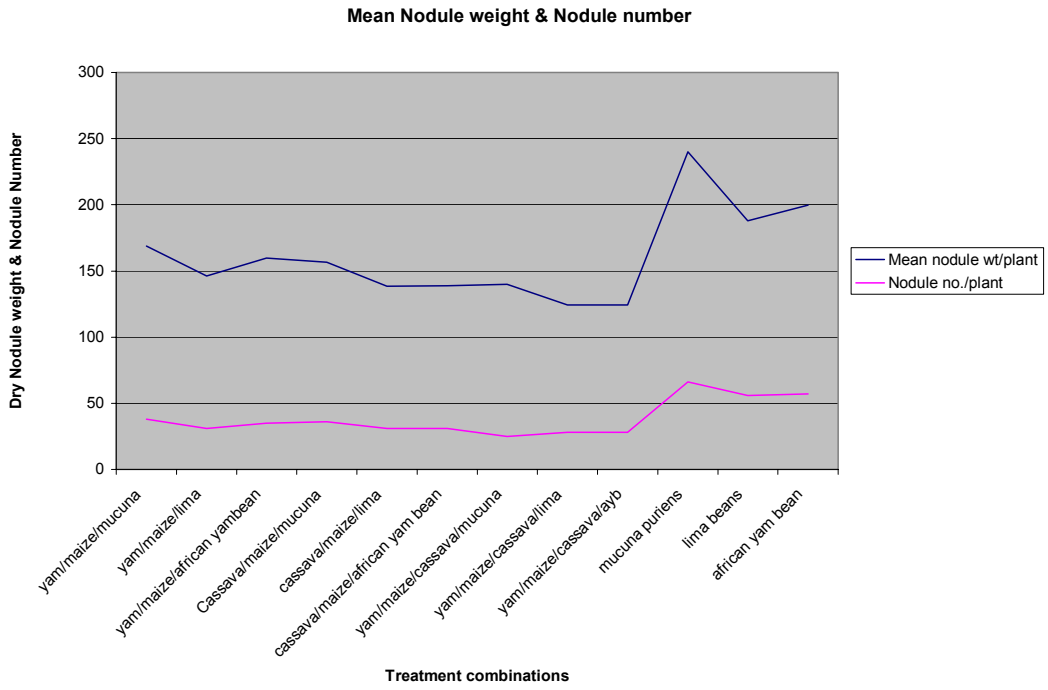

Figure 1. Relationship between mean nodule weight & nodule numbers for yam /cassava-based cropping systems & sole cropping of the three landrace legumes

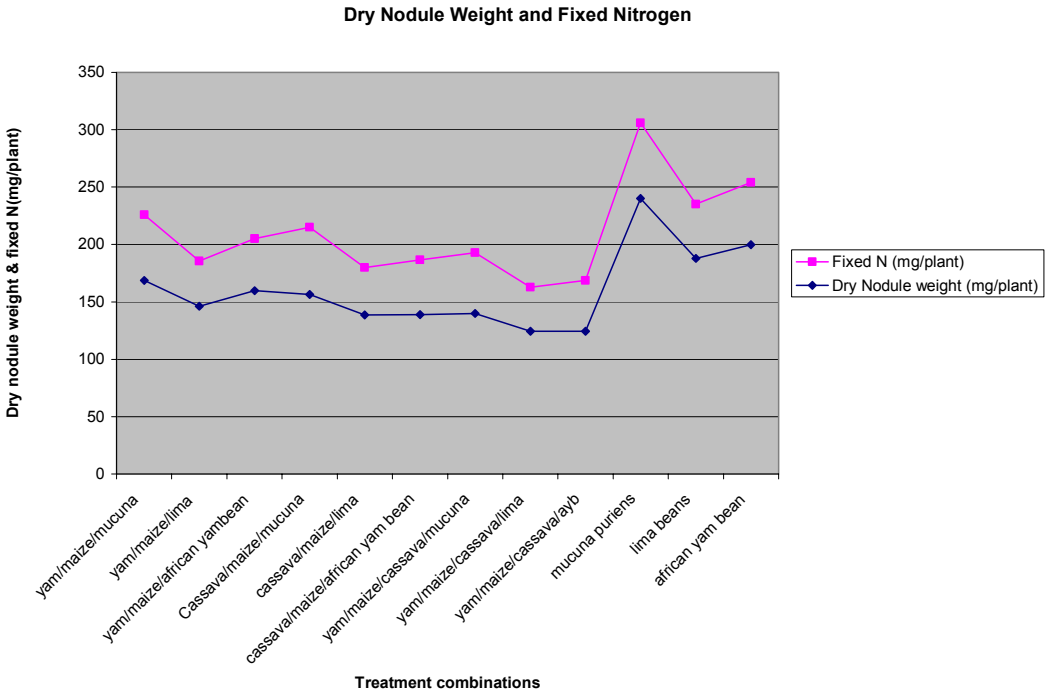

Figure 2. Relationship between mean dry nodule weight & Fixed N (mg/plant) for yam/cassava-based cropping system & sole cropping of the three landrace legumes.

Table 4: Mean value of fixed N, Symbiotic dependence (SD), Nodulation Efficiency (NE), and specific activity as influenced by cropping systems.

Cropping Systems	Fixed N (mg/plant)	Symbiotic Dependence(SD) (Fixed N/Total Plant N)*100	Nodulation Efficiency(NE) (Nodule dry wt.(mg)/(plt dry wt(g))	Specific Nodule Activity (Fixed N(mg)/Nodule Dry wt(mg))
Yam-based:				
yam/maize/Mucuna	57.1	57.44	24.82	0.34
yam/maize/lima	39.5	45.56	34	0.27
yam/maize/African yam bean	45.2	50.05	36.76	0.28
Cassava-based:				
Cassava/maize/mucuna	58.3	57.44	25.06	0.35
cassava/maize/lima	41.2	45.3	27.18	0.3
cassava/maize/African yam bean	47.7	50.32	26.96	0.34
Yam/Cassava based :				
yam/maize/cassava/Mucuna	52.8	57.02	21.51	0.38
yam/maize/cassava/lima	38.3	45.15	30.04	0.31
yam/maize/cassava/Ayb	44.2	50.05	30.56	0.36
Sole Cropping:				
mucuna puriens	65.8	57.62	27.3	0.27
lima beans	47.5	45.63	32.63	0.25
African yam bean	54.2	56.47	34.47	0.27
LSD (0.05)	10.8	11.75	11.39	0.06

NB: SD= (Fixed N)/(Total Plant N) x100/1
NE = (Nodule dry weight /Plant)/(Plant dry Weight)
SNA =(Fixed N)/(Nodule dry Weight)

Discussion

Nodule Dry Weight and Nodule Number

Nodule formation was noticed within 4 WAP. Field records show that some nodules were green, white or grey while some were pink or red when scratched with finger. The pink or red nodules are those believed to have leghemoglobin and capable of N- fixation. Lindemann and Glover (1998) reported that young nodules were white or grey and were not fixing nitrogen but as they grew they turned pink or reddish in colour indicating that nitrogen fixation has started. Nodule dry weight and number decreased with increasing numbers of plants population in each crop combination with the lowest in yam / cassava-based cropping system. It may be that nodule weight and number are energy dependent. This agreed with the report by Tang *et al (*2001) that phosphorus increased nodule number 35 WAP. However, nodule number and weight could be as a result of legumes genetic character to have up-to a certain number if favoured by environmental factors. Simple relationship exists between nodule dry weight and nodule number per plant as they are indices of N – fixation (Vincent – Chandlar *et al* 1964; Oti and Agbim 2000a).

Nodulation Efficiency (N.E) and Specific Nodule Activity (SNA).

These are derived technical expressions of the symbiotic permanence of the landrace legumes and point out the effectiveness or otherwise of nodules and their relationship with fixed-N_2. Therefore, the nodulation efficiency (NE) could be more dependent on the genetic inheritance of the legumes while specific nodule activity (SNA) seems more an environmentally controlled factor since it was significantly affected by the different cropping systems and the former was not. This view was shared by Oti and Agbim (2000b) who reported, that nodulation efficiency tended to be more an inherent attribute of legumes while specific nodule activity was more controlled by environmental factors

Total Dry Matter.

Dry matter accumulation is one of the measures of plant growth, (Noggle and Fritz 1983) and reflects the relative growth rate as regards to net assimilation rate. Dry matter is a function of crop species and soil fertility (Jones 1976; Oti and Agbim 2000(b}. The result suggests that inter-cropping system influenced dry matter accumulation. The inter-cropping systems involving yam and cassava, which have high demand for soil P and K (Ustimenko – Bakumovsky 1983, Onwueme and Sinha 1991), must have affected adversely the performance and growth of the land race legumes. This agreed with the report by Vincent – Chandlar *et al* (1964), Oti and Agbim (2000a) that low P in soils or its deficiency limits legumes growth and performance in tropical soils. However, large quantities of dry matter were obtained from sole cropping systems. This has its agronomic significance since total dry matter is one of the key factors in soil nitrogen fixation (West and Wedin 1985).

Fixed – N and Symbiotic Dependence (SD)

The significantly high quantity of N-fixed by the sole planted legumes reflected the number of nodules per plant, dry nodule weight and total dry matter content per plant. This observation agreed with the results obtained by Ibeawuchi *et al* (2004), who reported that nodule weight, nodule numbers and total dry matter are all indices of nitrogen fixation since they have either direct or indirect relationship. The high nodule weight and number of mucuna planted sole in the trial and its ability to fix-high quantity of N in the experiment is an indication of the importance of their relationship in N-fixation. This agreed with the report by Miller *et al* (1982) who reported that nodule weight was a major contributing factor to N-fixation activity while nodule numbers was important in its relationship with nodule weight. Symbiotic dependence (SD) being a mathematical expression in percentage of the fixed-N per total plant nitrogen may not be a dependable measuring technical attribute for nitrogen fixation potentials of the landraces. This observation agreed with Oti and Agbim (2000b) who stated that symbiotic dependence is influenced by soil and may not be a reliable indicator of screening the N– fixing potentials of legumes.

Conclusion:

Landrace legumes had been found to fix reasonable quantities of nitrogen in the soil and by implication help to improve soil fertility. This will go a long way in reducing the use of chemical fertilizers, thus sustaining our environments. Our farming environment is governed by high rainfall and temperature, which encourages leaching and volatilization losses. The soil being a living body is dynamic and these factors will not allow one to give accurately the N status of the soil at any particular point in time. However, farmers are encouraged to practice intercropping with landrace legumes since they have been found to fix large and economical amounts of nitrogen and dry matter which decay to sustain soil organic matter content. *Mucuna pruriens* is a crop of the future and emphasis should be laid on its research as human food and other endeavours of human life.

Acknowledgments

We acknowledge Mrs. Rosita Ibeawuchi, Okechukwu Nwaneri and Mr. & Mrs. Chika Ibeawuchi for all their efforts in fieldwork and data collection. We also thank the Chief Technologist Mr. C.I. Akaerue, of Department of Crop Science Laboratory, Mr. Simon Nti of the Department of Soil Science Laboratory Federal University of Technology Owerri and the Chief Technologist and Staff members of the Department of Soil Science the University of Nigeria Nsukka for all the laboratory analysis.

Correspondence to:
Ibeawuchi I.I., Obiefuna J. C., Nwufo, M. I. and Ofoh, M.C.
Department of Crop Science and Technology
Federal University of Technology
P.M.B. 1526, Owerri Nigeria
ii_ibeawuchi@yahoo.co.uk

Received: 10/31/2007

References

1. Agboola, S.A. (1979). An Agricultural Atlas of Nigeria: London, Oxford University Press. Pp 16-47
2. Brady, N. (1990) Nature and Properties of Soils. Macmillan publishing company, New York.
3. Bremmer, J.M. (1965) Total nitrogen. In: C.A. Black et al (ed) Methods of soil analysis Part 2. Agron No. 9. American Society of Agronomy, Madison, Wisconson USA pp1149-1178.
4. Boddey, R.M, Sa, J.C, D.M, Alues, B JR and Urquiaga, S. (1997). The contribution of biological nitrogen fixation for sustainable agricultural systems in the tropics. Soil biology and bniochemistry 29 (5/6) 287-799.
5. Daisy E.K. (1979) Food legumes: TPI Crop Product Digest. No. 3. Tropical Product Institute Circular 716.
6. Darbie,M; William, T.K and George, (1999). Lima bean :Commercial Vegetable Production.Goeogia Extention Services Publicarion Circular 716.
7. Degras. L. (1993) The Yam: A Tropical Root Crop. The Macmillan Press Ltd, London, pp.1-344.
8. Eshett, E.T. (1993) Wetlands and ecotones studies on land water. National Institute of Ecology, New Delhi and International Scientific Publications, New Delhi pp 232-234.
9. Ezeilo, W.N.O, Klinn, J.C. and Williams, L.B. (1975) Cassava Production in the East Central State of Nigeria. IITA Ibadan, Nigeria. Pp.27.
10. Farooqi, A.A., M.M. Khan and Asundhara (1999) Production technology of medicinal and aromatic crops. Natural Remedies. Put Ltd., Bangalore, India pp 26-28.
11. Giller *K .E (2001)Nitrogen fixing in tropical cropping systems. 2nd Edition .CAB International , Wallford . Pp. 423.*
12. Howard Bradbury. J. and Warren D. H. (1988). Chemistry of Tropical Root Crops. Significance for Nutrition and Agriculture in the Pacific. Ware Printing Melbourne ACIAR Monograph No. 6. pp. 27-37.
13. Ibeawuchi, I.I Obiefina J.C; Ofoh,. M.C.; Ihejirika, G.O; Tom, C.T, Owneremadu, E.U and Opara, C.C (2004) An Evaluation of four soybean varieties intercropped with Okra in Owerri Ultisol of Southeastern Nigeria. Pakistan Journal of Biological sciences (PJBS) 70 2004 ISSN 1028-8880.(*In press.)*
14. Ibeawuchi, I.I. and M.C. Ofoh (2000) Productivity of maize/cassava/food legume mixtures in south eastern Nigeria. J. Agric. and Rural Dev. 1(1): 1-9.
15. IPRI – FAO (International Plant Genetic Resources Institute – Food and Agricultural Organisation) (2001) Cultivation and use of African yam bean (Spenostylis stenocarpa) in the Vvolta regions of Ghana. PGR Newsletter No. 124 pp 13-16.
16. Jones, R..J. (1976) Yield potential for tropical pasture legumes NIFTAL college of tropical Agriculture Misc . Publ. 145:39-55
17. Koutsoyiannis, A (1986) Theory of Econometrics: An introduction of Econometric methods: 2nd Edition. Macmillan Education Ltd, London. Pp :11-666.
18. Liol, L., Esquivel M. and Castineiras, L. (1991) Lima bean (*Phaseolus lunatus* L.) landraces from cuba, electophoretic analysis of seed storage protein. Biologiches Zen tralolatt 110 (1) 76-79.
19. Lothar, D. (1982) Smallholder Farming System with yam in the Southern Guinea Savannah of Nigeria. GTZ. No. 126. Pp. 1-221.
20. Micro Soft Excel Package (2000) Microsoft Inc. USA
21. Miller, J.C, J.S. Scott, K.W Zary and S.K O' Hair 1982. The influence of available nitrate levels on N-fixation in 3 cultivars of cowpea Agron. J. 74:14-19
22. NAS (National Academy of Sciences) (1979b) Microbial Processes. Promising Technologies for Developing Countries. National Academy of Sciences, Washington D.C. Pp. 47-71

23. Noggle, G.R. and G.J. Fritz(1983) Introductory plant physiology. 2nd edition prentice-Hall Inc. Engle wood cliffs. New Jersey Pp 625.
24. Nwosu, A.C. and E.O. Adeniyi (1980) Imo state: A survey of resources for development. Nigeria Institute for Social and Economic Research (NISER), Ibadan, Nigeria pp 310.
25. Ofomata, G.E.K. (1975) Nigeria in maps. Eastern states. Ethiope Pub. House, Benin City, Nigeria pp 33-40.
26. Okigbo, B.N. and Greenland, D, J. (1976) Intercropping Systems in Tropical in Africa. In; R.L. Papendick, A. Sanchez and G..B triplet (Editors). Multiple Cropping ASA. Special publication No. 27,, Madison W.I. USA Pp. 63-101.
27. Onwueme I.C. and T.D. Sinha (1991) Field Crop Production in the tropical Africa CTA. Ede Netherlands. Pp. 1-319.
28. Oris J. B.(2000) Megastat (8.8) Microsoft Inc.2000.
29. Oti, N.N and Agbim N.N (2000a) Comparative studies of Nitrogen fixing potentials of some wild and cultivated legumes 1 Green house trial. J. Agric and Rural Dev 1(1) 27-44.
30. Oti, N.N. and Agbim, N .N (2000b) comparative studies of Nitrogen fixing potentials of some wild and cultivated legumes 2. Field Evaluation. J. Agric and Rural Dev. (1) 79-89.
31. Oudhia, P. (2001a) Records of *Aphis craccivora* Koch (*Hemiptera* aphididea) on medicinal crop *Mucuna pruriens* L., Chhattisgarh (India) Insect Environ. 7 (1): 24-36
32. Oudhia, P. (2001b) Kapikachu or cowhage (Mucuna pruriens). Society for Parthenium Management (SOPAM) 28-A Geeta Nagar Raipar 492001, India.
33. Oudhia, P. and Tripathi, R.S. (2001) The possibilities of commercial cultivation of rare medicinal plants in Chhattisgarth In: Abstract of the VII National Science Conference, Bhartiya Krishi Anusandhan Samittee, Directorate of cropping system research, Meerut, India.
34. Pierre, S. (1989) Cassava: The Tropical Agriculturist. CTA Macmillian London and Basingstoke pp 22-64.
35. Singh, B.M; V.K. Srivastava; M.A. Kidwai; V. Gupta and R. Gupta (1995), Aloe, Psoralea and Mucuna Pp 515 -525 In K L Chadha and Rajendra Gupta (eds), Advances in Horticulture Vol;II Medicinal and aromatic plants, 1995 Malhotra publ. House ,New Delhi
36. Statistical Package for Social Scientists (SPSS) (2004).SPSS Inc. Northern Michigan Avenue – Chicago. Version 11.
37. Tang, C; Hinsinger P; Drevon, J.J. and Jaillard B (2001): Phosphorus Deficiency impairs early nodule functioning and enhances proton Release in Roots of medical truncutula L.
38. Ustimenko-Bakumovsky, G.V. (1983) Plant Growing in the tropics and sub tropics MIR Publishers. Moscow Pp. 28-264.
39. Van der Measeen, L.J.G. and Sadikin, S. (1989) (eds) Plant resources of south east Asia No 1 Pulses Pudoc Wageningen. Pp56-60.
40. Vincent- Chandler JR, R .W Car-Coastas, R.W Pearson, F. Abruna, J. Figarella and S. Silva (1964). The intensive management of tropical forages in Puerto-Rico University of Puerto-Rico Agr Exp sta Bull N0 187.
41. Wahua, T.A.T. (1999) Applied statistics for scientific studies. Afrika-link books Aba Nigeria
42. Walkley, A.A. and J.A. Black (1934) An examination of the Degtjareff method for determining soil organic matter and proposed modification of chromic acid titration method. Soil Science. 37: 29-38.
43. Webstar, C and Wilson, P. (1998) Agriculture and tropics. Blackwell science, Oxford.
44. West, C.P and Wedin, W.F (1985) Dinitrogen fixation in Alfalfa orchard grass pasture Agron. J. 77:89-94.

Hemolysis production and resistance to fluoroquinolones among clinical isolates of *Escherichia coli* in Osogbo Metropolis, Southwest, Nigeria.

Olowe, O.A[1], Ogungbamigbe TO[2,], Kolawole SO[2], Olowe RA[5] and Olayemi AB[6].

1). Department of Medical Microbiology and Parasitology, College of Health Sciences, Ladoke Akintola University of Technology, Osogbo.
2). Department of Pharmacology and Therapeutics, College of Health Sciences, Ladoke Akintola University of Technology, Osogbo.
3). Department of Chemical Pathology, College of Health Sciences, Ladoke Akintola University of Technology. Osogbo.
5). Department of Biology, Federal University of Technology, Akure., Nigeria
6). Department of Biological Sciences, University of Ilorin. Nigeria.

Abstract: The activities of ampicillin, amoxycillin-clavulanic acid, gentamicin, tetracycline, nalidixic-acid, ciprofloxacin, pefloxacin and ofloxacin against 82 clinical isolates of *Escherichia coli* were determined by micro-dilution technique, according to NCCLS guidelines. Twenty two (27.3%) isolates were hemolytic, of which 16 (72.7%) were from urine samples, while 60 (72.7%) were non-hemolytic isolates. The percentage of resistance to quinolones - pefloxacin, ciprofloxacin, ofloxacin, nalidixic acid and amino-glycosides, among both hemolytic and non-hemolytic isolates were not significant ($P>0.05$). However it is very significant for the penicillins- ampicillin, amoxicillin-clavulanic acid, tetracycline and Cotrimoxazole. ($P<0.05$). Thus we conclude that susceptibility pattern to quinolones, nalidixic acid and aminoglycosides by *E. coli* is independent of the hemolysis factor since the level of resistance is not significantly different between the two isolates. While the susceptibility to the penicillins, tetracyclines and Cotrimoxazole is dependent on hemolysis factor since there is a significant difference between the sensitive hemolytic isolates and the non hemolytic isolates. [New York Science Journal. 2008;1(1):13-16]. (ISSN: 1554-0200).

Keywords: Hemolysis, Resistance, Fluoroquinolones, Escherichia coli, southwest, Nigeria.

Introduction:

Resistance to fluoroquinolones in *Escherichia coli* is an increasing problem in Nigeria and other countries. [Daini, 2005]. Most *Escherichia coli* isolates are normal, benign residents in the intestines of animals. However, small percentages of *E. coli* are pathogenic and cause a variety of diseases ranging from diarrhea to septicemia. The properties which allow pathogenic *E. coli* to invade infect, and damage host cells are conferred by adhesins, toxins, and haemolysins. *E. coli* can produce several types of haemolysin, including an extracellular protein (α-haemolysin), a cell-bound protein (ß-haemolysin) and a haemolysin expressed by nalidixic acid-resistant mutants (γ-haemolysins). [Cavalier, 1984; Walton, 1969]. Several mechanisms are known to determine this resistance in *E. coli*, including mutations in the topoisomerase (II and IV) genes, and decreased accumulation because of outer membrane alterations and or the expression of efflux pumps. [Everett, 1996].

In uropathogenic *E. coli* and other isolates that cause extra intestinal disease, the alpha haemolysin, (hlyA) is a particularly important virulence factor [Beutin,1991] This haemolysin belongs to a family of proteins called repeat-in-toxins (RTX) because of the tandem arrays of a nine amino acid repeat with the consensus sequence [Weich,1988; Bauer, 1996]. While determining antimicrobial susceptibility in our clinical laboratory we have often observed that majority of *E. coli* strains resistant to quinolones were non-hemolytic. In this study therefore we intend, to establish the relationship of hemolysis with the levels of resistance of *E.coli* strains to quinolones and determine whether strains of *E.coli* resistant to quinolones that are hemolytic are from specific body fluid.

Materials and methods.

Bacterial strains

Eighty-two isolates from, urine, cerebrospinal fluid, peritoneal fluid, blood culture, wound exudates were cultured for hemolysis testing from different patients referred to the clinical laboratory of the Ladoke Akintola University of Technology Teaching Hospital, Nigeria, from October 2004 to December 2005 were evaluated.

Susceptibility testing

Bacterial identification to susceptibility testing was performed by micro-dilution, according to NCCLS guidelines. The following antimicrobial agents were studied: ampicillin, amoxicillin-clavulanic acid, gentamicin, tetracycline, nalidixic acid, ciprofloxacin, pefloxacin and ofloxacin. Organisms were considered resistant to the antimicrobial agents evaluated when the corresponding MICs were 16mg/ml for ampicillin, 16.2mg/ml for amoxicillin-clavulanic acid, 8mg/ml for gentamicin, tetracycline and pefloxacin, 32mg/ml nalidixic acid and 2mg/ml ciprofloxacin and ofloxacin. These breakpoints allowed comparison of susceptible versus non-susceptible (either intermediate or resistant) isolates, according to NCCLS guidelines. [NCCLS, 1997]

Determination of hemolytic activity.

An organism was considered hemolytic when a clear halo was observed around isolated colonies after overnight incubation. The organisms were considered -haemolysin producers when hemolysis was observed on agar base containing sheep blood (5%, BioMérieux, Marcy l' Etoile, France) but not when containing human blood (5%).

Statistical methods.

The statistical significance of differences in resistance to antimicrobial agents between hemolytic and non-hemolytic isolates was tested using the 2 test and (in the case of gentamicin) Fisher's exact test. Differences were considered significant when P was <0.05

Results:

Among the eighty-two isolates tested for hemolysis 22 (26.8%) isolates produced hemolysis while 60 (73.2%) are non-hemolytic isolates. Of the hemolytic isolates 16 (72.1%) were isolated from the urine samples, 4 (18.2%) from stool samples and 2 (9.1%) from blood samples. The resistance pattern among both hemolytic and non-hemolytic isolates showed that 90.9%and 100% for ampicillin (P=0.06), 81.8% and 100% for amoxycillin-clavulanic acid (P=0.004), 9.1% and 11.7% for gentamicin (P=1.00),81.8% and 98.3% for tetracycline (P=0.017), 31.8% and 40.0% for nalidixic acid (P=0.61), 31.8% and 24.0% for ciprofloxacin (P=0.61), 18.2% and 38.3% for pefloxacin (P=0.11) 50.0% and 60.0% for co-trimoxazole (P=0.46). Twenty two (26.8%) isolates were haemolytic on both sheep and human blood agar, suggesting that these organisms produce -haemolysins. When compared, the percentages of resistance of both isolates to quinolones- ciprofloxacin, pefloxacin, nalidixic acid, co-trimoxazole and gentamicin were not significant statistically (P=0.61, 0.11, 0.61, 0.46 and 1.0 respectively) While the percentage resistance of the two isolates to tetracycline, ampicillin and amoxicillin-clavulanic acid were statistically significant (P=0.017, 0.06 and 0.0042 respectively).

Table I: Showing the comparative resistance pattern of hemolytic and non-hemolytic isolates of Escherichia coli to various antimicrobial agents.

Drugs	Hemolytic isolates N=22 (26.8%)		Non-hemolytic isolates N=60 (73.2%)		P-value
	Sensitive (%)	Resistant (%)	Sensitive (%)	Resistant (%)	
Ampicillin	2 (9.1%)	20 (90.9%)	0 (0%)	60 (100%)	P=0.06
Amo-clacid	4 (18.2%)	18 (81.8%)	0 (0%)	60 (100%)	P=0.004
Gentamicin	20 (90.9%)	2 (9.1%)	53 (88.3%)	7 (11.7%)	P=1.00
Tetracycline	4 (18.2%)	18 (81.8%)	1 (1.7%)	59 (98.3%)	P=0.017
Nalidixic-acid	15 (68.2%)	7 (31.8%)	36 (60%)	24 (40%)	P=0.61
Ciprofloxacin	15 (68.2%)	7 (31.8%)	36 (60%)	24 (40%)	P=0.61
Pefloxacin	18 (81.8%)	4 (18.2%)	37 (61.7%)	23 (38.3%)	P=0.11
Cotrimoxazole	11 (50%)	11 (50%)	24 (40%)	36 (60%)	P=0.46

Amo-clavid = amoxicillin and clavulanic acid.

Table II: Showing the body fluid distribution of hemolytic isolates of E. coli.

Source of body fluid	No of samples with hemolysis.
Urine	16 (72.7%)
Blood	2 (9.1%)
Stool	4 (18.2%)
Cerebrospinal fluid	Nil
Peritoneal fluid	Nil
Wound swab	Nil

Discussion:

Although several workers have reported various different properties of virulence of *Escherichia coli* strains and their possible risk to health in humans [Wieler, 1998; Olowe, 2003] Hemolysis is one type of virulence factor that assist in the pathogenesis of Escherichia coli both in man and avian [Reingold, 1999]. Expression of cytotoxicity by potential pathogens of *Escherichia coli* was also believe to have been initiated by the presence of hlyA gene, which may be part of Pathogenicity island [Xin-Helai, 1999].

It is not known if resistance to quinolones and loss of haemolysis are caused by common or related mechanisms or if these phenotypes are derived from independent mutations. Most clinical isolates of *E. coli* resistant to quinolones are gyrA mutants [Everett, 1996].The mechanisms responsible for the predominance of non-haemolytic *E. coli* strains among those expressing resistance to quinolones are unknown. Ciprofloxacin-resistant mutants (MIC of ciprofloxacin ranging from 0.03 to > 32 mg/L) derived in vitro from haemolytic-susceptible isolates still produced haemolysis. These mutants are not related to the previously described -haemolysin producers (selected in the presence of nalidixic acid) as they still haemolyse human erythrocytes which agrees with the previous work of Martinez [Martinez, 1998]. The relationship between haemolysin production and resistance to ofloxacin could not be evaluated, as all strains were susceptible to ofloxacin. Our data for tetracycline are similar to those obtained by other authors. But contrary to other authors our isolates showed a significant difference in resistance to Gentamicin among haemolytic and non-haemolytic isolates. In fact, the few gentamicin-resistant strains in our study were from both haemolytic and non-haemolytic. The only difference is that there are more Gentamicin resistance in non-haemolytic than haemolytic, and the degree of resistance is not significantly difference P=1.0 It was initially reported that most clinical isolates of *E. coli* resistant to quinolones are gyrA mutants [Everett, 1996] and it is possible that altered super coiling of DNA in these mutants may affect the expression of genes involved in haemolysis production. Another possibility is the existence of pleiotropic mutations in quinolone-resistant *E. coli* strains that may interfere with the expression or activity of haemolysin, as has recently been reported for mutations affecting the genes involved in lipopolysaccharide synthesis. [Bauer, 1997] Our study shows that haemolysin is becoming pronounced among our clinical isolates especially among the gram negative organisms which have led to increasing development of resistant strains to the common antimicrobial agents that is currently available. Also the study shows that haemolysin is less frequently produced by quinolone-resistant isolates of *E. coli* when compared with the penicillin, tetracycline and co-trimoxazole even though the amino-glycosides have superior sensitivity, with marked reduction in the production of haemolysin compared with the quinolones. It is possible that resistance to quinolones may be indirectly attributable to the cost of the drug which has reduced the drug pressure, consequently decreasing bacterial virulence, this finding agrees with the work of Martinez [Martinez, 1999].

Further testing is required to fully determine hemolysis of *Escherichia coli* in various body fluids as linked with antimicrobial resistance with more emphasis on the current trends of resistance development to the quinolones.

The rates of quinolone resistance reported here are similar to those presented in other studies from Spain, [Daini, 2005; Martinez, 1999] and higher than those of a previous study in our institution, [Olowe et al unpublished communication] confirming the tendency to increased quinolone resistance during recent years. Hariharan et al. have shown that resistance to co-trimoxazole, neomycin and tetracycline in E. coli strains isolated from piglets with diarrhoea was less frequent among strains producing heat-labile enterotoxin (LT) and haemolysin than among those lacking both factors, while the resistance to gentamicin was more frequent in LT-haemolysin producers than among LT-haemolysin non-producers.

Corresponding author:
Olowe OA.
Department of Medical Microbiology and Parasitology,
College of Health Sciences,
Ladoke Akintola University of Technology, Osogbo, Nigeria
E-mail:- olowekunle@yahoo.com
.Mobile phone: - 08033800026- Fax: 035 – 240110.

Reference

1. Daini, OA, Ogbolu, OD, Ogunledun. A. Quinolones resistance and R- plasmid of some gram – negative enteric bacilli. *African Journal of clinical and experimental microbiology* (Jan) **2005,** VOL 6, NOS 1
2. Everett, MJ, Fang Jin, Y., Ricci, V. & Piddock, LJV. Contribution of individual mechanisms to fluoroquinolones resistance in 36 *Escherichia coli* strains isolated from human and animals. *Antimicrobial Agents and Chemotherapy* (1996) **40**, 2380–6
3. Cavalier, SJ, Bohach, GA & Snyder, IS. *Escherichia coli* -haemolysin: characteristics and probable role in Pathogenicity. *Microbiological Reviews.* (1984). **48**, 326–43
4. Walton, JR & Smith, DH. New haemolysin ( ) produced by *Escherichia coli. Journal of Bacteriology.* (1969). **98**, 304–5
5. Beutin, L The different hemolysis of Escherichia coli: *Medical Micr6biology and Immunology.* (Berlin). (1991). 180, 167- 182.
6. Welch, RA & Pellet, S. Transcriptional organization of the *Escherichia coli* haemolysin genes. *Journal of Bacteriology.* (1988) **170**, 1622–30
7. National Committee for Clinical Laboratory Standards. (1997). *Methods for Dilution Susceptibility Tests for Bacteria that Grow Aerobically: Approved Standard M7-A3.* NCCLS, Wayne, PA.
8. Luis Martinez-Martinez., Felipe, Fernandez and Evelio J. Perea: Relationship between haemolysin production to fluoroquinolones among clinical isolates of Escherichia coli: *Journal of antimicrobial chemotherapy:* (1999) 43, 277-279.
9. Wieler LH, Anja Schwanitz, Elke Vieler, Barbara Busse., H, Steinruch, JB. Kaper and Baljer. Virulence properties of shiga-toxin producing Escherichia coli (STEC) strains of serogroup 0118, a major group of STEC pathogens in calves. *Journal of Clinical Microbiology.* (1998). June, 3 (6): 1604- 1607.
10. Olowe OA, Olayemi AB, Eniola, KIT, and Adeyeba AO. Aetiological agents of diarrhea in children under 5 years of age in Osogbo. *African Journal of clinical and experimental microbiology* (2003).4 (3) 62- 66.
11. Reingold J, Starr. N, Maurer J, Lee MD: Identification of a new strains Escherichia coli **she** haemolysin homolog in avian Escherichia coli. *Veterinary microbiology.* (1999) April (1) 66 (2): 125-35.
12. Xin-Helai, Su-Yan Wang and Bernt Eric: Expression of cytotoxicity by potential pathogens in the standard Escherichia coli collection of reference (ECOR) strains. *Microbiology* (1999), 145, 3295-3303
13. Martinez-Martinez, L, Paschal A, Jacoby GA, Quinolones resistance from transferable plasmid. *Lancet* 1998; 351: 277- 279.
14. Bauer, ME. & Welch, RA. Pleiotropic effects of a mutation in *rfaC* on *Escherichia coli* haemolysin. *Infection and Immunity* (1997) **65**, 2218–24
15. Bauer, ME & Welch RA. Characterization of an RTX toxin from enterohemorrhagic E. coli. 0157:H7. *Infectious Immunology*. 1996: 64: 165-171.

Impact Of Industrial Effluents On Quality Of Segment Of Asa River Within An Industrial Estate In Ilorin, Nigeria

ADEKUNLE, Adebayo S.[1] and ENIOLA, I. T. Kehinde[2]

[1] Department of Mechanical Engineering, Faculty of Engineering & Technology, University of Ilorin, Ilorin, Kwara State, Nigeria. adekunlebayo@yahoo.com
[2] Environmental and Public Health Research (EPHR) Laboratory, Department of Microbiology, University of Ilorin, P.M.B. 1515, Ilorin, Kwara State jiket@unilorin.edu.ng

ABSTRACT: The impact of industrial effluent on water quality criteria of a river within Asa Dam industrial estate, Ilorin was investigated. Physicochemical and bacteriological properties of samples of the river were examined to determine the quality and extent of pollution. The effluents were found to cause gross pollution of the river. Total hardness ranged between 51 and 175.5mg/l; while conductivity was between 65 and 318µs. Calcium and Magnesium ions varied between 33.7 and 102.3mg/l, and 3.5 and 57.1mg/l respectively. *E. coli* was found in the samples and the coliforms counts were high. The major sources of pollution were identified to be the direct runoff from the industries and refuse dumps within the estate. [New York Science Journal. 2008;1(1):17-21]. (ISSN: 1554-0200).

KEYWORDS: Pollutants, Surface water, Asa Dam, Nigeria.

Introduction

Industrialization is considered the cornerstone of development strategies due to its significant contribution to the economic growth and human welfare. It has become a yardstick for placing countries in the League of Nations and an index of its political stature (FEPA, 1991). Industrialization, like other human activities that impact on the environment, often results in pollution and degradation. It carries inevitable costs and problems in terms of pollution of the air, water resources and general degradation of the natural environment (Suflita *et al*., 1983; Thomas *et al*., 1992).

Worldwide water bodies are the primary means for disposal of waste, especially the effluents, from industries that are near them. These effluent from industries have a great deal of influence on the pollution of the water body, these effluent can alter the physical, chemical and biological nature of the receiving water body (Sangodoyin, 1991). The initial effect of waste is to degrade the physical quality of the water. Later biological degradation becomes evident in terms of number, variety and organization of the living organisms in the water (Gray, 1989). Often the water bodies readily assimilate waste materials they receive without significant deterioration of some quality criteria; the extent of this is referred to as its assimilative capacity (Fair *et al*., 1971). The input of waste into water bodies therefore does not always impact negatively on aquatic environment because of the self purification property of the water bodies.

Industries turn out wastes which are peculiar in terms of type, volume and frequency depending on the type of industry and population that uses the product (Odumosu, 1992). Industrial waste is the most common source of water pollution in the present day (Ogedengbe and Akinbile, 2004) and it increases yearly due to the fact that industries are increasing because most countries are getting industrialized. The extent of discharge of domestic and industrial waste is such that rivers receiving untreated effluent cannot give dilution necessary for their survival as good quality water sources. The transfer of unfavorable releases from industries is detrimental to human and animal health and safety (Sangodoyin, 1991). There is thus a challenge of providing water in adequate quantity and of required quality to minimize hazards to human health and conserve the water bodies and the environment.

Population explosion, uncontrolled urbanization and industrialization have caused a high rate of waste generation in Nigeria (Rosegrant, 2001). Akpata (1990) pointed out that aquatic pollution problem in Nigeria was increasing in scope and dimension. Olayemi (1994) identified that regular, unregulated indiscriminate dumping of waste into water bodies worsen aquatic pollution. This study is intended to assess the impact of industrial effluents on the surface water at Asa Dam industrial estate and its environs. It also identifies common pollutants in the water. The impact is assessed in term of its physicochemical and bacteriological quality.

Materials and Methods

Study Area

The study carried out within the industrial estate located in Ilorin, North Central Nigeria (8^o 28'N, 4^o 38'E to 8^o 31'N, 4^o 40'E). It houses the major industries in the town: Global soap and Detergent, Unifoam, 7^{up} Bottling Company, Tuyil pharmaceuticals and Nigeria Bottling Company. The study was on Asa River, the major water body in Ilorin, its course enters the southern end of the industrial estate from Asa Dam located south of the estate, and runs northwards through residential areas.

Sample Collection and Analysis

Duplicate grab samples of water were taken from five (5) points on the river: point of entry (PE), three different points on the river within the estate (L_1, L_2, L_3) and point of leaving (PL). Samples were collected using the conventional WHO (2004) methods. The pH of the samples was determined using a pH meter. The colour, turbidity, calcium ion, total hardness, chloride, dissolved oxygen were determined using standard methods. Bacterial count was determined using standard plate count (APHA, 1992). Bacterial isolates were characterized and identified using Cowan and Steel manual (Collines et al., 1989; Barrow and Feltham. 1995).

Results

The pH varied between pH 6.8 and 7.4, the highest pH was recorded at point L_2 and the lowest at PL. Turbidity varied between 4.6 and 189 (NTU), the highest value was obtained at L_2 while the lowest was obtained at PL. The colour varied between 153 and 1913 (Pt – Co), the highest value was obtained at L_2 and the lowest at PE. The temperature ranged between 26- 29^OC. The total hardness varied between 27 and 176 mg/l, Calcium and Magnesium hardness range from 62 to 338mg/l and from 9 to 73 mg/l respectively. The conductivity ranged from 65 to 318 us, with the highest obtained at L_3 and the lowest at PE. Variations in the pH, colour, turbidity, temperature, hardness and conductivity of the Asa River are shown on Table 1.

The total solid content varied between 220 and 670 mg/l; the highest value was obtained at L2 and the lowest at PE. The total suspended solid and total dissolved solids ranged between 172 and 445 mg/l and 48 and 225 mg/l respectively. The dissolved oxygen content ranged from 7 to 8 mg/l. The variations in the total solids, total suspended solids and total dissolved solids as well as the dissolved oxygen content are shown in Figure 1. The total bacterial count ranged between 3.0×10^4 to 7.5×10^4 cfu/ml; the highest values was at L_3 and the lowest at L_1 (Figure 2). Twelve bacterial species were identified: *Bacillus subtilis, Citrobacter diversus, E. coli, Micrococcus albus, Micrococcus luteus, Proteus vulgaris, Pseudomonas aeruginosa, Serratia* sp*, Shigella* sp*, Staphylococcus aureus, Streptococcus bovis* and *Streptococcus faecalis*. Their distribution is shown on Table 2.

Table 1: Physicochemical Characteristics of Asa Stream within the Estate

Parameters measured	PE	L_1	L_2	L_3	PL
pH	7.1	7.3	7.4	7.2	6.8
Colour (Pt-Co)	153	211	1913	1740	182
Turbidity (N.T.U)	4.6	8	189	162	1.5
Temperature (^oC)	28	26	27	29	27
Total Hardness (mg/l)	27	51	99	176	51
Calcium Hardness (mg/l)	16	21	74	85	21
Magnesium Hardness (mg/l)	12	30	25	91	30
Calcium ion (mg/l)	62	84	294	338	84
Magnesium ion(mg/l)	9	24	20	73	24
Conductivity (us)	65	73	299	318	85
Chloride (mg/l)	2	2	69	107	12

PE= Point of Entrance to Asa Dam Industrial Estate. L_1= Stream Location One in the Industrial Estate.

L_2= Stream Location Two in the Industrial Estate. L_3= Stream Location Three in the Industrial Estate.

PL= Point of Leaving Asa Dam Industrial Estate.

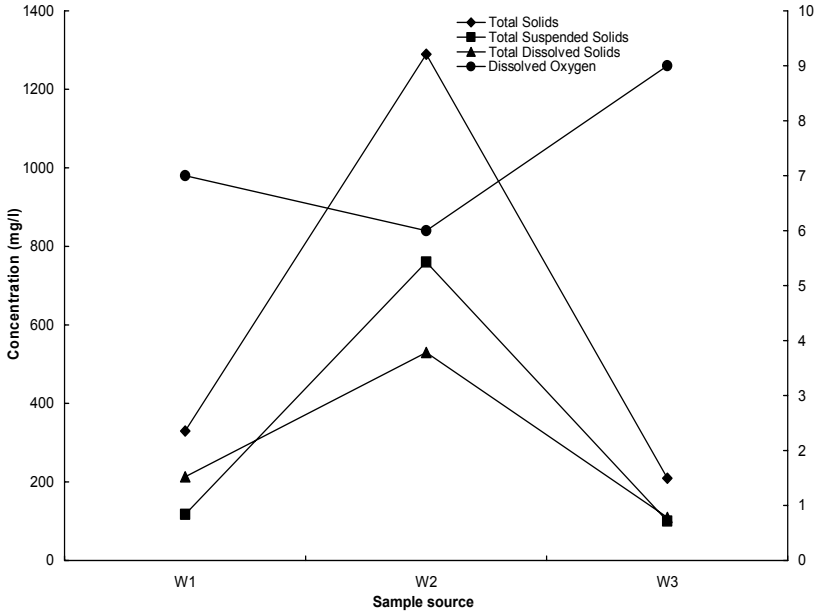

Figure 1. Variations in the total solids, total suspended solids, total dissolved solids as and dissolved oxygen content

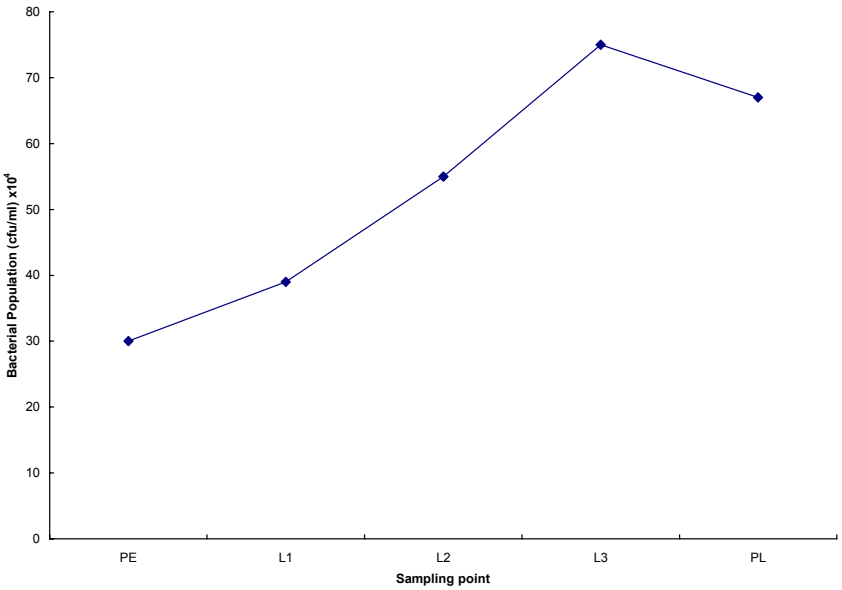

Figure 2. Variation in Bacterial Population in Asa River within the industrial Estate

Table 2: Identity and Distribution of bacteria isolated from Asa Stream within the Industrial Estate

Organisms	PE	L_1	L_2	L_3	PL
Bacillus subtilis	+	+	+	+	+
Citrobacter diversus	+	+	+	+	+
E. coli	+	+	+	+	+
Micrococcus albus	+	-	-	+	+
Micrococcus luteus	+	-	+	+	+
Proteus vulgaris	+	+	+	+	+
Pseudomonas aeruginosa	+	+	+	+	+
Serratia sp	+	-	+	+	+
Shigella sp	+	-	+	+	+
Staphylococcus aureus	+	+	+	+	+
Streptococcus bovis	+	-	-	+	+
Streptococcus faecalis	+	-	+	+	+

PE= Point of Entrance to Asa Dam Industrial Estate. L_1= Stream Location One in the Industrial Estate.
L_2= Stream Location Two in the Industrial Estate. L_3= Stream Location Three in the Industrial Estate.
PL= Point of Leaving Asa Dam Industrial Estate.

DISCUSSION

The higher concentrations of most of the measured parameters at points within the estate over values at the point of entry to the various points within the estate are suggestive of input of materials within the estate. The turbidity is directly related to the amount of materials present in the water, this is observed to be highest at the point within the estate after input of wastes from the industries. This is further buttressed by the higher concentrations of total solids, total dissolved solids and total suspended solids, which signify input of materials. Increased concentration of the measured parameters is probably due to the effect of the pollutants released by the industries into the water body.

The divalent metallic cations: Calcium and Magnesium contribute to the total hardness of the water (51 to 176mg/l). The water is hard and is thus largely unsuitable for direct use by communities that use it for laundry work and bathing. Turbidity of the water increased greatly from 4.6 N.T.U at the point of entry to 189 N.T.U for the water sample L_2 within the estate; this indicates an increase in the concentration of suspended matters in the water sample. The subsequent reduction to 1.5N.T.U at the point of leaving is indicative of self purification by the river (Gray 1989).

The river showed high bacterial count as is characteristic of water body receiving organic pollutant (Olayemi, 1994). The presence of *E.coli* is a definite indication of faecal contamination (WHO, 2004). The presence of the organism shows that the river can not be used directly as source of drinking water; it ranks among water that requires auxiliary treatment. In addition some of the organisms encountered in the water are potential pathogens contrary to the WHO (2004) recommendation that drinking water should be free of pathogens.

The presence of some of the organisms suggests that materials were being added to the water from other sources apart from the effluent. This is likely to be the refuse dumps within the estate. The dumps are exposed and hence can be washed into the river during rains or material be carried from it to the water during heavy winds. Summarily, water from Asa River requires elaborate treatment before it could be suitable for domestic purposes.

Correspondence to:
ADEKUNLE, Adebayo S.[1] and [2]
Department of Mechanical Engineering,
Faculty of Engineering & Technology,
University of Ilorin, Ilorin, Kwara State, Nigeria.
adekunlebayo@yahoo.com

ENIOLA, I. T. Kehinde
Environmental and Public Health Research (EPHR) Laboratory,

Department of Microbiology,
University of Ilorin,
P.M.B. 1515, Ilorin, Kwara State
jiket@unilorin.edu.ng

Received: 11/9/2007

REFERENCES

1. Akpata T. V. I. (1990) *Pollution Flora of Some Wetlands in Nigeria*. Nigerian Wetlands. Emmi Press, Ibadan, pp 130–137.
2. Barrow, G. I. and Feltham, R. K. A. (1995). *Cowan and Steel's Manual for the identification of Medical Bacteria*. 3rd Edition, Cambridge University Press.
3. Collins, C. H., Lyne, P.M. and Grange, J. M. (1989). Collins and Lyne's Microbiological Methods (6th Edition). Butterworth and Co. Ltd. London.
4. Federal Environmental Protection Agency (1991). Guideline and Standard for Environmental Pollution Control in Nigeria. FG Press 238pp.
5. Gray, N. F. (1989) *Biology of Water Treatment*. Oxford University Press, New York.
6. Ogedengbe, K. and Akinbile, C. O. (2004), "Impact Of Industrial Pollutants on Quality of Ground and Surface Waters at Oluyole Industrial Estate, Ibadan, Nigeria". Nigeria Journal of Technological Development, 4(2) 139-144.
7. Odumosu, A. O. T. (1992). Management of Liquid industrial wastes. Paper presented at a seminar on Industrial waste management, July 1. Inter match, Lagos 6pp.
8. Olayemi, A. B. (1994). Bacteriological water assessment of an urban river in Nigeria. *Intern. J. Environ. Health Res.* 4:156-164.
9. Rosegrant, M. (2001), "Dealing With Water Scarcity in the 21st Century in the Unfinished Agenda". (Per pinstrup Andersen and Rajul Pandya-Lorch, Eds), 1st edition, International Food Policy Research Institute, IPFRI, Washington, 145-150.
10. Sangodoyin, A.Y. (1991), "Groundwater and Surface Water Pollution by Open Refuse Dump in Ibadan, Nigeria". Journal of Discovery and Innovations, 3 (1) 24-31.
11. Suflita, J. M., Robinson, J. M., and Tiedje, J. M. (1983). Kinetics of Microbial dehalogenation of Haloaromatic substrates in methanogenic Environment. Applied and Environmental Microbiology 45(5) 1466- 1473
12. Thomas, J. M. Ward, C. H., Raymond, R. L. Wilson, J. T. and Lohehr, R. C. (1992). Bioremediation. In Encyclopedia of Microbiology I (J. Lederberg ed.) Academic Press London. 369-377.
13. World Health Organization (2004). World Health Organization guidelines for drinking water quality (3rd Edition). Geneva, Switerland..
14. American Public Health Association: APHA (1992). Water Pollution methods for the Examination of Water and Waste water (18th Edition) Washington D. C. 1437.

Amides as antimicrobial agents

Raymond C.Jagessar [1]*, Davendra Rampersaud [2]

*[1]Lecturer, Department of Chemistry, University of Guyana, South America
[2] Microbiologist, St. Joseph Mercy hospital, Parade Street, Georgetown, Guyana, South America.

raymondjagessar@yahoo.com

Abstract: The antimicrobial activities of amides: p-bromoacetanilide, acetanilide, nitrobenzamide and benzamide were investigated using the Stokes Disc diffusion sensitivity technique and the pour plate method. All compounds with the exception of benzamide exhibited both antibacterial and antifungal activities. Furthermore, the presence of nitro and bromo substituent on the phenyl ring seem to augment the antimicrobial activity. [New York Science Journal. 2008;1(1):22-26]. (ISSN: 1554-0200).

Keywords: Amides, Antimicrobial activity, Stokes Disc sensitivity technique, Pour Plate method.

1.0 Introduction:

Amides, RCONHR' are known to play a pivitol role in molecular recognition, being important components in Supramolecular chemical anion sensors[1-3] technology. Furthermore, in nature, the selective binding for substrates such as anion is achieved via the positional alignment of the amide hydrogen bonds[3].While plant extracts[5] and isolated pure natural products[6,7] have been used for antimicrobial activities, there are few reports of amides as antimicrobial agents[8,9].

This paper focuses on the antimicrobial activity of commercially available Aldrich amides: acetanilide (1), p-bromoacetanilide (2), benzamide (3) and nitrobenzamide (4), Fig 1.0.

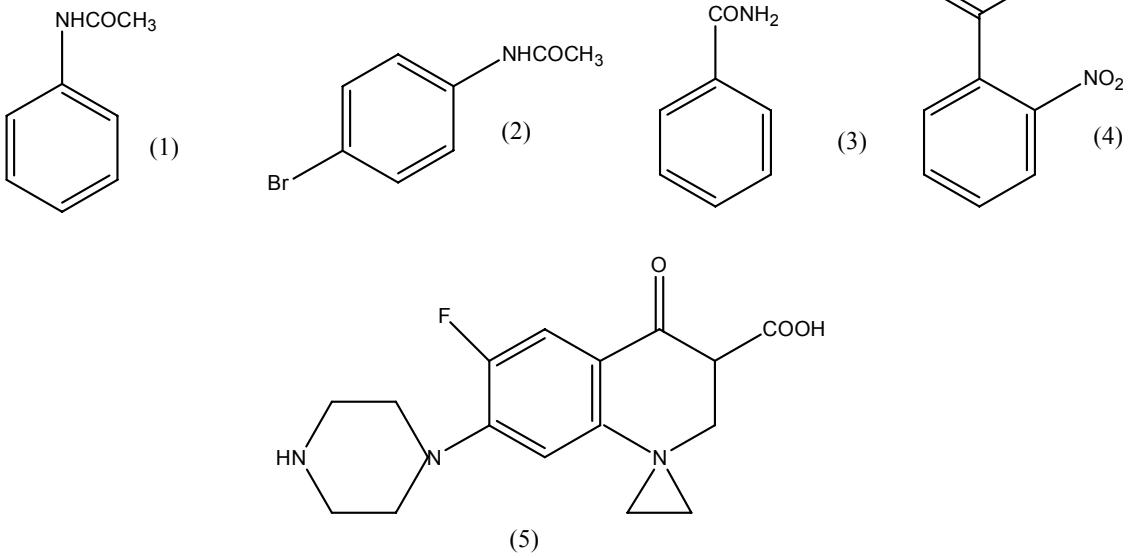

Fig. 1.0

2.0. Experiments:

2.1: Reagents and materials:

The amides, solvents and $BaCl_2.2H_2O$ were purchased from Aldrich. The antibiotic Ciprofloxacin and nystatin, Mueller Hinton agar, agar plates and microbial discs were purchased from the International Pharmacy Association in Guyana. Bacterial and fungal culture were obtained from Mercy hospital as necessary.

2.2. Preparation of Amide solution:

The amides were made to the appropriate concentration of 200 mg/ml in dichloromethane in a 25 ml round bottom flask and was sterilized by filtration through a 0.45 um membrane filter.

2.3 Preparation of Turbidity/opacity Standard (0.5 Mc Farland)

1% v/v solution of sulphuric acid was prepared by adding 1 ml of concentrated H_2SO_4 to 99 ml of distilled water and was mixed well.1.175% w/v solution of barium chloride was prepared ($BaCl_2.2H_2O$) by dissolving 2.35 g of dihydrate barium chloride ($BaCl_2.2H_2O$) in 200 ml of distilled water and was mixed well. To make the turbidity standard, 0.5 ml of the barium chloride solution was added to 99.5 ml of H_2SO_4 solution and was mixed thoroughly.The standard solution was dispensed into screw cap tubes as the same type as those for the preparation of the test and control inocula.The tubes were tightly sealed and stored in a dark room at room temperature (28-30ºC). The turbidity was vigorously agitated on a mechanical vortex mixer.

2.3. Source of microorganism:

For the bacterial organisms, both gram positive and gram negative bacteria were used. Gram positive and gram negative bacteria can be differentiated in the physical appearance of their cell envelopes. Gram positive and Gram negative bacteria used were *Escherichia coli* (ATCC 25922) and *Staphylococcus aureus* (ATCC 25923) respectively. For the fungi, yeast of the *Candida albicans* (ATCC 1023) species were investigated. These microorganisms were stored in a refrigerator at the microbiology laboratory of the hospital.

2.4. Screening for Antimicrobial activities: Stokes Disc diffusion sensitivity technique.

Antimicrobial activities were investigated using Stokes Disc diffusion sensitivity and the pour plate method.Using Stokes Disc diffusion sensitivity testing technique[4] , an inoculum containing bacterial or yeast cells was applied on Muller-Hinton agar plates. On each plate, a reference or control antibiotic ciprofloxacin (CIPRO), 1–cyclopropyl-6-fluoro-1,4-dihydro-4-oxo-7-(1-piperazinyl)-3-quinolinecarboxylic acid (5) was also applied.The reference antibiotic disc contained 10mg of antibiotic/disc. For fungal tests, nystatin was used. With the above testing technique, each disc was impregnated with the anticipated antimicrobial amide at appropriate concentration of 200 mg/ml using a microlitre syringe. This was then placed on a plate of sensitivity testing Mueller Hinton agar which was then incubated with the test organism:Bacteria/fungi. Incubation was done at 37ºC for 24 hr and 48 hr for the bacteria and *Candida albicans* species respectively. The antimicrobial compound diffuses from the disc into the medium. Following overnight incubation, the culture was examined for areas of no growth around the disc (zone of inhibition). The radius of the inhibition zone was measured from the edge of the disc to the edge of the zone.The end point of inhibition is where growth starts. Larger the inhibition zone diameter, greater is the antimicrobial activities. It is anticipated through the antimicrobial activity of amide, no area of growth will be induced around the disc.Bacteria or fungal strains sensitive to the antimicrobial are inhibited at a distance from the disc whereas resistant strains grow up to the edge of the disc.

2.5. Pour Plate Method.

With the pour plate method, 1 ml of microorganism (bacteria or fungi) was first tested against 1 ml of the amide solution i.e a 1:1 ratio of the microorganism to amide.This was followed with varying dilution of amide. This been 1:5, 1:10, 1:20 and 1:40 microorganism: amide concentration. The microorganism was placed in sterile water and was compared against the 1.0 Mc Farland standard so as to ensure that the turbidity exactly matches that of the standard. The density of the made up solution could be

adjusted either by (i) adding more colonies or (ii) adding more sterile water. For each ratio, the solution containing the microorganism and the amide solution were placed in vials and shaken vigorously so as to ensure a uniform mixture.

After the made up (adding water to the agar), nutrient agar was placed in the autoclave at 120^{o}C for one and half hour, taken out and left to semi cool in a sterilized environment and then poured into 100 mm sterile glass plates with an even depth of 4mm on a level surface The mixture of microorganism and amide solution was vigourously shaken and then placed into the liquid, almost cool agar. A sterile glass rod was used to uniformly stir the mixture into the nutrient agar and left to harden or solidify in the glass plate. While this process is taking place, a 96% alcohol flame was used and the environment was sterilized with bleach and alcohol.

The inoculated plates were incubated for 48hrs at 37˚C in an inverted position (lid on bottom) to prevent collection of condensation on the agar surface. Unless the surface is dry, it will be difficult to obtain discrete surface colonies. The plates were examined for the appearance of individual colonies growing throughout the agar medium. The number of colonies were counted so as to determine how effective the amides were antibacterial and antifungal.

3.0. Results and Discussion: Interesting results were obtained as shown in **Table 1.0 – 5.0**.

Table 1.0 Antimicrobial activity of amides as shown by the inhibition zone diameter.

Gram-negative Bacteria, Area of inhibition.	**Gram-positive Bacteria, Area of inhibition.**	**Compounds (1)-(4)**	**Yeast (*candida* species) Area of inhibition.**	***Control disc***
17 mm	15 mm	Compound 1	12 mm	22 mm
21 mm	19 mm	Compound 2	11 mm	21 mm
No inhibition	No inhibition	Compound 3	No inhibition	19 mm
22 mm	17 mm	Compound 4	14 mm	22 mm

Compound (1), acetanilide and compound (2) induced an inhibition zone of 15 mm and 19 mm for gram positive bacteria, *Escherichia coli* respectively whereas inhibition zone of 17 mm and 21 mm were observed for compounds (1) and (2) against gram negative bacteria, *Staphylococcus aureus* respectively. For compound (4), nitrobenzamide, inhibition zone of 17 mm and 22 mm were obtained against gram positive and gram negative bacteria respectively. Compound (3), benzamide produced no inhibition zone on both gram positive and gram negative bacteria. Thus, compound (3) cannot be used as an antimicrobial compound. Both compounds (2) and (4) with electron withdrawing groups such as bromo and nitro exhibit a greater degree of inhibition against bacteria. For example, compound (2) and (4) induced zones of inhibition of 21mm and 22mm respectively against gram negative bacteria. Compound (1), (2) and (4) induced a smaller zone of inhibition against the fungal species, *candida albicans*. These been 12 mm, 11mm and 14 mm for compound (1), (2) and (4) respectively. It is interesting to note that compound (4) bearing a nitro group seem to produce the largest inhibition against gram negative bacteria and fungal strain. Again compound (3) produce no degree of inhibition on the fungal strain. These results are all summarized in Table 1.0. Pour plate results are summarized in Table 2.0-5.0.

Antimicrobial activity of amides as investigated using the pour plate method.

Table 2.0. compound 1.0

Bacteria	Fungi	Time(hrs)	Dilution(microorganism:amide)	Observations
S. aureus	*C.albicans*	48	1:1	No organism grown
S. aureus	*C.albicans*	48	1:5	No organism grown
S.aureus	*C.abicans*	48	1:10	No organism grown
S.aureus	*C.albicans*	48	1:20	Few colonies seen
S.aureus	*C.albicans*	48	1:40	Moderate amount of colonies seen

Table 3.0, **Compound 2**.

Bacteria	Fungi	Time (hrs)	Dilution (microorganism:amide)	Observations
S. aureus	*C.albicans*	48	1:1	No organism grown
S. aureus	*C.albicans*	48	1:5	No organism grown
S.aureus	*C.abicans*	48	1:10	No organism grown
S.aureus	*C.albicans*	48	1:20	Moderate colonies seen
S.aureus	*C.albicans*	48	1:40	Moderate colonies seen

Table 4.0. **Compound 3**.

Bacteria	Fungi	Time (hrs)	Dilution (microorganism:amide)	Observations
S. aureus	*C.albicans*	48	1:1	Few colonies seen
S. aureus	*C.albicans*	48	1:5	Few colonies seen
S.aureus	*C.abicans*	48	1:10	Moderate colonies seen
S.aureus	*C.albicans*	48	1:20	Large colonies seen
S.aureus	*C.albicans*	48	1:40	Large colonies seen

Table 5.0. **Compound 4.0**

Bacteria	Fungi	Time (hrs)	Dilution (microorganism:amide)	Observations
S. aureus	*C.albicans*	48	1:1	No organism grown
S. aureus	*C.albicans*	48	1:5	No organism grown
S.aureus	*C.abicans*	48	1:10	No organism grown
S.aureus	*C.albicans*	48	1:20	Few colonies seen
S.aureus	*C.albicans*	48	1:40	Moderate amount of colonies seen

The pour plate method indicates that as the concentration of the amide decrease (increasing dilutions) whilst the concentration of microorganism remaining constant, the number of colonies increase i.e the antimicrobial properties of the amide decrease with decreasing concentration of the amide.

All compounds show their strongest antimicrobial activities (i.e no organism growth or zero colonies) when the ratio of microorganism to amide is 1:1 and 1:5, Table, 2-5 Compound (1), (2) and (4) showed no organism growth at microorganism: amide ratio of 1:1, 1:5 and 1:10. With microorganism:amide ratio of 1:20 and 1:40, compound (1), (2) and (4) showed identical results. Thus, the results obtained via the pour plate method mirror that obtained via the disc diffusion method for compound (1), (2) and (4). Also, the pour plate method results for compound (3) also mirror those obtained via the disc diffusion method. For compound (3), colonies were seen at micro organism/amide ratio of 1:5, 1:10, 1:20, 1:40. These been few, moderate, large and large. With the exception of (3), no colonies were seen for

compound (1), (2) and (4) at microorganism:amide ratio of 1:1. These results strongly suggest that compound (3), benzamide, clearly is not an antimicrobial.

Conclusion:

In conclusion, the results obtained via the the disc diffusion and pour plate method support each other. Thus, based on the above, compounds (1), (2) and (4) can be used as antibacterial agents against gram positive bacteria and gram negative bacteria and as an antifungal agents against yeast or useful in the future design of drugs. It is anticipated that well designed macrocyclic amides will produce more potent results.

Acknowledgement: We thank the University of Guyana, Department of Chemistry for funding and the use of the microbiology laboratory at St.Joseph Mercy hospital, Georgetown, Guyana.

Correspondence to:
Dr.Raymond C. Jagessar,
Department of Chemistry,
University of Guyana,
Turkeyen Campus,
Greater Georgetown,
South America
Email: raymondjagessar@yahoo.com

References:

1. P.D.Beer, M.G.B.Drew, C.Hazelwood, D.Hesek, J.Hodacova, S.E.Stokes, *J. hem. oc. hem. ommun*. 1993, 229.
2. P.D.Beer, M.G.B.Drew, D.Hesek, R.Jagessar, *J.Chem.Soc., Chem.Commun*., 1995, 1187.
3. P.D.Beer, M.G.B.Drew, R.Jagessar, *J.Chem.Soc., Dalton Trans*., 1997, 881-886.
4. Stokes, J.E., and Ridgway, G.L. *Clinical Bacteriology*, Ch.7, Edward Arnold Publishers, 5th edition, 1980.
5. Rojas, A., L. Hernandez, R. Pereda-Miranda, R.Mata. 1992. Screening for antimicrobial activity of crude drug extracts and pure natural products from Mexican medicinal plants. *J. Ethnopharmacol*. 35: 275-283.
6. Silva, O., A.Duarte, J.Cabrita, M.Pimentel, A. Diniz and E. Gomes. 1996. Antimicrobial activity of Guinea-Bissau traditional remedies. *J.Ethnopharmacol*. 50: 55-59.
7. Navaro, V., M.L.Villarreal, G.Rojas, X. Lozoya, J. *Ethanopharmacology*, 1996,143-147.
8. B. Narasimhan, D. Belsare, A.Dhake, *Eur.J.Med. Chem*. 2004; 39(10): 827-34.
9. B.Priya, S.N Swamy, K.S. Rangapa. *Bio.Org.Med.Chem*. 2005.13(7).

Anatomical Features of the Roots and Leaves of *Hibiscus Rosa-Sinensis* and *Abelmoschus* Esculenta

Nwachukwu C.U. *, Mbagwu F.N. **, Iwu Jane Ijeoma ***

* Alvan Ikoku College of Education., Owerri, Imo State, Dept. of Biology.
** Imo State University., Owerri, Imo State, Dept. of Plant Science and Biotechnology.
*** Dept. of Plant Science and Biotechnology, Imo State University

ABSTRACT: Roots and leaves anatomical features of *Hibiscus rosa sinensis* and *Abelmoschus esculenta* found in different parts of Imo State Nigeria were studied with the aid of a light microscope. The aim is to ascertain the taxonomic importance of roots and leaf anatomical features in establishing intraspecific relationship among these taxa. Result obtained showed presence of long chain and numerous epidermal calls in *Hibiscus rosa seninsis* while they are short chains small and numerous in *Abelmoschus esculenta*. Similarly the xylem vessels are numerous and circular in *Hibiscus rosa seninsis* while they are few and cuboidal in *Abelmoschus esculenta*. Furthermore in the leaf anatomy of *Hibiscus rosa seninsis* the central cells are large with dark stained calcium oxalate crystala while in *Abelmoschus esculenta* the mesophyll layer is made up of 3 – 4 layers of regular shaped cells. An analysis of the root and leave anatomical features studied showed that these taxa possessed vital characteristic that could be attached to other taxonomic information and used in their description hence the biosystematic implication of this finding have been discussed in the light of the current literature. [New York Science Journal. 2008;1(1):27-32]. (ISSN: 1554-0200).

KEYWORDS: Anatomy; *Hibiscus rosa sinensis; Abelmoschus esculenta;* Malvaceae

INTRODUCTION

The plants *Hibiscus rosa sinensis* and *Abelmoschus esculenta* belong to the Subkingdom *Tracheobionta* (vascular plants); Division magnoliopsida and family malvaceae Tiadak, 1979, Green sill 1976 and stern 2001).

The family malvacaea is one of the most important families consisting of 82 genera and 1,500 species with Hibiscus over 200 species, sida 200 species, ablition 190 species and malva 40 species. The family is world wide in distribution but is mostly represented in the tropical and subtropical region. Members may be herbs, shrubs or trees with mucilage.

Leaves of the family may be simple, alternate, stipulate, petiolate, palmatified (as in cotton) or multifoliate as in silk cotton. Inflorescence is solitary as in cymes though occasional they are in panicle raceme, regular polypetalous, bisexual, hypogynous, conspicuously mycilaginous, with a whorl of bracteoles known as epicalyx except in (Ablition and sida). The pollen grains are large and spiny; placentation is axile with the style passing through the staminal tube.

The fruit could be capsule in the cotton plant or a schizocarp as in Abutilon and Althaea rosea, the seed is endospermic (Vidyarthi and tripathi, 2002).

Hibiscus rosa sinensis is an evergreen shrub growing up to 2.5 inches high. It is a tender perennial plant and it prefers light (sandy) medium (loamy) and heavy (clay) soils. The plant prefers neutral and basic soils and cannot grow in shade (Burkill, 1995). Similarly *Abelmoschus esculenta* grows best in warm climates with a minimum temperature of 18^{o}c. The plant is known and called different names in Nigeria such as Okra (Igbo name) Etighi in Efik, Kabewa in Hausa and Ila in Yoruba land (Harpert 1977). It can grow up to 1.8m in height depending on the variety as long as the soil is not water logged. The stem is erect and hairy and leaves are also hairy with long leaf stalk (Azah 1968). *Hibiscus rosa sinensis* and *Abelmoschus esculenta* have been found to possess wide range of uses to mankind ranging from economic, medicinal and agronomic. The young leaves *Hibiscus rosa sinensis* are most times used as substitute for spinach in most parts of eastern Nigeria. The fibre is used for coarse fabrics, nets and paper making (Akroroda 1985). The essential oil in the seed has a strong antispasmodic effect and has been successfully used to ease the pains for intestine pile or kidney colic. The flower extract is used internally in the treatment of excessive and painful menstruation, veneral diseases and to promote hair growth (Burkill 1995). *Abelmoschus esculenta* on the other hand is also used for variety of purposes e.g., the stem is used as paper manufacturing, the unripe fruits are used as vegetable while the sauces or soup used in active cooking known as palaver in Sireerleone is got from the leaves and fruits of *Abelmoschus esculenta* (Greenisill, 1976).

Despite the numerous economic, medicinal and agronomic importance of *Hibiscus rosa sinensis* and *Abelmoschus esculenta*, there is absence of a clear taxonomic criteria especially in root and leaf anatomy to delineate these two taxa. The probable lack of anatomical (roots and leaf). Information on these two taxa does not make them irrelevant considering the various roles anatomy has played in taxonomic delieanation of species (Schewell 1957). Contributions on the anatomy of plants of various areas includes the works of Nwachukwu and Mbagwu, 2007 in Eight *Indigofera* species, Mbagwu and Edeoga in Vigna, Okoli in Telfairia. Further contributions of anatomical features in systematics are the works of Curcibitacaea and Metcalfe and chalk 1950 in selected Dicotyledons.

This investigation therefore reports the root and leaf anatomical characters in *Hibiscus rosa sinensis* and *Abelmoschus esculenta* as observed with a light microscope. This investigation further assesses the relevance of these anatomical features (root and leaf) in deducing similarities and differences among the taxa studied as well as utilizing the anatomical characters obtained from these two taxa for the systematic grouping and characterization of the two taxa.

Materials and Methods

Section of mature and fresh roots and leaves of Hibiscus rosa sinensis not longer than 1 x0.5cm each of the two taxa colleted from the cultural garden of IMSU and Songhi farms Nekede Owerri-West Local Government in Imo State were put into labeled vials and fixed in FAA (1:1:18). 40% formaldehyde, 70% ethanol v/v for at least 72 hours. These were then rinsed in several changes of distilled water and passed through different alcohol series (30, 50, 95 and 100%). The dehydrated materials were infiltrated with wax by passing through different proportions of alcohol and chloroform gradually replaced the alcohol; pure chloroform and wax were added in the bottles. The idea was to gradually infiltrate the tissues with wax which would be hard enough to microtomy. The metal mould, were later removed and the specimens within the wax cube were trimmed and section on Reichert rotary microtome at 20 – 24cm. The ribbons were placed on clean slides smeared with a film Haupt's albumen and allowed to dry and drops of water added prior to mounting.

Drops of alcian blue were put on the specimen for five minutes, washed off with water and counter stained with safranin for two minutes, then dehydrated in a series of alcohol 50%, 70%, 80%, 90%, xylene/absolute alcohol solution (i.e. 1:3 and 1:1 v/v) and pure xylene at intervals of a few seconds and mounted in Canada Balsam. Photomicrographs were taken from the slides using a Leitz Wetzlar artholus microscope fitted with a vivitar v-335 cmera.

Result

The anatomical features of the root and leaf of *Hibiscus rosa sinensis* and *Abelmoschus esculenta* investigated are summarized in Tables 1 and 2 and illustrated in (Figs 1a – b and 2a – b). The root epidermal layer of the two taxa studied shows that the epidermal cells are in form of short chains (kioned) small and numerous in *Hibiscus rosa sinensis* while they are of long chains big and numerous in *Abelmoschus esculenta* (Fig. 1a – b). Similarly the cortex tissue show the presence of small sized parenchyma cells in *Hibiscus rosa sinensis* while in *Abelmoschus esculenta* the parenchyma cells are bigger in size. Both taxa show presence of angular collenchyma. The xylem vessels are numerous circular in shape and are radially grouped in *Hibiscus rosa sinensis* while they are few and cuboidal in shape in *Abelmoschus esculenta* (Fig. 1a – b). The root anatomy of both taxa studied shows presence of calcium oxalate crystal in the cortex region of the two taxa though the crystal are not stained in *Hibiscus rosa sinensis* while they are dark stained in *Abelmoschus esculenta* (Fig. 1a – b).

Furthermore the leaf anatomy (Fig. 2a – b) of both taxa studied show variations in *Hibiscus rosa sinensis*, the mesophyll which is confined to the center of the lamina is composed of 4 – 6 epidermal layers of cells and are irregular in shape while in *Abelmoschus esculenta* the mesophyll layer though confined to the centre of the lamina is composed of 3 – 4 epidermal layers of cells and are regular in shape (Fig. 2a – b). There are also well developed selerenchymatous and parenchymatous cells and calcium oxalate crystal in the leaves of the two taxa studied.

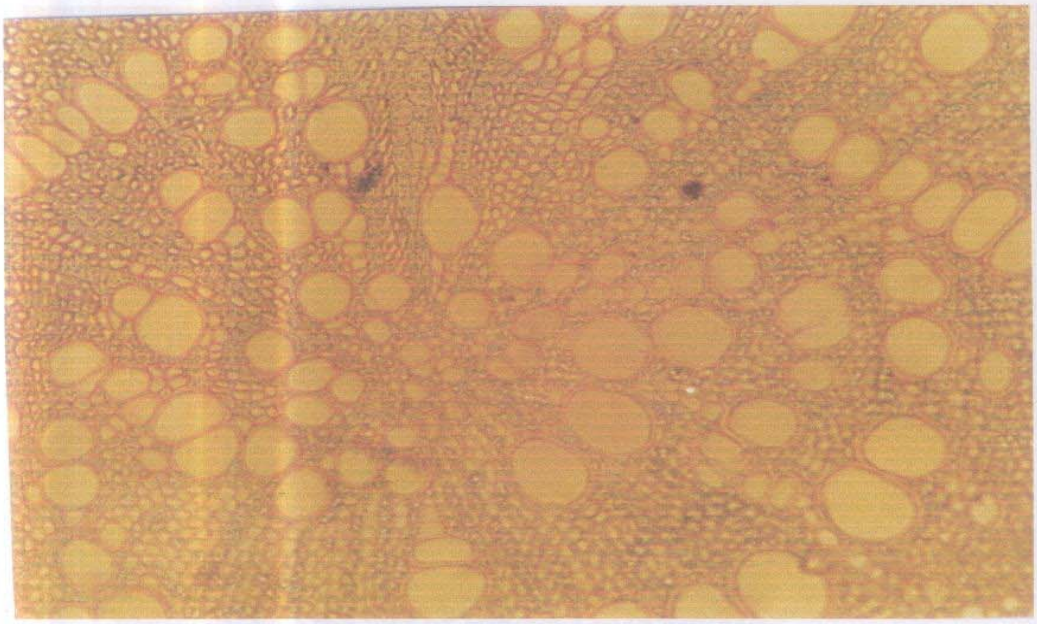

Fig 1a: T.S of the Root of Hibiscus rosa senensis

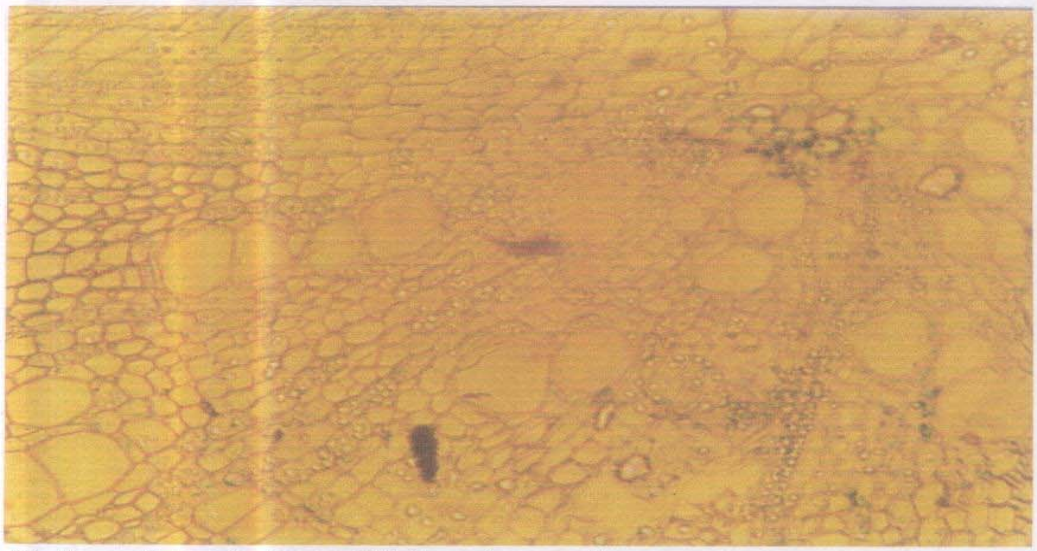

Fig 1b: T.S of the Root of Abelmoschus esculentus

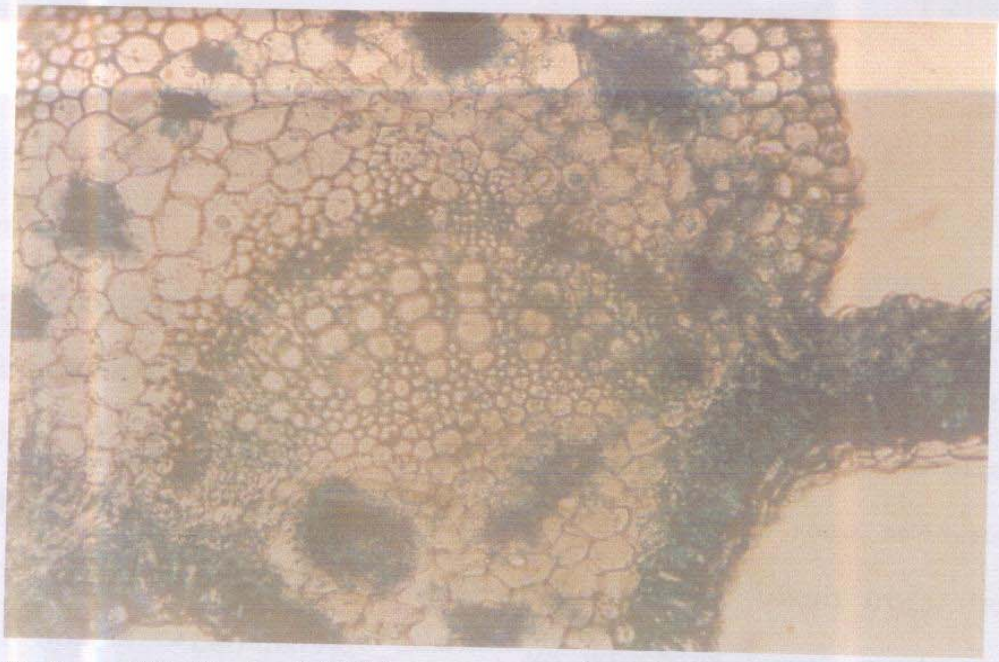

Fig 2a: T.S of the Leaf of Hibiscus rosa senensis

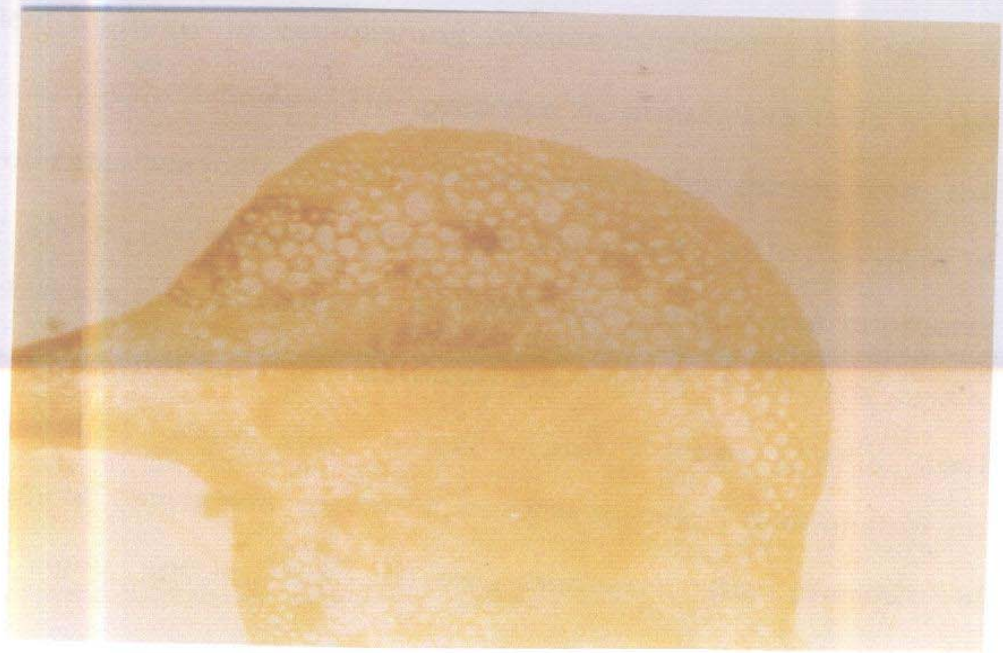

Fig 2b: T.S of the Leaf of Abelmosclus esculentus

Table 1: Anatomical Characters of the Roots of the two taxa studied.

Characters	*Hibiscus rosa senensis*	*Abelmoschus esculenta*
Epidermal cells	Short chains, small	Long chain, big
Parenchyma cells	Small in size	Big in size
Number of crystals	3	2
Xylem vessels	Numerous, circular in shape	Few, cuboidal in shape
Collenchyma cells	Angular	Present Angular
Xylem fibres	Present	Absent
Metaxylem	Many	Few
Pith	Present	Present
Phloem	Present	Present
Stains of Oxalate	No stain of Oxalate	Dark stain of Oxalate

Table 2 Anatomical Characters of the Leaves of the two taxa studied.

Characters	*Hibiscus rosa senensis*	*Abelmoschus esculenta*
Nature of central cells	Large with dark stained contents of Calcium Oxalate	Large without stains of Calcium Oxalate
Mesophyll	4 – 6 layers with irregular shape	3 – 4 layers with regular shapes
Xylem vessels	Very big and numerous	Very small and few
Sclerenchymatous and Parenchymatous	Well developed	Well developed
Crystals	Present	Present
Crystals	Present	Present
Phloem	Present	Present

Discussion

The *Hibiscus rosa sinensis* and *Abelmoschus* taxa investigated possesses features in their root and leaf anatomy that could be vital in their description and in their taxonomy. The variation in the epidermal cells: Short chains, small and numerous in *Hibiscus rosa esculentus* and long chains, big and numerous in *Abelmoschus* could be used to separate these two taxa. The mesophyll layer which is irregular comprised of 4 - 6 layers in *Hibiscus rosa sinensis* and regular with 3 - 4 layer in *Abelmoschus esculenta* could further strengthen the difference among the two taxa (Fig. 1a - b and Fig. 2a - b) This observation is inline with the work of Okoli (1987), Edeoga and Okoli (1997, 2001) who used both the root and leaf anatomical features in the family Cucurbitaceae and Dioscoraceae in establishing relationship among taxa. The reported small sized paranchyma cells of root anatomy in *Hibiscus rosa sinensis* and bigger sized cell in *Abelmoschus esculenta* is not strange since Nwachukwu 2005 had reported that cells of parenchyma vary greatly in size, shape and could also be elongated or lobed. The parenchyma cells are metabolically active and are modified for photosynthetic and secretary function. The nature of xylem vessels in both taxa, are very big, numerous and circular in shape in *Hibiscus rosa sinensis* further separates it from the very small few and ovoid in shape xylem cells in *Abelmoschus esculenta*. This observation is equally significant since no previous work has been reported on the root and leaf of the two taxa studied. Hence this variation in vascular bundle types among the taxa could be used to distinguish them (Fig. 1a - b) similarly variations in

other features of the roots and leaves of the plants studied Table 1 and 2 could further be used to separate this taxa, while the presence of Protoxylem, Metaxylem, Crystals, Angular collenchyma cells in both taxa studied are typical of most dicot plants. This study is therefore based on the principles that root and leaf anatomy has played a major role in the identification, characterization and delimination of plants. Hence the need to incorporate information from root and leaf anatomy with data derived from other botanical disciplines remains vital when formulating conclusions on the systematic of the taxa investigated.

Corresponding Author:
Nwachukwu C.U.
Dept. of Biology,
Alavan ikoku College of Education,
P.M.B 1033 Owerri, Imo State, Nigeria.
E-mail Address: nwachukwucu2005@yahoo.co.uk

REFERENCES

1. Akorod M.O (1985) Edible fruits productivity and harvest duration of *Abelmoschus esculenta* in Southern Nigeria Nihort, Ibadan, Nigeria Pp. 110 - 113.
2. Azah Y.E.A (1968) Applied agronomic research on field food crops in Northern Ghana, Food and Agricultural Organization. NO. 2596:5 - 8.
3. Burkill H.M (1995) The useful plants of West Tropical Africa (2nd edition) Royal Botanic Gardens Kew. Pp. 654 - 670.
4. Edeoga H.O and Okoli B.E (1997) Anatomy and Systematics in *Costus lucanusianus* Complex (costaceae) Acta Phytolax Gebot 48:155 - 158.
5. Edeoga H.O and Okoli B.E (2001) Midrib anatomy and Systematics in Dioscoreae. *J.Econ. Tax. Bot,* 23:1 - 5.
6. Greensill T.M (1976) Growing better vegetable 4th edition Evans Brothers Ltd. London Pp. 14 - 15.
7. Harpert L. (1997) Population biology of plants. London Academic press Pp. 3 - 15.
8. Metcafe C.R and Chalk L. (1950) Anatomy of the Dicotylendon 2nd edition Clarendon press, Oxford 2:860 - 900.
9. Mbagwu F.N and Edeoga H.O (2000) Anatomical studies on the
10. roots of some vigna species (Leguminosae - Papilionoideae) Agric Journal (1) 8 - 10.
11. Nwachukwu C.U (2005) Anatomy and Histology of Spermatophytes, (A basic approach) 1st edition Beth Vin Publishers 55 Osuji Street Owerri, Imo State Nigeria.
12. Nwachukwu C.U and Mbagwu F.N (2006) Anatomical studies on the petiole of some species of *Indigofera. Medwell, Agricultural Journal 1* (2): 55 : 58.
13. Okoli B.E (1987) Anatomical studies in the leaf and protract of *Telfairia Hoker* (Curcurbitaceae) *Feddes Repertorium, 98*:231 - 236.
14. Schewell-Copper W.E (1957) Basic book on vegetable growing (2nd edition) Barrie and Jenkin Ltd London Pp. 19 - 26.
15. Stern K.R (2000) Introduction plant Biology, Macgraw-Hill Company Inc. United States of America. 603 Pp.
16. Tindale H.O (1979) Commercial Vegetable growing. University Press, London Pp. 14 - 50.
17. Vidyard R.D and Tripathi S.C (2002) A test book of Botany, Chand and Company, Ram Nagar. New Delhi Pp. 649 - 650.

Temperature Increased for Atherosclerotic Artery after Lasing

Ma Hongbao

Brooklyn, New York 11212, The United States

hongbao@gmail.com

Abstract: Introduction: Usefulness of laser angioplasty for endovascular surgery was recognized especially for patients having short segments of severe atherosclerotic changes in vessels. Acute thrombotic occlusion of arteries and veins is the leading causes of death worldwide. Difference of temperature increasing in normal and atherosclerotic arteries after the lasing is not clearly established. **Materials and Methods:** NZW rabbits were induced to atherosclerosis with balloon deendothelialization and feeding a high cholesterol diet (1%) for 9 months. The thermal couple was induced to rabbit aortas (control n=9; atherosclerotic n=12) wrapped by rabbit skin and the temperature of artery was measured during lasing with different energies of 2, 3, 4, 5 W. **Results:** There is linear relationship between the temperature and lasing energy ($r=0.99$, $p<0.0005$). After 2, 3, 4, 5 W lasing, the temperature of atherosclerotic rabbit arteries was 2.63, 4.18, 6.98 and 9.40^{o}C higher than the temperature of normal rabbit arteries. **Conclusions:** Laser angioplasty for endovascular surgery was a useful procedure but there is a significant higher temperature increasing after lasing. Consequently, this method should be recommended especially for high-risk patients with atherosclerosis. [New York Science Journal. 2008;1(1):33-42]. (ISSN: 1554-0200).

Keywords: artery; atherosclerosis; laser; temperature

Introduction

Over one million patients present yearly with cardiovascular events in the United States. Vulnerable plaques are responsible for development of unstable and acute cardiovascular syndromes. Extensive data from investigations in other fields have demonstrated that the laser can alter collagen structure as shown for skin resurfacing and from our recent work on thermal coagulation of collagen in the arterial wall. The problem of ischemic heart disease is widely prevalent. These patients have heart attacks and unstable angina symptoms. Although various medical and technological advances have reduced the mortality, many patients continue to die suddenly from coronary artery disease because of vulnerable plaques (Lipinski et al, 2004; Schaar et al, 2004; Vink et al, 2003).

The pathology of vulnerable plaque has demonstrated it to be composed of a rich lipid core covered by a thin collagen cap. However, recently inflammatory cell activity has been shown to participate in weakening the collagen cap by producing enzymes that digest collagen (Bhatia et al, 2003; Hartung et al, 2004). After heart attacks, vulnerable lesions are noted to have ruptured collagenous caps leading to exposure of the lipid core to the circulating blood causing thrombotic occlusion of the artery (Virmani et al, 2002). Although investigations have demonstrated that the vulnerable plaque can be detected, it is not clear what type of intervention will alter its course to rupture (Shah, 2003).

The temperature elevation is critical problem for the laser clinical practice. Temperature difference between atherosclerotic plaque and healthy vessel wall is related to clinical instability. It is correlated with systemic markers of inflammation and is a strong predictor of adverse cardiac events after percutaneous interventions. Thermography is the first in a series of novel "functional" imaging methods and is moving to clinical trials (Madjid et al, 2002). Usefulness of laser angioplasty for endovascular surgery was recognized especially for patients having short segments of severe atherosclerotic changes in vessels. Acute thrombotic occlusion of arteries and veins is the leading causes of death worldwide. Difference of temperature increasing in normal and atherosclerotic arteries after the lasing is not clearly established. The objective of this proposal is to use laser radiation to stabilize vulnerable plaques by altering their collagen structure, and detect the temperature after lasing.

Materials and Methods

Bench Studies: In this project we have established the technique that will be used in the rabbit model by in vitro testing. A 300 μm core optical fiber was placed in the flush channel of a balloon angioplasty catheter (Figure 1). The argon ion beam was noted to diffuse via the crystalloid fluid filling the balloon and lucent balloon walls. Using a single perfusion chamber, segments of both normal and atherosclerotic aorta were irradiated. Thermocouples were placed on the arterial wall surface while the balloon catheter was advanced into the perfusion chamber via a t-connection. The balloon was inflated and the argon laser activated at various powers and temperatures measured on the arterial wall surface (Figure 2).

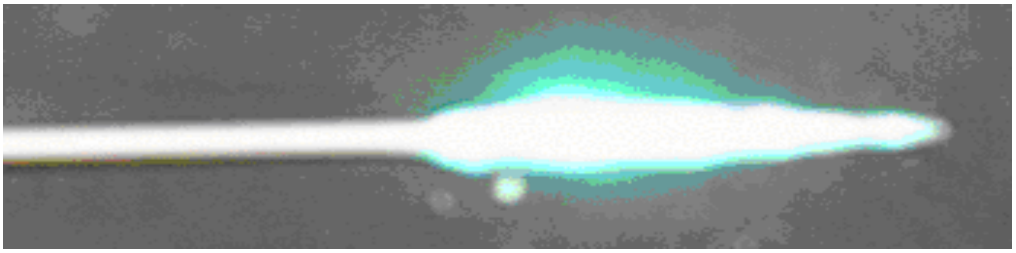

Figure 1. A standard angioplasty balloon catheter was used with a 300 μm optical fiber centered within the balloon. Argon ion laser irradiation can be seen as a bright light diffusing around the body of the inflated balloon.

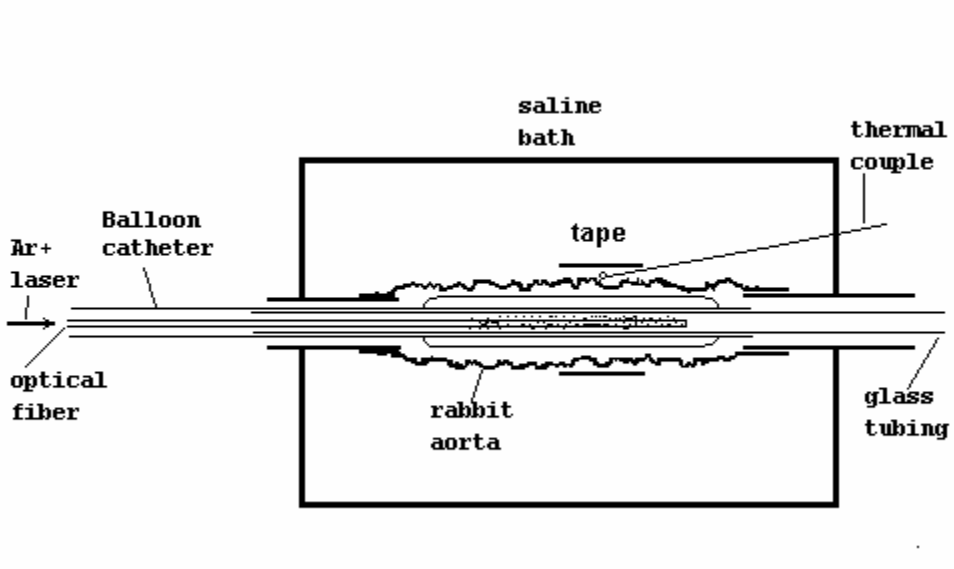

Figure 2. Sectional view of a single organ perfusion chamber. The balloon catheter is seen advanced into the lumen of the rabbit artery. Thermal couples are placed on the surface to measure temperature and these are held in place using umbilical tape.

Temperature rise on the arterial surface was proportional to the laser energy delivered via the balloon. Following irradiation the balloon material was left intact. Figure 3 is an example of the temperature rise and peak over about 60 seconds at five power levels (2, 3, 4, 5, 5.5W). After the study, the rabbit aortas are perfusion fixed and stored for histological analysis using light and electron microscopy.

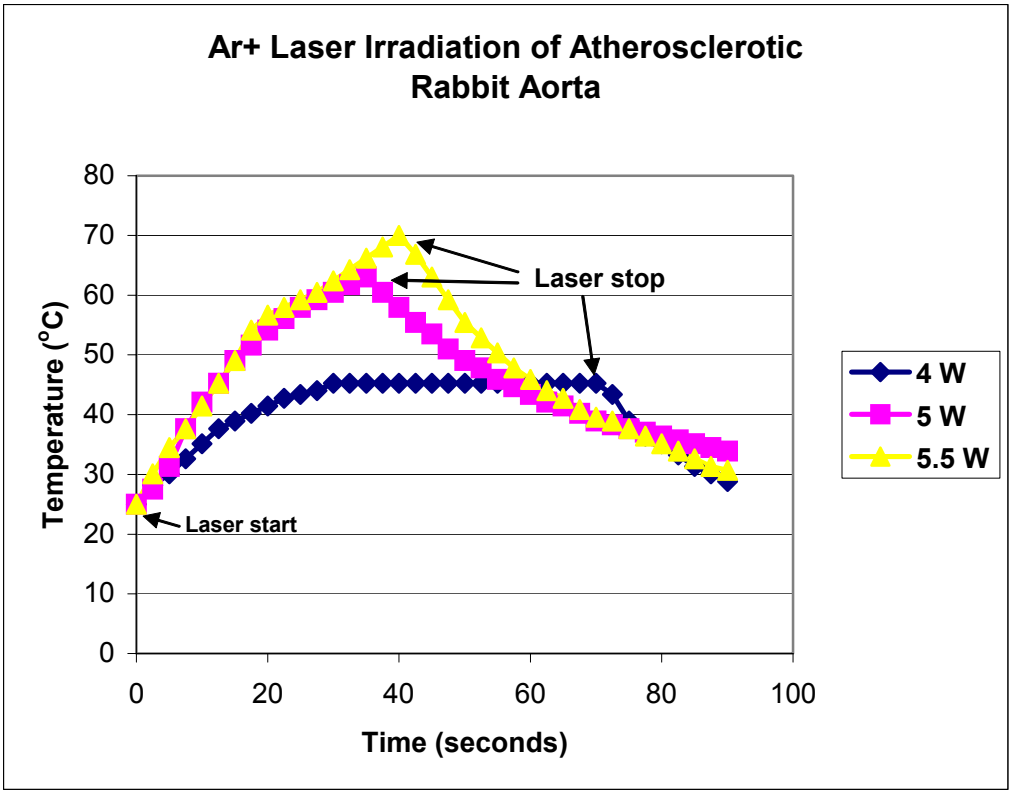

Figure 3. Temperature curves measured at the surface of the rabbit abdominal aorta during Ar^+ laser irradiation. These measurements were performed in a bath at 23ºC.

If the bath temperature was 37ºC then there was a higher target of temperature achieved using lower laser energy. Also, the temperature profile formed a plateau with a more consistent temperature profile (Figure 4). These data will guide how we will implement the laser delivery in the rabbit experiments. While under general anesthesia, the rabbit body temperature will be monitored and a warming pad used to maintain a 37ºC body temperature.

In vivo Rabbit Studies: New Zealand white (NZW) rabbits are made atherosclerotic by feeding a high cholesterol diet (1%) and balloon deendothelialization. After maintaining the cholesterol enriched diet for 4 months, rabbits will be ready to undergo pharmacological triggering to induce myocardial infarction and platelet rich thrombus on the aorta. Presently, two rabbits were made atherosclerotic and their aortas used in the bench top studies to determine the lasing parameters for the in vivo study described above. We have already demonstrated in the above experiments that we can raise the arterial wall temperature to levels that will cause cross-linking of collagen in the arterial wall. These are the same temperatures we had used in prior reports using other laser devices (i.e. laser activated thermal probes).

Currently, ten NZW rabbits are being fed an atherogenic diet and will undergo balloon deendothelialization in two weeks according to the protocol. Prior to triggering, balloon angioplasty of the mid-abdominal aorta with associated laser irradiation will be performed in a group of five rabbits and only a sham using the balloon without irradiation will be performed in the remaining five rabbits. Another group of ten rabbits will be staggered to conduct the same study and prepared two months after the first group was begun.

The thermal couple was induced to rabbit aortas (control n=9; atherosclerotic n=12) wrapped by rabbit skin and the temperature of artery was measured during lasing with different energies of 2, 3, 4, 5 W.

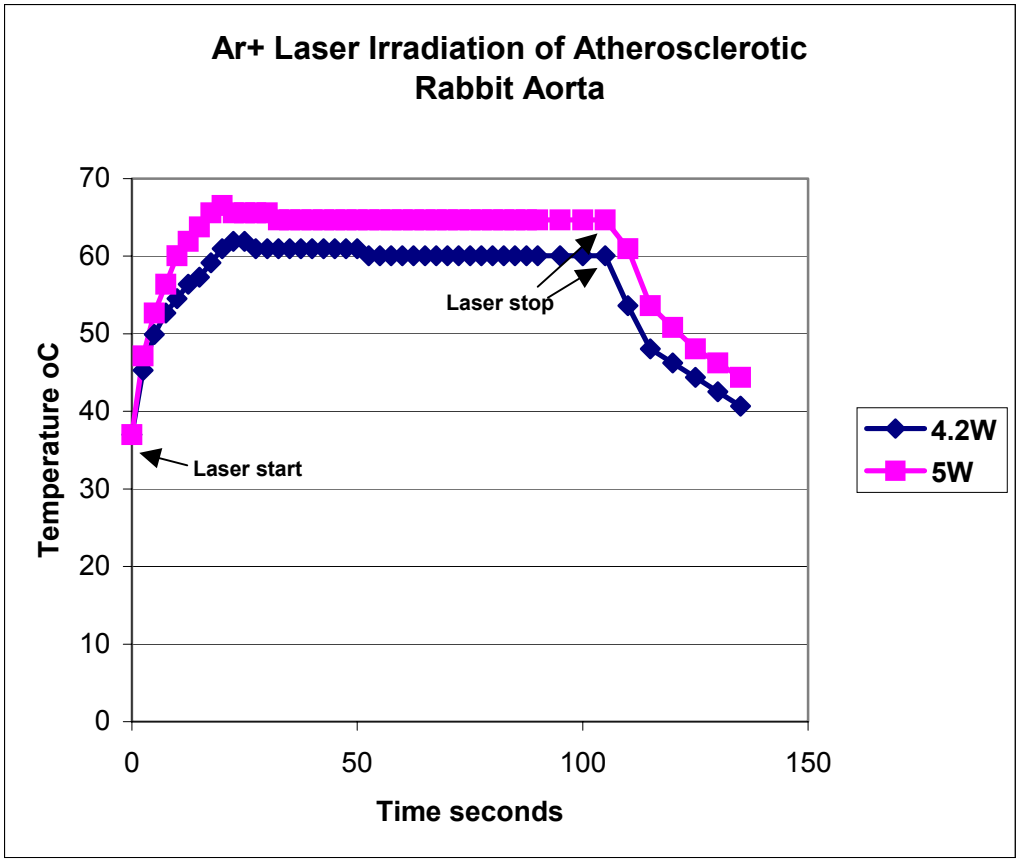

Figure 4. Temperature curves measured at the surface of the rabbit abdominal aorta during Ar^+ laser irradiation. These measurements were performed in a bath at 37ºC to simulate the body temperature. The bath at 37ºC provides a more stable thermal environment for the arterial wall.

Results

If our hypothesis that lasing of the arterial wall that cross links the collagen to stabilize the plaques were correct we would expect to see a significantly reduced number of pharmacologically triggered thrombi in the section of the aorta that was treated. We know from earlier studies that most of the thrombus occurs in the mid abdominal aorta. Thus, we will select that section of the aorta to conduct our preliminary laser-balloon treatment sites.

1. Temperature Measurement in vitro

In this project, we measured the temperature with the thermal camera. First, the temperature of isolated aorta was measured using a thermal camera. There was a linear relationship of the energy and temperature ($r=0.99$; $p<0.0001$). After 3, 4, 5 W lasing, the temperature of atherosclerotic rabbit arteries was 1.87°C, 2.99°C, and 4.96°C higher than the temperature of normal rabbit arteries ($p<0.001$) (Figure 5).

Second, we measured the temperature of the aortas wrapped with rabbit skin using a thermal couple. There was a linear relationship of the energy and temperature ($r=0.99$; $p<0.001$) in this measurement either. After 2, 3, 4, 5 W lasing, the temperature of atherosclerotic rabbit arteries was 2.63°C, 4.18°C, 6.98°C and 9.40°C higher than the temperature of normal rabbit arteries (Figure 6).

Third, we measured the temperature of the aortas wrapped with Nu Gauze plain packing strip using a thermal couple. There was a linear relationship of the energy and temperature ($r=0.99$; $p<0.001$) in this measurement either. There was no significant temperature difference between normal aorta and atherosclerotic aorta (Figure 7).

The temperature of the aorta with rabbit skin wrap measured by thermal camera was 8-20°C higher than the temperature measured by thermal couple (8.05°C, 11.58°C and 15.00°C after 3, 4 and 5 W lasing respectively for normal arteries; 10.37°C, 15.57°C and 19.45°C after 3, 4 and 5 W lasing respectively for atherosclerotic arteries) (Figure 8).

Using the thermal couple, the temperature of aorta wrapped with rabbit skin was higher that the temperature of aorta wrapped with Nu Gauze plain packing strip (Figure 9).

The temperature distribution of rabbit aorta during 5 W argon lasing is shown in Figure 10. The temperature peak is about located in a 15 mm length of the artery during the lasing.

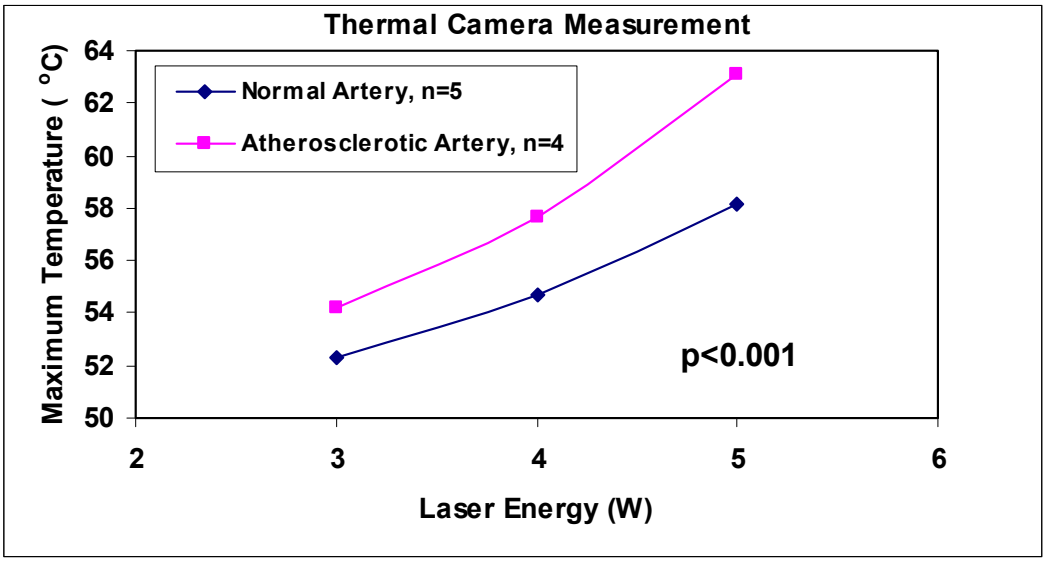

Figure 5. Temperature measurement of rabbit aorta by thermal camera.

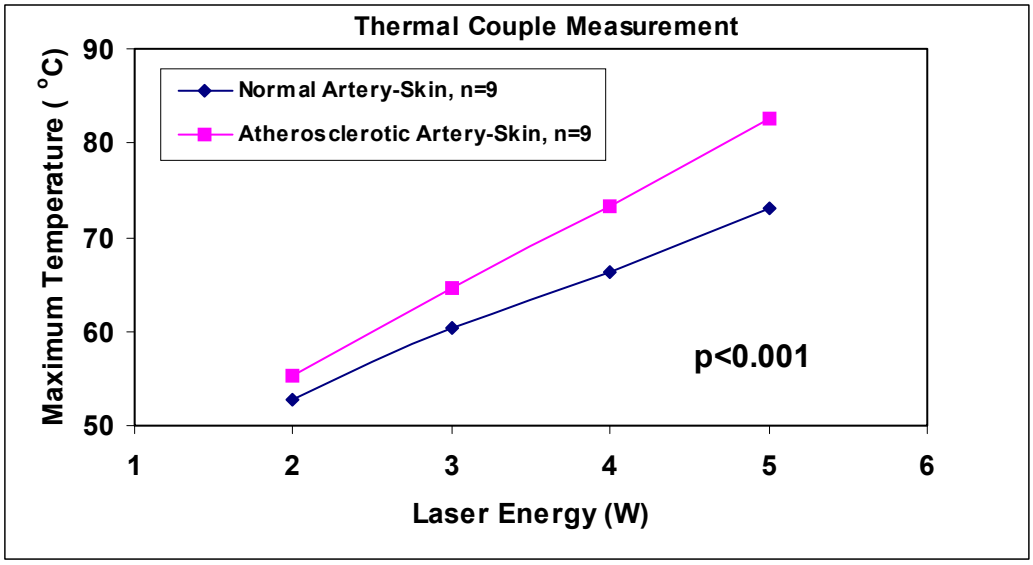

Figure 6. Temperature measurement of rabbit aorta with skin wrap.

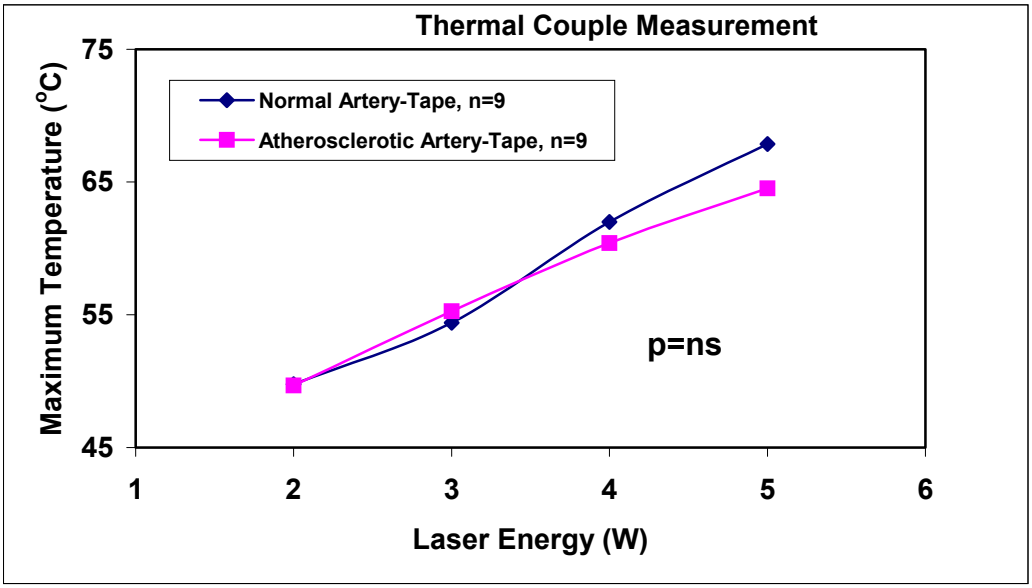

Figure 7. Temperature measurement of rabbit aorta wrapped with clothes tape.

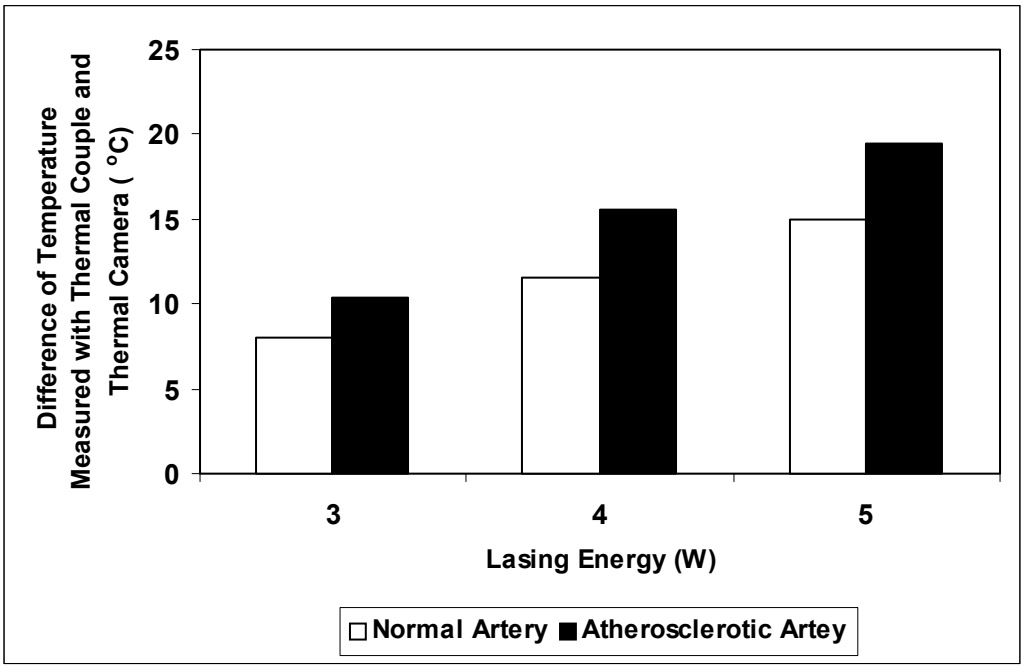

Figure 8. The temperature of the aorta with rabbit skin wrap was 8-20°C higher than that of without rabbit skin wrap (8.05°C, 11.58°C and 15.00°C after 3, 4 and 5 W lasing respectively for normal arteries; 10.37°C, 15.57°C and 19.45°C after 3, 4 and 5 W lasing respectively for atherosclerotic arteries).

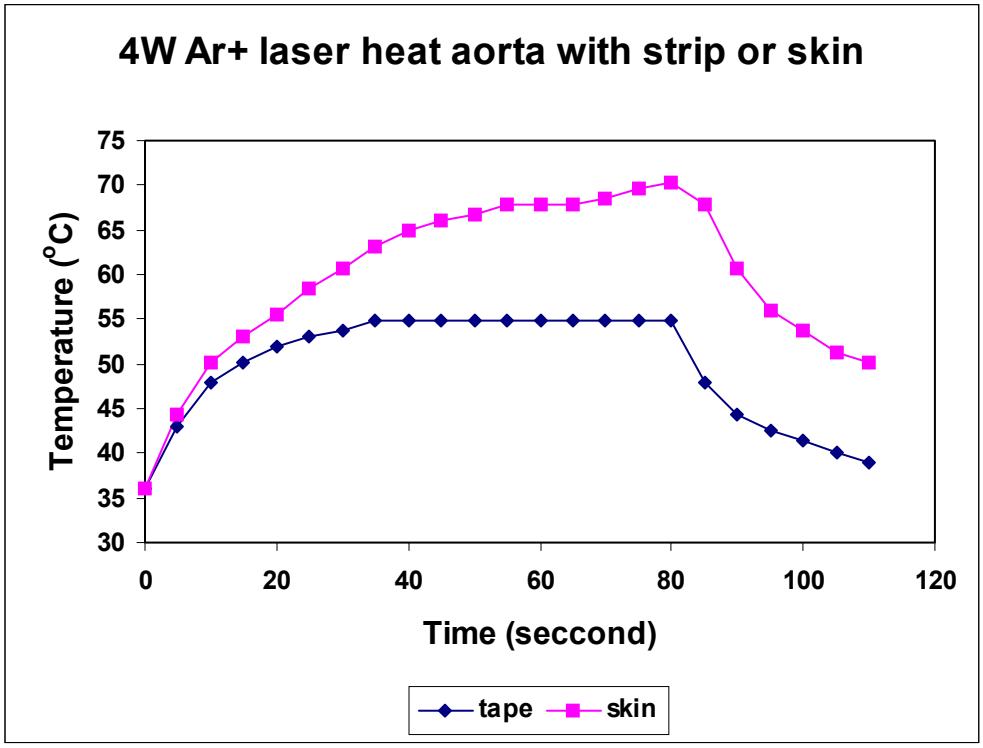

Figure 9. Comparison of the temperature of lased rabbit aortas (4 W Ar+) wrapped with Nu Gauze plain packing strip and rabbit skin. The result shows that the temperature of the artery wrapped with skin is higher than that of the artery wrapped with strip.

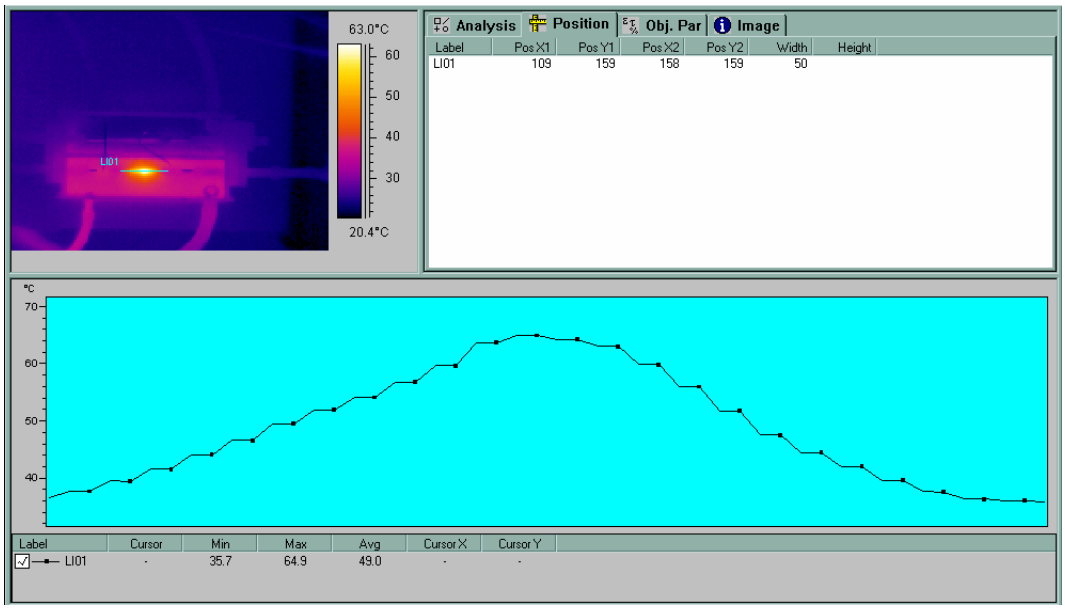

Figure 10. Temperature distribution on rabbit aorta during argon lasing by 5 W. The artery is lased for 30 sec and the total length of the cures is 30 mm.

2. Temperature Measurement in vivo

In this project, we measured the temperature in vivo with the thermal couple. The rabbit abdomen was opened under general anesthesia and rabbit aorta temperature was measured in vivo.

With 3.5 W argon lasing, the temperature will be elevated to the peak from 45 sec lasing (Figure 11). It is highly correlated between laser energy and rabbit aorta temperature ($r=0.95$; $p<0.0001$) (Figure 12).

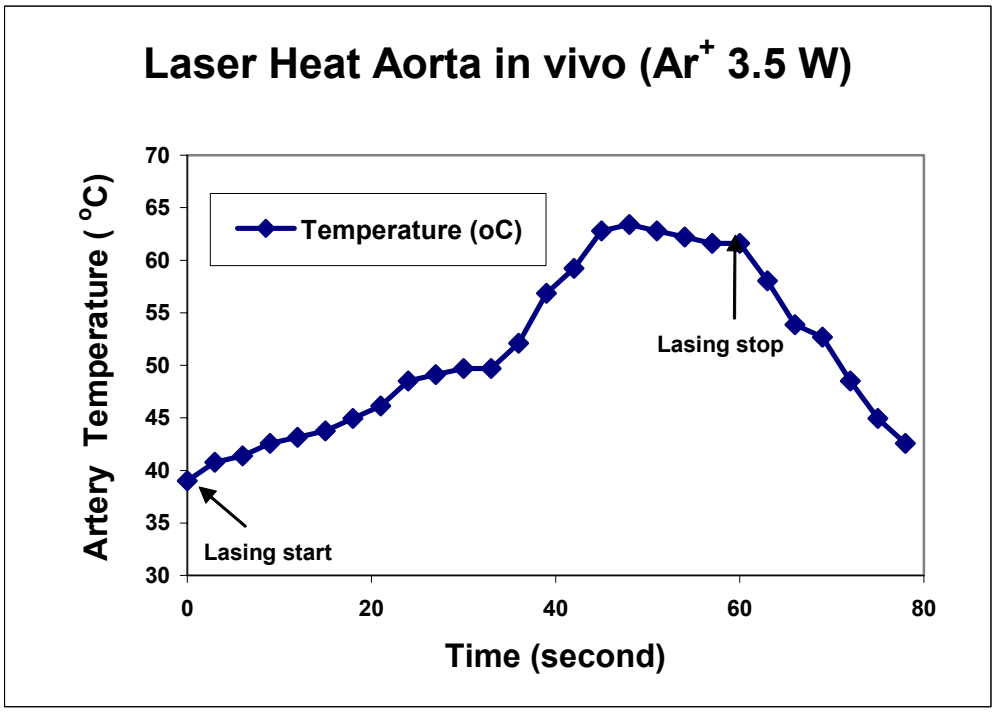

Figure 11. Temperature measurement in vivo for rabbit aorta after lasing by argon laser (3.5 W).

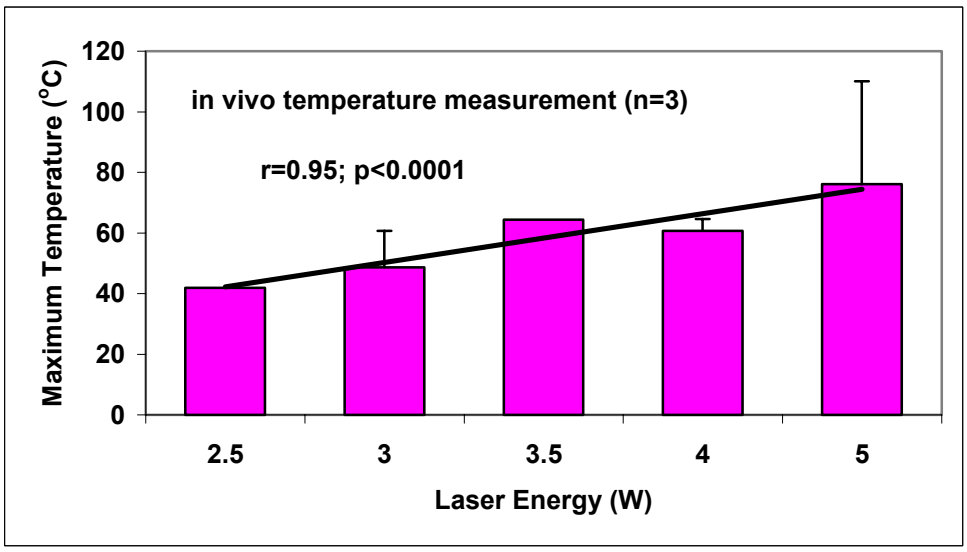

Figure 12. Temperature measurement in vivo for rabbit aorta after lasing by argon laser with different energy.

Discussion

According to the report of Madjid et al in 2002, areas with lower pH had higher temperature, and areas with a large lipid core showed lower pH with higher temperature. They also developed a thermography basket catheter and showed in vivo temperature heterogeneity in atherosclerotic lesions of atherosclerotic dogs and Watanabe rabbits. Thermal heterogeneity was later documented in human atherosclerotic coronary arteries in Madjid's group. Temperature difference between atherosclerotic plaque and healthy vessel wall is related to clinical instability. It is correlated with systemic markers of inflammation and is a strong predictor of adverse cardiac events after percutaneous interventions. It may be useful for a variety of clinical and research purposes, such as detection of vulnerable plaques and risk stratification of vulnerable patients (Madjid et al, 2002).

Arteriosclerosis is an inflammatory disease. Inflammatory processes play a role in the initiation of plaque development and the early stages of the disease as well as in complex plaques and complications such as intraarterial thrombosis. A method to detect inflammation in coronary arteries has the potential to characterize both local and systemic activation of arteriosclerotic plaque disease. It could help to define in more detail what constitutes a vulnerable plaque or vulnerable vessel and thus improve the prediction of acute coronary syndromes. Intracoronary thermography records a cardinal sign of inflammation. Heat is probably produced by (activated) macrophages. Experimental work has suggested that thermal heterogeneity is present in arteriosclerotic plaques and that increased temperature is found at the site of inflammatory cellular-macrophage-infiltration. Preliminary experience in patients undergoing coronary angiography has demonstrated that it is safe and feasible to perform intracoronary thermography using various systems. A graded relationship between thermal heterogeneity and clinical symptoms has been reported, with the greatest temperature elevation in acute myocardial infarction. Increases in thermal heterogeneity appeared to be associated with a comparably unfavorable long-term prognosis. Intracoronary thermography has the potential to provide insights into location and extent of inflammation as well as the prognostic consequences. Currently, this novel method and the underlying concepts are extensively evaluated (Schmermund et al, 2003).

The detection of temperature during laser execution is important to monitor the laser effect. In this study, we have developed the technique with thermal couple to detect the temperature during laser angioplasty in vivo. We propose to use laser and laser-thermal techniques in an atherosclerotic rabbit model to demonstrate a reduction in the plaque disruption and thrombosis. This could be translated to applications in humans with lesions that can cause heart attacks. Laser angioplasty for endovascular surgery was a useful procedure but there is a significant higher temperature increasing after lasing. Consequently, this method should be recommended especially for high-risk patients with atherosclerosis.

Laser angioplasty for endovascular surgery was a useful procedure but there is a significant higher temperature increasing after lasing. Consequently, this method should be recommended especially for high-risk patients with atherosclerosis.

Correspondence to:
Ma Hongbao, Ph.D.
Brooklyn, New York 11212
The United States
hongbao@gmail.com

References

1. Bhatia V, Bhatia R, Dhindsa S, Virk A. Vulnerable plaques, inflammation and newer imaging modalities. J Postgrad Med 2003;49(4):361-8.
2. Hartung D, Narula J. Targeting the inflammatory component in atherosclerotic lesions vulnerable to rupture. Z Kardiol 2004;93(2):97-102.
3. Lipinski MJ, Fearon WF, Froelicher VF, Vetrovec GW. The current and future role of percutaneous coronary intervention in patients with coronary artery disease. J Interv Cardiol 2004;17(5):283-94.
4. Madjid M, Naghavi M, Malik BA, Litovsky S, Willerson JT, Casscells W. Thermal detection of vulnerable plaque. Am J Cardiol 2002;90(10C):36L-39L.

5. Schaar JA, Muller JE, Falk E, Virmani R, Fuster V, Serruys PW, Colombo A, Stefanadis C, Ward Casscells S, Moreno PR, Maseri A, van der Steen AF. Terminology for high-risk and vulnerable coronary artery plaques. Eur Heart J 2004;25(12):1077-82.
6. Schmermund A, Rodermann J, Erbel R. Intracoronary thermography. Herz 2003;28(6):505-12.
7. Shah PK. Mechanisms of plaque vulnerability and rupture. J Am Coll Cardiol 2003;41(4 Suppl S):15S-22S.
8. Vink A, Pasterkamp G. Atherosclerotic plaques: how vulnerable is the definition of "the vulnerable plaque"? J Interv Cardiol 2003;16(2):115-22.
9. Virmani R, Burke AP, Kolodgie FD, Farb A. Vulnerable plaque: the pathology of unstable coronary lesions. J Interv Cardiol 2002;15(6):439-46.

Effects Of Intercropping On Root-Gall Nematode Disease On Soybean (*Glycine max (L) Merril*)

C. M. AGU

Department of Crop Science and Technology, Federal University of Technology, Owerri. P. M. B. 1526, Imo State, Nigeria. E-mail: cmagu2001@yahoo.com

ABSTRACT: Six intercrops (maize, melon, okra, *Telfairia*, *Amaranthus* and pepper) were tested for control of root-gall nematode disease on soybean in a loamy sand soil naturally infested with *Meloidogyne javanica*. The experiment was laid out in a randomized complete block design replicated four times. Results based on root-gall indices and number of juveniles (J_2) recovered from roots and rhizospheric soil showed that intercropping soybean with *Telfairia*, pepper and *Amaranthus* effectively suppressed infection on soybean roots. Okra, maize and melon intercropped with the soybean aggravated root-gall damage and caused yield reductions. [New York Science Journal. 2008;1(1):43-46]. (ISSN: 1554-0200).

Keywords: Disease, intercrop, nematode, root-gall, soybean, Owerri, Imo State, Nigeria.

INTRODUCTION

Soybean is the cheapest source of dietary plant protein (Judd, 1970). It produces the highest yield of protein per unit land area and has the ability to succeed on nearly all soils (Perman, 1982). The crop is usually grown sole and suffers a great deal of nematode damage which has led to some farmlands being abandoned to some parasitic nematodes (Lehman, 1978). Total crop failure in soils heavily infested with root-gall nematode (*Meloidogyne spp*) has also been reported (Agu, 2006). A number of control methods and practices have however, been developed. These included: inclusion of non-hosts in rotation sequence (Adesiyan *et al*, 2000), introduction of resistant varieties (Odihirin, 1981); heat and chemical treatments (Adesiyan *et al*, 2000); use of biological control agents (Adesiyan, 1985) and the use of organic manures (Egunjobi and Onayemi, 1981 and Amosu, 1981). The success and adoption of any one of these methods however depends mainly on the level of expertise and socio-economic conditions of the farmers.

In Nigeria, root crops, cereals, legumes and vegetables are grown together in mixtures in various combinations. Besides yield advantages (Wahua *et al*, 1981) mixed cropping systems also provide an effective strategy in controlling nematode pests of agricultural crops (Idowu and Fawole, 1991). This is by intercropping a susceptible crop with non-host crops. Information on crop mixtures for effective control of soybean root-gall nematode is lacking. This study was therefore concerned with the evaluation of different soybean based intercrops for effective control of root-gall nematode disease on soybean.

METHODS

The study was conducted at the Teaching and Research Farm of Federal University of Technology, Owerri, located between latitudes 5^0 20'N and 5^0 27'N and longitude 7^0 00'E. The soil was loamy sand (84.08% sand; 12.56% clay and 3.36% silt) and naturally infested with root-gall nematode, *Meloidogyne javanica*. By sieving and Bearmann's funnel technique (Viglierchio and Schmitt, 1983), the nematode population density in the soil was estimated.

Before planting, the land was cleared and made into mounds (2 x 1 m) according to farmers' practice and laid out in a randomized complete block design with four replications on a 20 x 25 m plot size. Soybean cv. TGX 813-6D, moderately susceptible to *M. javanica* (Awolola, 1987); Okra cv. Awgu early; melon cv Red Queen, *Telfairia occidentalis*, maize cv. FARZ 7; pepper cv. Nsukka yellow and *Amaranthus cruentus* were combined as follows: soybean/melon/maize/okra; soybean / maize / okra / *Amaranthus*; soybean / pepper / *Telfairia* / *Amaranthus*; soybean / melon / *Amaranthus* / pepper; soybean / *Telfairia* / maize / melon; soybean / pepper / *Telfairia* / okra and interplanted the same day on the mounds using the sole populations of each (soybean, 240,000; okra, 37,037; melon, 10,000; *Telfairia*, 10,000; maize, 20,000; pepper, 17,778 and *Amaranthus*, 222,222 / ha, (Unanma *et al*, 1991). In each crop mixture, soybean was sown 2 seeds / hole on crest and the intercrops planted 15 cm away from soybean and in alternate arrangement. Mounds planted with sole soybean served as control.

Table 1: Host status of intercrops collected from around *M. Javanica* infected soybean

Intercrop	Mean root-gall indices (0 – 4)	Host status to *M. Javanica*
Okra cv. Awgu early	4.00	highly susceptible
Melon cv. Red Queen	3.10	moderately susceptible
Telfairia occidentalis	0.20	resistant
Maize cv. FARZ 7	2.90	moderately susceptible
Pepper cv. Nsukka yellow	0.00	highly resistant
Amaranthus spp	0.00	highly resistant
$LSD_{0.05}$	1.00	

Table 2: Root-gall indices, number of *M. javanica* juvenile (J_2) recovered from roots and rhizospheric soil of soybean alone and in association with other intercrops

Crop mixture	Soybean root-gall indices (0 – 4)	Juvenile (J_2) population	
		/2g root system	/200 cm^3 soil
S/P/T/A	0.40	0.00	44.00
S/P/T/O	2.20	48.00	66.00
S/Me/A/P	3.20	188.00	148.00
S/T/M/Me	4.00	296.00	338.00
S/M/O/A	4.00	322.00	336.00
S/Me/M/O	4.00	350.00	402.00
Soybean sole (control)	3.00	174.00	152.00
$LSD_{0.05}$	1.20	56.02	69.31

S = soybean; P = pepper; T = Telfairia; A = Amaranthus; O = Okra, Me = melon; M = maize

Table 3: Soybean yields as affected by intercrops and root-gall nematode infection

Crop mixture	Mean soybean root-gall indices (0 – 4)	Mean soybean yields					
		Number of		Shoot weights (gm)		Grain yield (ton/ha)	Root dry weights (gm)
		Pods/plant	Seeds/pod	Fresh	Dry		
S/P/T/A	0.40	21.39	3.64	10.10	3.02	3.80	9.18
S/P/T/O	2.20	15.37	3.75	10.00	3.85	3.00	10.20
S/Me/A/P	3.20	13.61	2.99	9.30	3.60	2.60	13.87
S/T/M/Me	4.00	10.80	2.23	8.80	4.63	2.10	16.14
S/M/O/A	4.00	9.73	2.80	8.60	4.70	1.90	15.92
S/Me/M/O	4.00	10.75	1.39	8.70	6.99	1.20	18.32
$LSD_{0.05}$	1.20	3.94	1.61	0.50	2.08	1.00	3.47

S = soybean; P = pepper; T = Telfairia; A = Amaranthus; O = okra, Me = melon; M = maize

Compound fertilizer NPK 15:15:15 at 400 kg/ha was applied after first hoe-weeding (i.e. 3 weeks after planting) and second weeding done 10 weeks after planting. Twelve weeks after planting the crops were carefully lifted from soil and the crops separately washed free. The roots were examined and rated for galls on a scale of 0 to 4 according to Ogubji (1981) in which 0 = no infection (no galls present); 1 = rare infection (1 – 3 galls present); 2 = light infection (4 – 10 galls present); 3 = moderate infection (11 – 30 galls present) and 4 = severe infection (≥ 30 galls present). Juveniles second stage (J_2)/2 g of plant root system were extracted by the jar incubation method (Ayoub, 1977). Juveniles/120 cm^3 of soil were also extracted using a modified Bearman funnel technique (Tray method) (Hooper, 1969). The nematodes from roots and soil were counted using a dissecting microscope.

Data collected on soybean also included: number of harvested pods/plant, number of grains/pod; shoot weights (fresh and dry); grain yield/ha and root dry weights. These data were subjected to analysis of

variance (Steel and Torrie, 1981) and significant differences between means separated by Fisher's least significant difference method (Fisher, 1948) at P = 0.05.

RESULTS AND DISCUSSION

Crops roots rated for galls showed that the intercrops differed in host status to *M. javanica* (Table 1) and can be grouped as follows: (i) highly susceptible: okra; (ii) moderately susceptible: maize and melon; (iii) resistant: *Telfairia* and (iv) highly resistant: pepper and *Amaranthus*. The intercrops influenced root-galling on soybean (Table 2). Severe root-galls occurred on soybean plants intercropped with okra, maize and melon; also with *Telfairia*, melon and maize as well as with maize, okra and *Amaranthus*. Moderate root-galls occurred on the soybean when intercropped with melon, *Amaranthus* and pepper. Pepper, *Amaranthus* and *Telfairia* intercrops suppressed gall formation on the soybean.

These results showed that okra, maize and melon are not good crop associates with soybean in *M. javanica* infested soils. This observation agrees with Bridge (1978) who noted that planting susceptible crops alongside yam plants could increase nematode population density and the severity of damage by root-gall nematode (*M. incognita*) on yam plants. Atu and Ogbuji (1986) also reported that susceptible intercrops planted on yam mounds resulted in greater root-gall damage on the harvested tubers.

Rare root-galls on soybean caused by resistant pepper, *Amaranthus* and *Telfairia* intercrops was because these intercrops prevented nematode population increase around the soybean plants (Table 2). Fawole and Mai (1979) reported that gall indices corresponded with nematode population density.

Soybean yields varied with galling responses at different crop mixtures (Table 3). Significantly higher number of pods/plant were produced by soybean plants intercropped with pepper, *Amaranthus* and *Telfairia* with low gall index. Grain yield (tons/ha), fresh shoot weight and number of grains/pod consistently decreased with increases in galling response at the various crop mixtures. These decreases were significant on soybean plants intercropped with two or more of the intercrops susceptible to the root-gall nematode (*M. javanica*). This was due to significant increases in galling response at significantly increased nematode population attacking the soybean (Table 2). Galls are known to decrease the uptake of minerals, especially, N, P and K (Trudgill, 1987) and also do not translocate adequate water and nutrients to vegetative organs for photosynthesis (Otiefa and Elgindi, 1962).

Soybean root dry weights increased as galling response increased with increasing number of intercrops susceptible to the root-gall nematode (Table 3). This was because of the weight gain on the main roots caused by galls. Agu (2002) found that galled roots represented most of the total weight of the root system.

From this study, it is obvious that root-gall nematode disease on soybean can be effectively controlled and good grain yields obtained in *M. javanica* infested soils if *Telfairia*, pepper and *Amaranthus* were used as intercrops. *Telfairia*, pepper and *Amaranthus* are therefore recommended as intercrops for effective control of soybean root-gall nematode disease in soils infested with *M. javanica*.

ACKNOWLEDGEMENT

The author thanks the Centre for Agricultural Research, Federal University of Technology, Owerri for supporting this study and providing laboratory and farm facilities under its Research Programme.

REFERENCES

1. Adesiyan, S. O. 1985. Comparative in vivo studies on possible nematicidal effets of spores of *Aspergillus niger, Penicillium sderotigenum* and *Fusarium oxysporium* on yam nematode. Nigeria Journal of Plant Protection 9: 15 – 21.
2. Adesiyan, S. O., Caveness, F. E., Adeniyi, M. O. and Fawole, B. 2000. Nematode Pests of Tropical Crops. Heinemann Educational Books (Nigeria) Plc.
3. Agu, C. M. 2006. Susceptibility of soybean cultivars to root nematodes in south western Ethiopia. Tropical Sciences. 46 (3). 143 – 146.
4. Agu, C. M. 2002. Effect of urea fertilizer on root-gall disease of *Meloidogyne javanica* in soybean. Journal of Sustainable Agriculture, 20 (3), 95 – 100.
5. Amosu, J. O. 1981. Control of root-knot nematodes by cultural practices. Proceedings of the Third Research Planning Conference on Root-knot Nematodes, *Meloidogyne spp*. November 16 – 20, 1981, IITA Ibadan, p. 259 – 265.
6. Atu, U.G. and Ogbuji, R. O. 1986. Root-knot nematode problems with intercropped yam (*Discorea rotundata*). Phytoprotection, 67: 35 – 38.

7. Awolola, T. A. 1987. Studies on elite soybean cultivars to nematode infection and nodulation potentials. B. Agric Project Report (unpublished). Dept. of Crop Science, University of Nigeria, Nsukka, 44pp.
8. Ayoub, S. M. 1977. Plant nematology, an agricultural training aid. State of California Dept. of Food and Agriculture. 157pp.
9. Bridge, J. 1978. A review of plant parasitic nematode association with yams. International Foundation of Science Publication, Session III, No. 3, 305pp.
10. Egunjobi, O. A. and Onayemi, S. O. 1981. The efficacy of water extract of neem (*Azadirachta indica*) leaves as a systemic nematicide. Nigerian Journal of Plant Protection. 5: 70 – 74
11. Fawole, B. and Mai, W. F. 1979. Influence of plant age, light intensity, nematode inoculum level and their interactions on tomato growth and reproduction of *Meloidogyne haplaI*. Journal of Nematology II (2) 199 – 121.
12. Fisher, R. A. 1948. Statistical Tables for Biological, Agricultural and Medical Research. Edinburgh and London: Oliver and Boyd.
13. Hooper, D. J. 1969. Extraction and handling of plant and soil nematodes. Pages 20 – 36 in J. E. Peachy (ed), Nematodes of Tropical Crops common. Bur. Helminthol. Tech. Commun. No. 4.
14. Idowu, A. A. and Fawole, B. 1991. Effects of intercropping maize and cowpea on the pathogenicity of *Meloidogyne spp* and yields of cowpea. Nigeria Journal of Plant Protection. 14: 20 – 26.
15. Judd, R. W. 1970. Cost of protein. Soybean News 21: 6.
16. Lehman, R. O. 1978. The important nematode diseases of soybeans. Pages 69 – 76. In: D. K. Whigham (ed). Soybean Production, Protection and Utilization. INTSOY Series No. 6. Univ. of Illinois, Urban-Champaign.
17. Odihirin, R. A. 1981. Screening of some West African cowpeas for resistance to root-knot nematodes, *Meloidogyne incognita* and *M. javanica*. Proceedings of the Third Planning Conference on Root-knot Nematodes, *Meloidogyne spp*. November 16 – 20, 1981, IITA Ibadan, p. 232 – 240.
18. Ogbuji, R. O. 1981. Infectivity of three *Meloidogyne spp* on soybean in Nigeria. Der Tropenlandwirt 82: 149 – 152.
19. Otiefa, B. A. and Elgindi, O. N. 1962. Influence of parasitic duration of *Meloidogyne javanica* on host nutrient uptake. Nematologica 8: 216 – 220
20. Perman, G. K. 1982. Soybean research-more food for more people, In: Whigham D. K. (ed.) soybean Production, Protection and Utilization. INTSOY series. No. 6 University of Illinois, Urbana-Champaign.
21. Steel, G. D. and Torrie, J. H. 1981. Principles and Procedures of Statistics (2^{nd} edition). McGraw-Hill Book Company. Inc. N. Y. xxi – 633pp.
22. Trudgill, D. L. 1987. Effects of rates of nematicide and of fertilizer on the growth and yield of cultivars of potato which differ in their tolerance of damage. Plant and Soil: 235 – 243.
23. Unanma, R. O.; Anuebunwa, A.; Ezulike, F. O.; Udealor, T. O. and Ikeorgu, J. E. G. 1991. Evaluation of improvements on the basic cropping system of southeastern Nigeria. In: Olukosi J. O.; Ogungbile, A. O. and Kalu, B. A. (ed). Appropriate Agricultural Technologies for Resource - Poor Farmers N.F.S.R.N.
24. Viglierchio, D. R. and Schmitt, R. V. 1983. On the methodology of nematode extraction from field samples: comparism of methods for soil extraction. Journal of Nematology, 15: 438 – 444.
25. Wahua, T. A. T.; Babalola, O. and Aken'Ova, M. E. 1981. Intercropping morphologically different types of maize with cowpea: LER and growth parameters of associated cowpea. Experimental Agriculture. 17: 407 – 413.

How S-S' di quark pairs signify an Einstein constant dominated cosmology, and lead to new inflationary cosmology physics.

A. W. Beckwith

ABSTRACT

We review the results of a model of how nucleation of a new universe occurs, assuming a di quark identification for soliton-anti soliton constituent parts of a scalar field. Initially, we employ a false vacuum potential system; however, when cosmological expansion is dominated by the Einstein cosmological constant at the end of chaotic inflation, the initial di quark scalar field is not consistent w.r.t a semi classical consistency condition we analyze as the potential changes to the chaotic inflationary potential utilized by Guth . We use Scherrer's derivation of a sound speed being zero during initial inflationary cosmology, and obtain a sound speed approaching unity as the slope of the scalar field moves away from a thin wall approximation. All this is to aid in a data reconstruction problem of how to account for the initial origins of CMB due to dark matter since effective field theories as presently constructed require a cut off value for applicability of their potential structure. This is often at the cost of, especially in early universe theoretical models, of clearly defined baryogenesis, and of a well defined mechanism of phase transitions.

[New York Science Journal. 2008;1(1):47-91]. (ISSN: 1554-0200).

Correspondence: A. W. Beckwith: projectbeckwith2@yahoo.com

PACS numbers**:** 03.75.Lm, 11.27.+d, 98.65.Dx, 98.80.Cq, 98.80.-k

I. INTRODUCTION

As of June 2005, an effort was made to combine reconstruction of data gathering techniques with the requirement of the JDEM dark matter-dark energy search for the origins of dark matter in the early universe[1]. This has, among other things, lead to methodologies being presented which could shed light as to the initial formation of scalar potentials which could contribute to CMB background radiation. In doing so, it was noted that initial dimensions, as postulated by Quin, Pen, and Silk[2] presented evidence as to how three extra dimensions play a role in explaining how at very short distances gravity would have a r^{-5} spatial behavior dependence in force calculations. We do believe that in the initial stages of cosmic inflation, that space, indeed had additional dimensions and that the dimensions play a role as far as nucleation of a new universe.

We have, therefore, written up how to reconstruct potentials, using the methodology presented by Kadota et al[3], but we also think that it is important to pick out properties of the potential in question with respect to early universe models, since CMB data as presently configured is too imprecise to get anything other than the standard FRW flat space metric, 1000 or so years after the big bang. So being the case, we have constructed a list of properties of what an early universe potential system, composed of di quark constituents in order to help researchers investigate CMB data more accurately for very early universe configurations.

II. ORGANIZATION OF THE PAPER

Appendix I, parts A and B highlights what can be said about typical data reconstruction for early universe potential systems. **Appendix II** initiates setting up three regimes for an evolving potential model leading to chaotic inflation, in line with Dr.

Guths quartic potential system. **Appendix III** presents what is done with instanton models of what is called in the literature, QCD balls[4], for initially stable di quark pairs which we believe are the building blocks for a false vacuum nucleation of initial baryonic states of matter. Afterwards, in the main text of this document, I examine the break down of what Bunyi and Hsu of the U. of Oregon call a semi classical approximation[5], but which I call a consistency condition for di quark pair contributions to Guth style chaotic inflation. In making this consistency evaluation, I then refer to in **Appendix IV, part A and B** how and why the initial wave functionals used in forming this semi classical evaluation are formed. This uses the results of two accepted world press scientific articles, one published in IJMPB [6], and also another accepted already for publication in Modern Physics Letters B [7], which describe necessary and sufficient conditions for a false vacuum based construction of Gaussian wave functionals, which then have, due to the very short distances involved, a discrete state presentation which is then used in an inner product evaluation of potential systems.

It is interesting to note that the semi classical (consistency) condition so outlined in the main text works best initially for a modified driven washboard potential system, which is integrated over six dimensions, in line with Silks presentation as to the importance of higher dimensions being very significant for extremely small spatial dimensions. This is given more structure in **Appendix V**. I do believe that this is no accident, and is congruent with the Calabi Yau conjecture in string theory with the curling up of higher spatial dimensions, which after a certain phase in inflation no longer contribute significantly to the chaotic inflation paradigm presented by Guth[8].

How does this bend in with more observational techniques as given by astrophysics researchers? Early universe nucleation is too small a region of space for typical action integral arguments to be effectual. So I have presented an alternative, as given in **Appendix VII**, which I do believe is able to give a new structure as to how to consider the flux of particles from a cosmic nucleation stand point[9]. In addition, the initial configuration of matter states would not be treatable by the Einstein cosmological constant. But that the evolution of di quark states can, after the onset of inflation, evolve into an Einstein cosmological constant dominated epoch, as given by an argument based upon a modified Scherrer k essence argument. This argument is important, and is in the main text of this document. All of this has been presented in PANIC 2005, and will be included in the AIP proceedings of that conference[10].

This last step depends upon a break down of a thin wall approximation. I do believe that this is consistent with the quantum fluctuations of momentum discussed in the paper written by R. Aloisio[11] et al, about deformed special relativity and its relations to a supposed quantum gravitational background.

Finally, I make direct connection with Venzianos[12] postulates as to the links between Planck scale length, a scalar field term, and a wavelength approximately in sync with the initial scale of a nucleating universe. I suggest here that the initial cosmic nucleation diameter was of the order of Planck Length, and subsequently radically expanded afterwards, in a result consistent with cosmic inflation.

The initial impetus for making this effort was due to the following conundrum. As is commonly known in cosmology circles, one would expect a flat Friedman – Walker

universe after 60 e-foldings, but beforehand one could expect sharp deviations as to flat space geometry. The moment one would expect to have deviations from the flat space geometry would closely coincide with Rocky Kolb's model for when degrees of freedom would decrease from over 100 degrees of freedom to roughly ten or less during an abrupt QCD phase transition[13]. As was mentioned by Joe Lykken , the CMB model should yield a distinct 'signal' which is lending toward a non flat cosmological metric space potential which can be seen to be initiating a phase transition at about the end of the 60 e-folding regime of cosmological expansion[14]. My own model is useful for such QCD phase transitions; while Kenji Kadoka's potential reconstruction scheme is not specific as to a **UNIQUE** potential structure. It would be enough in itself to try to combine the two techniques as to go before the thousand year mark Kenji mentioned as to data sets permitting potential reconstruction, and to find evidence as to CMB background as to the initial phases of CMB generation leading to the datum Kolb mentioned as to the decrease in cosmic microwave radiation to its present value as a result of a QCD phase transition in the expansion of the early universe.

III. BRIEF RE CAP OF QINS EXTRA DIMENSIONS FROM DARK MATTER ARTICLE, PLUS THE EVOLVING POTENTIAL SYSTEM ACCOMODATING DI QUARK SCALAR FIELDS

As mentioned, Quinn's article[2] gives a new force law, with respect to distances at or below $1nm$ in length. As presented in the article [10], this appears to be a verification of the existence of small but non infinitesimal extra dimensions. The key assumption which was used in their paper was a force law of the general form for distances $r << R$:

$$F = \alpha \cdot \frac{GMm}{r^{2+n}} \tag{3.1}$$

Here, α is a constant with dimensions $[length]^n$, G is the gravitational constant, and M and m are the masses of the two particles and. $\alpha \equiv R^n$ was set , while the value of n was, partly to fit with an argument given by Volt and Wannier[15] that the quantum mechanical cross section for collision is twice the corresponding classical value, if one assumes a central force field dependence of r^{-5} This all together, if one assumes that initially r is of the order of magnitude of Planck's length l_P would lead to extremely strong pressure values upon the domain walls of a nucleated scalar field initial states, which I claim would lead to a quite necessary collapse of the thin wall approximation. This collapse of the thin wall approximation set the stage for an Einstein constant dominated regime in inflation, if one adheres to a version of Scherrer's K essence theory[16]results for modeling the di quark pairs used as an initial starting point for soliton-anti soliton pairs(S-S') in the beginning of quantum nucleation of our universe.[10]

We should note that **Appendix I** as given gives a necessary and sufficient condition for constructing a potential system, initially in the false vacuum mode of potential, due to a pop up of a di quark state[10]. Here, for reasons of scale, we set M_P as a Planck mass, and the 2nd mass, m, as considerably smaller. The scalar field term ϕ is constructed in terms of di quarks , in line with the soliton- anti soliton (S-S') used in the two accepted articles using similar constructions in IJMPB, etc [6,7], and ϕ^* is, here, picked in terms of the limits of quantum fluctuations of a scalar field, in line with Guths model of chaotic inflation[17]. Furthermore we write the potentials V_1, V_2, and V_3 in terms of S-S' di quark pairs nucleating and then contributing to a chaotic inflationary scalar potential system[10].

$$V_1(\phi) = \frac{M_P^2}{2} \cdot (1 - \cos(\phi)) + \frac{m^2}{2} \cdot (\phi - \phi^*)^2 \tag{3.2a}$$

$$V_2(\phi) \approx \frac{(1/2) \cdot m^2 \phi^2}{(1 + A \cdot \phi^3)} \tag{3.2b}$$

$$V_3(\phi) \approx (1/2) \cdot m^2 \phi^2 \tag{3.2c}$$

The difference between these potentials becomes extraordinarily important in considering how the nucleating universe system evolves in time from the onset of the big bang itself. Furthermore, as a convenience, I have bench marked the ϕ^* term via the following procedure. We consider if and when we have classical and quantum fluctuations approximately giving the same value for a phase value of [17]

$$\phi^* \equiv \left(\frac{3}{16 \cdot \pi}\right)^{\frac{1}{4}} \cdot \frac{M_P^{3/2}}{m^{\frac{1}{2}}} \cdot M_P \rightarrow \left(\frac{3}{16 \cdot \pi}\right)^{\frac{1}{4}} \cdot \frac{M_P^{3/2}}{m^{\frac{1}{2}}} \tag{3.3}$$

where we have set M_P as the typical Planck mass which we normalized to being unity in this paper for the hybrid false vacuum – inflaton field cosmology example , as well as having set the general evolution of our scalar field as having the form of [17]

$$\phi \equiv \tilde{\phi}_0 - \frac{m}{\sqrt{12 \cdot \pi \cdot G}} \cdot t \tag{3.4}$$

This then permits us to look at how consistent having a di quark model, with a thin wall approximation is, with the evolving potential system, given above. It is important, since we are finding that having the additional dimensions specified in the beginning permits us to have a more physically consistent picture of how the phase transition to an Einstein constant dominated cosmology occurs in the first place. This is especially relevant from going from the 1st to the 3rd potential given above. **Appendix III** presents what is done

with instanton models of what is called in the literature, QCD balls[4], for initially stable di quark pairs, which is what we are assuming with this construction of ϕ, and we can use to obtain S-S' type pairs which are then used to construct wave functional representation of early universe states. This is in part based upon **Appendix IV, part A and B** on how and why the initial wave functional used in forming this semi classical evaluation are formed. This uses the results of two accepted world press scientific articles, one published in IJMPB [6], and also another accepted already for publication in Modern Physics Letters B [7]. The important thing to consider here, though is that we are looking at understanding the existence of the phase transformation from the first to the third potential occurs, and what it says about the formation of conditions relevant toward an Einstein constant dominated cosmology

IV: CRITERIA USED BY BUNYI AND HSU, WHICH WE CALL A CONSISTENCY CONDITION REFLECTING THE OCCURANCE OF A PHASE TRANSITION.

Let us first consider an elementary definition of what constitutes a semi classical state. As visualized by Buniy and Hsu,[5] it is of the form $|a\rangle$ which has the following properties:

i) Assume $\langle a|1|a\rangle = 1$

(Where 1 is an assumed identity operator, such that $1|a\rangle = |a\rangle$)

ii) We assume that $|a\rangle$ is a state whose probability distribution is peaked about a central value, in a particular basis, defined by an operator Z

a) Our assumption above will naturally lead, for some *n* values

$$\langle a|Z^n|a\rangle \equiv \left(\langle a|Z|a\rangle\right)^n \tag{4.1}$$

Furthermore, this will lead to, if an operator Z obeys Eq. (4.1) that if there exists another operator, call it Y which does not obey Eq. (4.1), that usually we have non commutativity

$$[Y, Z] \neq 0 \tag{4.2}$$

Buniy and Hsu[5] speculate that we can, in certain cases, approximate a semi classical evolution equation of state for physical evolution of cosmological states with respect to classical physics operators. This well may be possible for post inflationary cosmology; however, in the initial phases of quantum nucleation of a universe, it does not apply. We do this with a potential system, with S-S' di quark constituents we model via using[10]

$$\phi \equiv \pi \cdot \left[\tanh b\left(x - x_a\right) + \tanh b\left(x_b - x\right)\right] \tag{4.3}$$

We can, in this give an approximate wave function as given by a discretized version of the wave functional given for the first potential system as in Appendix IV, B:

$$\psi \cong c_1 \cdot \exp\left(-\tilde{\alpha} \cdot \phi(x)\right) \tag{4.4}$$

Then we can look to see if we have[5,10]

$$\left(\int_{x_a}^{x_b} \psi \cdot V_i \cdot \psi \cdot 4\pi \cdot x^2 \cdot dx\right)^N \equiv \int_{x_a}^{x_b} \psi \cdot \left[V_i\right]^N \cdot \psi \cdot 4 \cdot \pi \cdot x^2 \cdot dx \Big|_{i=1,2,3} \tag{4.5}$$

This was later generalized, in the initial phases of nucleation for the 1st potential system as being, in six initial dimensions

$$\left(\int_{x_a}^{x_b} \psi \cdot V_i \cdot \psi \cdot 4\pi \cdot x^5 \cdot dx\right)^N \equiv \int_{x_a}^{x_b} \psi \cdot \left[V_i\right]^N \cdot \psi \cdot 4 \cdot \pi \cdot x^5 \cdot dx \Big|_{i=1} \tag{4.6}$$

In addition, the analysis of how to work with a ratio of the values of the left and right hand sides of eq (4.5 and (4.6)as a way of looking at the consistency of what has been called the semi classical approximation would lead to analyzing

$$\Phi_{i,n,N}(ratio) \equiv \left. \frac{\left(\int_{x_a}^{x_b} \psi \cdot V_i \cdot \psi \cdot x^{2+n} \cdot dx \right)^N}{\int_{x_a}^{x_{bf}} \psi \cdot [V_i]^N \psi \cdot x^{2+n} \cdot dx} \right|_{i=1,2,3} \tag{4.7}$$

The first coefficient, i, denotes which potential system is picked, and ranges in value from 1 to 3. The second coefficient, *n,* is either 0 or 3, depending upon what dimensionality is assumed for this problem. The third coefficient, N, is freely ranging in values from 1 up to 100. I as a convenience often worked with N= 9. This eventually led to the calculations of **Appendix V**, which highlight the importance of higher dimensionality in the initial stages of nucleation, for the first potential system.

Assuming that this is a valid initial dimensional approximation, we did the following for the three potentials.

a. Assumed that the scalar wave functional term was decreasing in '*height*' and increasing in '*width*' as we moved from the first to the third potentials. ϕ also had a definite evolution of the domain wall from a '*near perfect*' thin wall approximation to one which had a considerable slope existing with respect to the wall.

b. We also observed that in doing this sort of model that there was a diminishing of magnitude from unity for Eq. (4.7) for large *N* values, regardless if or not the thin

wall approximation was weakened as we went from the first to the third potential system. In doing to, we also noted that even in Eq. (4.7) for the first potential, Eq. (4.7) had diminishing applicability as a result for decreasing *b* values in Eq. (4.3), which corresponded to when the thin wall approximation was least adhered to.

We also observed that for the third potential, that there was never an overlap in value between the left and right hand sides of Eq. (4.5) and Eq. (4.6), regardless of whether the thin wall approximation was adhered to. In other words, the third potential was least linkable to a semi classical approximation of physical behavior linkable to a physical system, while Eq. (4.5) and Eq. (4.6) worked best for a thin domain wall approximation to Eq. (4.4) in the driven sine Gordon approximation of a potential system. In all this, we assumed that the small perturbing term added to the $(1-\cos(\phi))$ part of Eq. (3.2a) was a physical driving term to a very classical potential system $(1-\cos(\phi))$ which had a quantum origin consistent with the interpretation of a false vacuum nucleation of the sort initially formulated by Sidney Coleman.[18] Furthermore, as we observed an expanding 'width' in Eq. (4.3), the alpha term in Eq (4.4) shrank in its value, corresponding to a change in the position of constituent S-S' components in the scalar field given in this model. The S-S' terms roughly corresponded to di quark pairs.

c. Chaotic inflation in cosmology is, in the sense a quartic potential portrayed by Guth,[17] a general term for models of the very early Universe which involve a short period of extremely rapid (exponential) expansion; blowing the size of what is now the observable Universe up from a region far smaller than a proton to about the size of a grapefruit (or even bigger) in a small fraction of a second. This process smoothes out space-time to make the Universe flat, but is not in the model presented linkable in the chaotic inflationary region given by the third potential to any semi classical arguments. The relative good fit of Eq. (4.7) for the first

potential is in itself an argument that the thin wall approximation breaks down past the point of baryogenesis after the chaotic inflationary regime is initiated by the third potential as modeled by Guth.[17]

Since we have established this, we should then attempt to consider if the higher dimensional physical state relevant to the 1st potential system are countable. Yes they are, but not by ordinary least action principal arguments[19]. I give a variant of what could be analyzed in **Appendix VII**, after stating that the earlier least action counting algorithms referenced in **Appendix VI** (summary of Garrigas work)[20] is not germane to such a small scale physical system. This then leads to to consider what the evolving state of di quark pairs says about , from a Scherrer k essence stand point of how the evolution to Guth chaotic inflation, as given by the third potential corresponds to the rise of an Einstein constant dominated inflationary cosmology[10].

V.HOW DARK MATTER TIES IN, USING PURE KINETIC *K* ESSENCE AS DARK MATTER TEMPLATE FOR A NEAR THIN WALL APPROXIMATION OF THE DOMAIN WALL FOR ϕ

We define k essence as any scalar field with non-canonical kinetic terms. Following Scherrer,[10,21,22]we introduce a momentum expression via

$$p = V(\phi) \cdot F(X) \tag{5.1}$$

where we define the potential in the manner we have stated for our simulation as well as set[10,21,22]

$$X = \frac{1}{2} \cdot \nabla_{\mu} \phi \quad \nabla^{\mu} \phi \tag{5.2}$$

and use a way to present F expanded about its minimum and maximum[10,21,22]

$$F = F_0 + F_2 \cdot \left(X - X_0\right)^2 \tag{5.3}$$

where we define X_0 via $F_X\big|_{X=X_0} = \left.\frac{dF}{dX}\right|_{X=X_0} = 0$, as well as use a density function[10,21,22]

$$\rho \equiv V(\phi) \cdot \left[2 \cdot X \cdot F_X - F\right] \tag{5.4}$$

where we find that the potential neatly cancels out of the given equation of state so[10,21,22]

$$w \equiv \frac{p}{\rho} \equiv \frac{F}{2 \cdot X \cdot F_X - F} \tag{5.5}$$

as well as a growth of density perturbations terms factor Garriga and Mukhanov[20] wrote as

$$C_x^2 = \frac{\left(\partial p / \partial X\right)}{\left(\partial \rho / \partial X\right)} \equiv \frac{F_X}{F_X + 2 \cdot X \cdot F_{XX}} \tag{5.6}$$

where $F_{XX} \equiv d^2F / dX^2$, and since we are fairly close to an equilibrium value, we pick a value of X close to an extremal value of X_0.[10,21,22]

$$X = X_0 + \tilde{\varepsilon}_0 \tag{5.7}$$

where, when we make an averaging approximation of the value of the potential as very approximately a constant, we may write the equation for the k essence field as taking the form (where we assume $V_\phi \equiv dV(\phi) / d\phi$)

$$\left(F_X + 2\cdot X\cdot F_{XX}\right)\cdot\ddot{\phi} + 3\cdot H\cdot F_X\cdot\dot{\phi} + \left(2\cdot X\cdot F_X - F\right)\cdot\frac{V_\phi}{V} \equiv 0 \tag{5.8}$$

as approximately

$$\left(F_X + 2\cdot X\cdot F_{XX}\right)\cdot\ddot{\phi} + 3\cdot H\cdot F_X\cdot\dot{\phi} \cong 0 \tag{5.9}$$

which may be re written as[10,21,22]

$$\left(F_X + 2\cdot X\cdot F_{XX}\right)\cdot\ddot{X} + 3\cdot H\cdot F_X\cdot\dot{X} \cong 0 \tag{5.10}$$

In this situation, this means that we have a very small value for the growth of density pertubations[10,21,22]

$$C_S^2 \cong \frac{1}{1+2\cdot\left(X_0+\widetilde{\varepsilon}_0\right)\cdot\left(1/\widetilde{\varepsilon}_0\right)} \equiv \frac{1}{1+2\cdot\left(1+\dfrac{X_0}{\cdot\widetilde{\varepsilon}_0}\right)} \tag{5.11}$$

when we can approximate the *kinetic energy* from

$$\left(\partial_\mu\phi\right)\cdot\left(\partial^\mu\phi\right) \equiv \left(\frac{1}{c}\cdot\frac{\partial\phi}{\partial\cdot t}\right)^2 - \left(\nabla\phi\right)^2 \cong -\left(\nabla\phi\right)^2 \rightarrow -\left(\frac{d}{dx}\phi\right)^2 \tag{5.11a}$$

and, if we assume that we are working with a comparatively small contribution w.r.t. time variation but a very large, in many cases, contribution w.r.t. spatial variation of phase

$$\left|X_0\right| \approx \frac{1}{2}\cdot\left(\frac{\partial\phi}{\partial x}\right)^2 >> \widetilde{\varepsilon}_0 \tag{5.11b}$$

$$0 \le C_S^2 \approx \varepsilon^+ << 1 \tag{5.12}$$

And [10,20]

$$w \equiv \frac{p}{\rho} \cong \frac{-1}{1-4\cdot\left(X_0+\widetilde{\varepsilon}_0\right)\cdot\left(\dfrac{F_2}{F_0+F_2\cdot\left(\widetilde{\varepsilon}_0\right)^2}\cdot\widetilde{\varepsilon}_0\right)} \approx 0 \tag{5.13}$$

We get these values for the phase ϕ being nearly a box, i.e. the thin wall approximation for b being very large in Eq. (4.3); this is consistent with respect to Eq. (5.13) main result, with $w \equiv \frac{p}{\rho} \cong 0 \Rightarrow$ treating the potential system given by the first potential (modified sine Gordon with small quantum mechanical driving term added) as a semi classical system leading to Eq. (4.7) nearly being unity. This also applies to the formation of S-S' pair formation due to the di quarks as alluded to in Zhitinisky's[16] formulation of QCD balls with an axion wall squeezer having a 'thin wall' character.

When we observed

$$\left|X_0\right| \approx \frac{1}{2}\cdot\left(\frac{\partial\phi}{\partial x}\right)^2 \cong \frac{1}{2}\left[\delta_n^2\left(x+L/2\right)+\delta_n^2\left(x-L/2\right)\right] \tag{5.14}$$

with

$$\delta_n\left(x\pm L/2\right) \xrightarrow[n\to\infty]{} \delta\left(x\pm L/2\right) \tag{5.15}$$

as the slope of the S-S' pair approaches a box wall approximation in line with thin wall nucleation of S-S' pairs being in tandem with $b \to$ *larger*. Specifically, in our simulation, we had $b \to 10$ above, rather than go to a pure box style representation of S-S' pairs; this could lead to an unphysical situation with respect to delta functions giving infinite values of infinity, which would force both C_s^2 and $w \equiv \frac{p}{\rho}$ to be zero for

$\left|X \approx X_0\right| \cong \frac{1}{2} \cdot \left(\frac{\partial \phi}{\partial x}\right)^2 \to \infty$ if the ensemble of **S-S'** pairs were represented by a pure thin wall approximation,[20] i.e., a box. If we adhere to a finite but steep slope convention to modeling both C_s^2 and $w \equiv \frac{p}{\rho}$, we get the following: When $b \geq 10$ we obtain the conventional results of

$$w \cong \frac{-1}{1-4 \cdot \frac{X_0 \cdot \widetilde{\varepsilon}_0}{F_2}} \to -1 \tag{5.16}$$

and recover Scherrer's solution for the speed of sound [10,21,22]

$$C_S^2 \approx \frac{1}{1+4 \cdot X_0\left(1+\frac{X_0}{2 \cdot \widetilde{\varepsilon}_0}\right)} \to 0 \tag{5.17}$$

(If an example $F_2 \to 10^3, \widetilde{\varepsilon}_0 \to 10^{-2}, X_0 \to 10^3$). Similarly, we would have if $b \to 3$ in Eq. (4.5)

$$w \cong \frac{-1}{1-4 \cdot \frac{X_0 \cdot \widetilde{\varepsilon}_0}{F_2}} \to -1 \tag{5.18}$$

and

$$C_S^2 \approx \frac{1}{1+4 \cdot X_0\left(1+\frac{X_0}{2 \cdot \widetilde{\varepsilon}_0}\right)} \to 1 \tag{5.19}$$

if $F_2 \to 10^3$, $\widetilde{\varepsilon}_0 \to 10^{-2}$. Furthermore $|X_0| \to$ *a small value*, which for $b \to 3$ in Eq. (5) would lead to $C_S^2 \approx 1$, i.e., when the wall boundary of a S-S' pair is no longer approximated by the thin wall approximation. This eliminates having to represent the initial state as behaving like pure radiation state (as Cardone[23] postulated), i.e., we then recover the cosmological constant. When $|X_0| \approx \frac{1}{2} \cdot \left(\frac{\partial \phi}{\partial x} \right)^2 >> \widetilde{\varepsilon}_0$ no longer holds, we can have a hierarchy of evolution of the universe as being first radiation dominated, then dark matter, and finally dark energy.

If $|X \approx X_0| \cong \frac{1}{2} \cdot \left(\frac{\partial \phi}{\partial x} \right)^2 \to \infty$, neither limit leads to a physical simulation that makes sense; so, in this problem, we then refer to the contributing slope as always being large but not infinite. We furthermore have, even with $w = -1$

$$C_s^2 \equiv 1 \xrightarrow[b1 \to 3]{} 1 \tag{5.20}$$

indicating that the evolution of the magnitude of the phase $\phi \to \varepsilon^+$ corresponds with a reduction of our cosmology from a dark energy dark matter mix to the more standard cosmological constant models used in astrophysics. This coincidently is when the semi classical evaluation involving S-S' di quark pairs breaks down, as given by Eq. (4.7) being much smaller than unity and corresponds to the b of Eq. (4.3) for $\phi \to \varepsilon^+$ being quite small. It also denotes a region where there is a dramatic reduction of the degrees of freedom of the FRW space time metric, as Kolb postulated[24,25] so that we can then visualize cosmological dynamics being governed by the Einstein constant at the conclusion of the cosmological inflationary period

VI: CONCLUSION

Veneziano's model [12] gives us a neat prescription of the existence of a Planck's length dimensionality for the initial starting point for the universe via:

$$l_P^2 / \lambda_S^2 \approx \alpha_{GAUGE} \approx e^{\phi} \tag{6.1}$$

where the weak coupling region would correspond to where $\phi << -1$ and λ_S is a so called quanta of length, and $l_P \equiv c \cdot t_P \sim 10^{-33} cm$. As Veneziano implies by his 2nd figure [6], a so called scalar dilaton field with these constraints would have behavior seen by the right hand side of his figure one, with the $V(\phi) \to \varepsilon^+$ but would have no guaranteed false minimum $\phi \to \phi_F < \phi_T$ and no $V(\phi_T) < V(\phi_F)$. The typical string models assume that we have a present equilibrium position in line with strong coupling corresponding to $V(\phi) \to V(\phi_T) \approx \varepsilon^+$ but no model corresponding to potential barrier penetration from a false vacuum state to a true vacuum in line with Coleman's presentation.[5,20] However, FRW cosmology[26] will in the end imply

$$t_P \sim 10^{-42} \text{ sec} onds \Rightarrow size \quad of \quad universe \approx 10^{-2} cm \tag{6.2}$$

which is still huge for an initial starting point, whereas we manage to in our S-S' 'distance model' to imply a far smaller but still non zero radii for the initial 'universe' in our model.

We find that the above formulation in Eq. (6.1) is most easily accompanied by the given S-S' di quark pair basis for the scalar field used in this paper, and that it also is consistent with the initial scalar cosmological state evolving toward the dynamics of the cosmological constant via the *k* essence argument built up near the end of this document.

Furthermore, we also argue that the semi classical analysis of the initial potential system as given by Eq. (4.7) and its subsequent collapse is de facto evidence for a phase transition to conditions allowing for CMB to be created at the beginning of inflationary cosmology.

We are fortunate as shown in **Appendix V** that for determining the relative good fit of Eq. (4.7) that the relative domain walls slope of the initial phase given by Eq. (4.5) was not terribly significant, for the first potential system, which dove tails with Eq. (4.1) merely pushing out the domain walls, as a primary effect, for a driven sine Gordon type modeling of false vacuum nucleation. As ,mentioned earlier, this was actually heightened by the extra dimensionality as alluded to by the power law relationship in Eq. (4.1) making an almost perfect equality between the left and right hand sides of Eq. (4.7). That the ratio Eq. (4.7) in **Appendix V** had varying values, showing different degrees of break down of this relationship for the 2^{nd} transitional potential, due to differences in dimensionality and slope of the scalar field as given by Eq. (4.3) is probably due to this representing the abrupt loss of numbers of degrees of freedom Rocky Kolb has mentioned as part of a phase transition. Needless to say though, as we evolve toward the Einstein cosmological constant era and chaotic inflation, as given by the 3^{rd} potential, we should keep in mind very real limits as to the comparative sharpness of the slope of the scalar field as given by Eq. (4.3)

K essence analysis argues against making *b* in Eq. (4.3) too large, i.e., if we have a 'perfect' thin wall approximation to our S-S' di quark pairs, we will have the unphysical speed of sound results plus other consequences detailed in the k essence section of the document which we do not want. On the other hand, the semi classical analysis brought

up in the section starting with Eq. (4.5), Eq. (4.6) and summarized by Eq. (4.7) shows us that a close to the thin wall approximation for S-S' di quark pairs gives an optimal fit for consistency in the potential with the wave functions exhibiting a thin wall approximation 'character'. It is useful to note that our kinetic model can be compared with the very interesting Chimentos [27]purely kinetic k –essence model, with density fluctuation behavior at the initial start of a nucleation process. The model indicate our density function reach $\rho =$ constant after passing through the tunneling barrier as mentioned in our nucleation of a S-S' pair ensemble. This is when the Einstein constant becomes dominant and that the semi classical approximation in Eq. (4.7) for a domain wall at the time the comparative thin wall approximation S-S' pair ceases to be relevant.

Our initial attempt here very likely should be re visited, especially if the sort of brane world objects referred to by Trodden et a[28] are used in a future calculation for initial nucleation states. However, this should all be done to re calibrate how to fill in the CMB contribution toward reconstruction of a suitable class of potentials which could shed light not only on the origins of baryogenesis, in early universe models, but also in determining how dark matter-dark energy could contribute to the formation of initial inflationary cosmology parameters. The hope is that if suitable data reconstruction methodology is obtained and refined, that one could as an example determine how the initial physical fundamental constants could be set as they are, as well understand how dark matter-dark energy contribute to the initial origins of CMB itself This also would allow us to improve upon the particle flux from nucleation argument we used, using Gongs [29] approximate construction in order to get around limitations in least action principles due to tiny spatial dimensions.

[Insert figures 1a, 1b, and then figures 2a, 2b *with captions* here]

Furthermore, we should note that these nucleation configurations fit in well with the following model of false vacuum nucleation.

[Insert figure 3 *with caption* here]

This is in line with the first specified potential as given in Eq. (3.2a) which we claim eventually becomes in sync with Eq. (3.2c). Further progress in investigating this phenomenology should take into account the datum so mentioned in the text, about the original multiple dimensions in the initial phases of a nucleating universe, which subsequently are reduced as the scalar potential evolves toward the chaotic potential given in Eq. (3.2c). This should permit us to be able to reconstruct potentials far closer to the big bang itself, than the 1000 or so year limit alluded to by Dr. Kadota in his May 2005 Pheno talk given in Madison, Wisconsin[30]. This in its own way will entail considerable additional analytical work, along the lines first specified by *Edmund J. Copelan et al.* in their ground breaking tome on potential reconstruction techniques applied to cosmology[31] .It is worthwhile to note that the orientation of my white paper was in unifying certain techniques, and methodology of what is known in the literature as QCD balls in an instanton configuration to use data reconstruction in order to obtain information on dark matter physics. In doing so, I wound up using a lot of ideas, as was done by other physicists considering early universe nucleation models, from condensed matter physics. The emphasis though of the presented concept was in setting up a template as to examine what actually constitutes dark matter. This should be what future inquiry should be directed toward.

Figure captions

Fig 1a,b: Evolution of the phase from a thin wall approximation to a more nuanced thicker wall approximation with increasing L between S-S' instanton components. The 'height' drops and the 'width' L increases correspond to a de evolution of the thin wall approximation. This is in tandem with a collapse of an initial nucleating 'potential' system to the standard chaotic scalar ϕ^2 potential system of Guth. As the 'hill' flattens, and the thin wall approximation dissipates, the physical system approaches standard cosmological constant behavior.

Fig 2a,b: As the walls of the S-S' pair approach the thin wall approximation, a normalized distance, $L = 9 \rightarrow \boldsymbol{L} = 6 \rightarrow L = 3$, approaches delta function behavior at the boundaries of the new nucleating phase. As L increases, the delta function behavior subsides dramatically. Here, the $L = 9 \Leftrightarrow$ conditions approaching a cosmological constant. $\boldsymbol{L} = 6 \Leftrightarrow$ conditions reflecting Scherrer's dark energy-dark matter mix. $L = 3 \Leftrightarrow$ approaching unphysical delta function contributions due to a pure thin wall model.

Fig 3: Initial configuration of the domain wall nucleation potential as given by Eq. (4.4a) which we claim eventually becomes in sync with Eq. (4.4c) due to the phase transition alluded to by Dr. Edward Kolbs model of how the initial degrees of freedom declined from over 100 to something approaching what we see today in flat Euclidian space models of space time (i.e. the FRW metric used in standard cosmology)

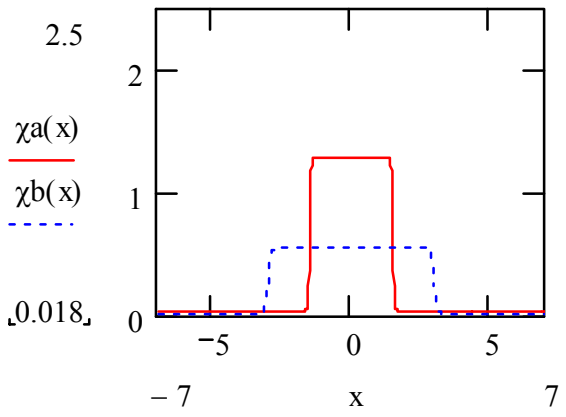

Figure 1a, 1b

Beckwith

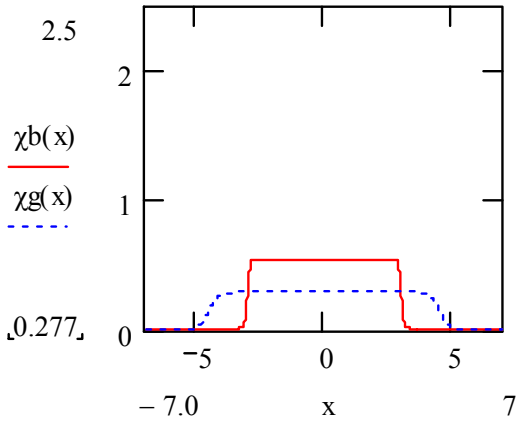

Figure 2a, 2b

Beckwith

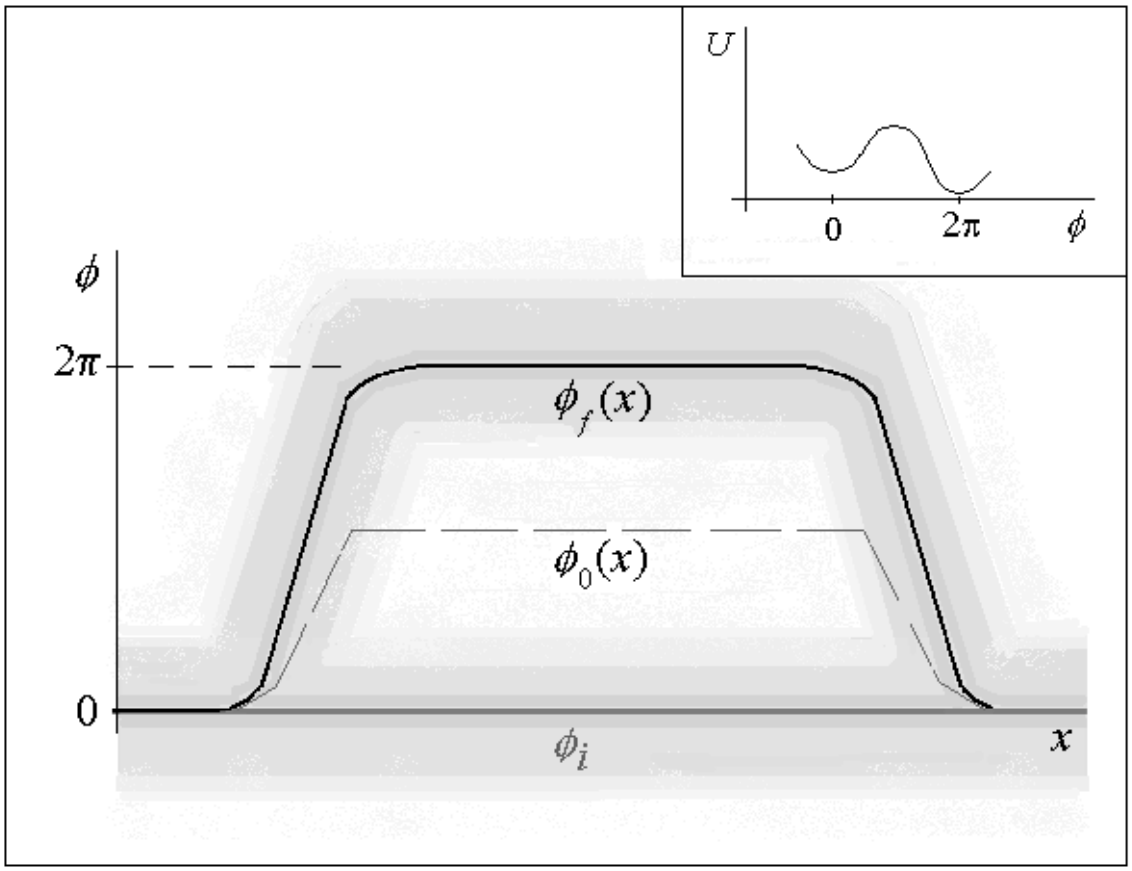

Figure 3

Beckwith

APPENDIX IA: INITIAL STATEMENT OF KADOTAS POTENTIAL RECONSTRUCTION METHODOLOGY

Kenji Kadot*a* of FNAL in Pheno 2005 [30] and also in arXIV [3] talked of comparing two graphs, one with a combination of scalar potential terms $\left[3\cdot\left(\frac{V'}{V}\right)^2-2\cdot\frac{V''}{V}\right]$ against $[(\xi)]$ (Mpc) with a graph of

$m(j)$ against ***mode numbers***. Here, in this situation,

$$m(j)= \text{ linear combination of } \{P(j)\} \tag{1a}$$

And when we set t_{END} = the demarcation of the end of time for the inflation, for a scale factor a leads to

$$\xi \equiv -\int_{t}^{t_{END}} \frac{dt'}{a(t')} \tag{1b}$$

In this situation, the $\{P(j)\}$ refer to pixel data slices which show up in

$$\left[3\cdot\left(\frac{V'}{V}\right)^2-2\cdot\frac{V''}{V}\right]\equiv\sum_i p_i\cdot B_i(\ln\xi) \tag{2}$$

We should identify the left hand side of equation 2 with the derivative of a function $G(\xi)$, i.e.

$$\frac{dG(\xi)}{d\xi}\equiv\sum_i p_i\cdot B_i(\ln\xi) \tag{2a}$$

This is when Kadota et al defined

$$B_i(\ln\xi)=\begin{cases}1\\0\end{cases} \quad \text{with a value of 1 iff} \quad \ln\xi_i<\ln\xi<\ln\xi_{i+1} \tag{3}$$

In the most recent arXIV article, Kadota defined a procedure as to how to identify useful entries as to acceptable $\{P(j)\}$ values as to a simplified scalar potential structure which is $V(\phi) \equiv \left(V_0 \cdot e^{\lambda \cdot (\phi - \phi_0)}\right) \cdot \left[1 + c \cdot e^{-\nu \cdot (\phi - \phi_0)^2}\right]$ for a perturbation centered at $\phi \equiv \phi_0$ where this has $|\lambda|, c << 1, \ |\nu| >> 1$, so then after Kadota defined

$$\phi \cong \lambda \cdot \ln \xi \tag{4}$$

so one could write

$$\phi_0 \equiv \lambda \cdot \ln \xi_0 \tag{5}$$

He, Kadota, obtained graphical behavior as seen in his fig 8 and fig 9 of his arXIV article[3]. An even simpler situation graphically emerged when Kadota set the left hand side of Eq. (1a) equal to a constant which permitted him, using Eq. (2)and Eq. (3)above to give constant values to the p_i pixels, which was equivalent to his figure 7 which was for a potential system leading to a constant spectral index value, *n* when he defined via linking *n* – 1 to the derivative with respect to *k* of an expression of the primordial power spectrum $\mathrm{P}(k)$ via

$$n - 1 = \frac{d\mathrm{P}(k)}{dk} \tag{6}$$

Here, in this situation we have that if we interpret $\vartheta(1)$ as an order of magnitude constant of about $1 < \vartheta(1) < 10$. We should also note that often $\vartheta(1)$ is often set very close to 1 itself.

$$k = \vartheta(1) \cdot a \cdot H \equiv a \cdot H \tag{7}$$

The exact particulars of the power spectra $\mathrm{P}(k)$ are in Kadoka's well written arXIV paper, but it suffices to say that the natural logarithm of the power spectra $\mathrm{P}(k)$ is equal

to an integral over ξ values from zero to infinity, with part of the integrand involving a so called 'window function' times the power spectra $\mathrm{P}(k)$, for $G(k)$ of equation 2.2a above. I do believe one can say the following:

Kenji Kadoka's methodology permits the general reconstruction of potentials as up to about 1000 years after the big bang. The issue at stake though is if or not re constructive methodology using some of these same methods could be countenanced going up to the end of the 60 e-folding period commonly viewed as the demarcation between flat and curved space, with a curved space milieu being the regime of active nucleation of our universe. This would entail, among other things, finding traces in CMB data of the initial signature of the big bang itself and tying it into a QCD style phase transition.

APPENDIX I B: USING JDEM ANALYSIS OF DATA WITH THIS BUILT UP POTENTIAL SYSTEM, WITH KADOTAS POTENTIAL RECONSTRUCTION PROCEDURES

The first step would be to refine the analytical algorithms to, give reliable data inputs into the right hand side [3,30] of $\frac{dG(\xi)}{d\xi} \equiv \sum_i p_i \cdot B_i(\ln \xi)$, where the left hand side of this equation actually could use, in a modified format the procedure given in Eq (3.2a) to Eq (3.2c) of the main text , and this done to obtain a match up of the acceptable p_i entries with CMB data.

This would entail use of Monte Carlo simulations as well as far more developed analysis of how to obtain acceptable p_i entries in a more realistic manner than the toy problem

analyzed by *Kadoka's* toy problem[3,30] example which he presented in fig 7 of his arXIV article[3].

Afterwards, once acceptable procedures are outlined as to finding acceptable p_i entries for potentials other than the potential given by Kadoka's test scalar potential given as

$$V(\phi) \equiv \left(V_0 \cdot e^{\lambda \cdot (\phi - \phi_0)}\right) \cdot \left[1 + c \cdot e^{-\nu \cdot (\phi - \phi_0)^2}\right] \quad (1)$$

The potential reconstruction I believe could be greatly aided by some of the initial effective contributions of extra dimensionality and of side effects of the baryogenesis mentioned in the formation of our early universe potential nucleation model The idea would be to find ways to obtain data sets via techniques most congruent to reliable potential reconstruction of the early inflationary cosmos. Before the 1000 or so year limit specified by Kenji Kadota in discussions I had with him at Pheno 2005 [30].

If finding acceptable match up of data sets with how to reconstruct a complicated potential beyond the one given by Eq (1) above was completed in general. Then one would face a discussion with manufacturers of the satellite used for dark matter searching as to tailor made electronics which would be acceptable for obtaining sufficient data sets. I am assuming that this investigation would be one out of many being used in the upcoming satellite mission.

APPENDIX II: LINKS TO THE POTENTIAL SYSTEM USED FOR COSMOLOGICAL NUCLEATION

$$\begin{array}{lll} V_1 & \to V_2 & \to V_3 \\ \phi(increase) \le 2\cdot\pi & \to \phi(decrease) \le 2\cdot\pi & \to \phi \approx \varepsilon^{+} \\ t \le t_P & \to t \ge t_P + \delta\cdot t & \to t >> t_P \end{array} \tag{1}$$

We described the potentials V_1, V_2, and V_3 in terms of S-S' di quark pairs nucleating and then contributing to a chaotic inflationary scalar potential system.

$$V_1(\phi) = \frac{M_P^2}{2}\cdot(1-\cos(\phi)) + \frac{m^2}{2}\cdot(\phi-\phi^*)^2 \tag{2a}$$

$$V_2(\phi) \approx \frac{(1/2)\cdot m^2\phi^2}{(1+A\cdot\phi^3)} \tag{2b}$$

$$V_3(\phi) \approx (1/2)\cdot m^2\phi^2 \tag{2c}$$

APPENDIX III: INCLUDING IN NECESSARY AND SUFFICIENT CONDITIONS FOR FORMING A CONDENSATE STATE AT OR BEFORE PLANCK TIME t_P

For a template for the initial expansion of a scalar field leading to false vacuum inflationary dynamics in the expansion of the universe, Zhitnitsky's[4] formulation for how to form a condensate of a stable soliton style configuration of cold dark matter is a useful starting point for how an axion field can initiate forming a so called QCD ball. Zhitnitsky[4] uses quarks in a non-hadronic state of matter that, in the beginning, can be in di quark pairs. A di quark pair would permit making equivalence arguments to what is done with cooper pairs and a probabilistic representation as to find the relative 'size' of

the cooper pair. We assume an analogous operation can be done with respect to di quark pairs. In doing so, calculations[4] for quarks being are squeezed by a so called QCD phase transition due to the violent collapse of an axion domain wall. The axion domain wall would be the squeezer to obtain a so called S-S' configuration. This presupposes a formation of a highly stable soliton type configuration in the onset due to the growth in baryon mass

$$M_B \approx B^{8/9} \tag{1}$$

This is due to a large baryon (quark) charge B which Zhitnitsky[4] finds is smaller than an equivalent mass of a collection of free separated nucleons with the same charge. This provides criteria for absolute stability by writing a region of stability for the QCD balls dependent upon the inequality occurring for $B. > B_C$ (a critical charge value)

$$m_N > \frac{\partial M_B}{\partial B} \tag{2}$$

He[19] furthermore states that stability, albeit not absolute stability is still guaranteed for the formation of meta stable states occurring with

$$1 << B < B_C \tag{3}$$

If we make the assumptions that there is a balance between Fermi pressure P_f and a pressure due to surface tension, with σ being an axion wall tension value[4] so that

$$\left(P_\sigma \cong \frac{2\sigma}{R} \right) \equiv \left(P_f \cong -\frac{\Omega}{V} \right) \tag{4}$$

This pre supposes that Ω is some sort of thermodynamic potential of a non interacting Fermi gas, so that one can then get a mean radius for a QCD ball at the moment of formation of the value, when assuming $\tilde{c} \approx .7$, and also setting $B \approx B_C \propto 10^{+33}$ so that

$$R \equiv R_0 \cong \left(\frac{\widetilde{c} \cdot B^{4/3}}{8 \cdot \pi \cdot \sigma} \right)^{1/3} \tag{5}$$

If we wish to have this of the order of magnitude of a Planck length l_P, then the axion domain wall tension must be huge, which is not unexpected. Still though, this pre supposes a minimum value of B which Zhitnitsky[4] set as

$$B_C^{\exp} \sim 10^{20} \tag{6}$$

We need to keep in mind that Zhitnitsky[4] set this parameterization up to account for a dark matter candidate. I am arguing that much of this same concept is useful for setting up an initial condensate of di quark pairs as, separately S-S' in the initial phases of nucleation, with the further assumption that there is an analogy with the so called color super conducting phase (CS) which would permit di quark channels. The problem we are analyzing not only is equivalent to BCS theory electron pairs but can be linked to creating a region of nucleated space in the onset of inflation which has S-S' pairs. The S-S' pairs would have a distance between them proportional to distance mentioned earlier, R_0, which would be greater than or equal to the minimum Planck's distance value of l_P. The moment one would expect to have deviations from the flat space geometry would closely coincide with Rocky Kolb's model for when degrees of freedom would decrease from over 100 degrees of freedom to roughly ten or less during an abrupt QCD phase transition[4]. The QCD phase transition would be about the time one went from the first to the second potential systems mentioned above.

APPENDIX IV A: WAVE FUNCTIONALS USED IN THIS MODEL AND THEIR ANALOGIES TO BLACK HOLE NUCLEATION

This idea of pair creation arose once again in a later context in an article by Dias and Lemos called 'Pair creation of black holes on a cosmic string background' where the so called 'amplitude' for the propagation from 'nothing' to a three dimensional surface boundary Σ was given by the wave function [32](wave functional):

$$\psi\left(h_{ij}, A_i\right) = \int d\left[g_{uv}\right] \cdot d\left[A_u\right] \cdot \exp\left(-I\left(g_{uv}, A_u\right)\right) \tag{1}$$

where h_{ij} and A_i are the induced metric and electromagnetic potential on the boundary $\Sigma = \partial M$ of a compact manifold M , and $I\left(g_{uv}, A_u\right)$ is the Euclidian action , with $d\left[g_{uv}\right]$ and $d\left[A_u\right]$ measures of the metric g_{uv} and the Maxwell field A_u . Diaz and Lemos further state that a semi classical instanton approximation allows us to state that dominant contributions to the path integral come from metrics and Maxwell fields where are near the solutions which extremalize the Euclidian action and satisfy boundary conditions. So if we have this process, we may construct a wave function that that denotes the creation of a black hole via

$$\psi_{inst} \equiv B \cdot \exp\left(-I_{inst}\right) \tag{2}$$

where B is a one loop contribution from quadratic fluctuations in the fields, $\delta^2 I$, and I_{inst} is the classical action of the gravitational instanton that mediates the pair creation of black holes. Similarly, the wave function which describes the nucleation of a *dS* de Sitter space from nothing is:

$$\psi_{dS} \propto \exp(-I_{ds}) \tag{3}$$

where $I_{dS} = -\frac{3 \cdot \pi}{2 \cdot \Lambda}$ is the action of the S^4 gravitational instanton which according to Lemos 'mediates' this nucleation. So , then the nucleation probability of the *dS* space from nothing and then the *dS* space with a pair of black holes from nothing is given by $|\psi_{dS}|^2$ and $|\psi_{inst}|^2$ respectively. This then allows us to state then that if we take the ratio of these two probabilities that we obtain the pair creation rate of black holes in the *dS* background as

$$\Gamma \cong \eta \cdot \exp(-2 \cdot I_{inst} + 2 I_{dS}) \tag{4}$$

For the Bogomol'nyi inequality approach[6,7] we modify a de facto 1+1 dimensional problem in condensed matter physics to being one which is quasi one dimensional by making the following substitution, namely looking at the Lagrangian density ς to having a time independent behavior denoted by a sudden pop up of a S-S' pair via the substitution of the nucleation 'pop up' time by[6,7]

$$\int d\tau \cdot dx \cdot \varsigma \to t_P \cdot \int dx \cdot L \tag{5}$$

where t_P is the Planck's time interval. Then afterwards, we shall use the substitution of $\hbar \equiv c \equiv 1$ so we can write

$$\psi \propto c \cdot \exp\left(-\beta \cdot \int L \, dx\right) \tag{6}$$

A

PPENDIX IV B: REDUCING THE GIVEN WAVE FUNCTIONAL TO HAVING GAUSSIAN FUNCTIONAL BEHAVIOR

We wish to give an argument as to how we obtain [6,7]

$$\Psi_{i,f}\ \left[\phi(\mathbf{x})\right]\Big|_{\phi=\phi_{ci,cf}}\ =\ c_{i,f}\cdot\exp\left\{-\int d\mathbf{x}\ \alpha\left[\phi_{Ci,f}(\mathbf{x})-\phi_0(\mathbf{x})\right]^2\right\}, \tag{1}$$

In both cases, we find that the coefficient in front of the wave functional in Eq. (1) is normalized due to error function integration

This is due to

We also found that in order to have a Gaussian potential in our wavefunctionals that we needed to have in both interpretations

$$\frac{(\{\ \})}{2}\equiv\Delta E_{gap}\equiv V_E(\phi_F)-V_E(\phi_T) \tag{2}$$

where for the Bogomol'nyi interpretation of this problem we worked with potentials (generalization of the extended Sine-Gordon model potential) [6,7]

$$V_E\cong C_1\cdot(\phi-\phi_0)^2-4\cdot C_2\cdot\phi\cdot\phi_0\cdot(\phi-\phi_0)^2+C_2\cdot\left(\phi^2-\phi_0^2\right)^2 \tag{3}$$

We had a Lagrangian[15] we modified to be (due to the Bogomil'nyi inequality)

$$L_E\geq|Q|\ +\ \frac{1}{2}\cdot(\phi_0-\phi_C)^2\cdot\{\ \} \tag{4}$$

with topological charge $|Q|\to 0$ and with the Gaussian coefficient found in such a manner as to leave us with wave functionals [1,3,10] we generalized for charge density

transport .This same Eq. (1) was more or less assumed in the Gaussian wavefunctional ansatz interpretation while

$$\Psi_f[\phi(\mathbf{x})]\big|_{\phi\equiv\phi_{Cf}} = c_f\cdot\exp\left\{-\int d\mathbf{x}\;\alpha\left[\phi_{C\,f}(\mathbf{x})-\phi_0(\mathbf{x})\right]^2\right\}\rightarrow c_2\cdot\exp\left(-\alpha_2\cdot\int d\tilde{x}[\phi_T]^2\right)\cong\Psi_{final}, \tag{5}$$

and

$$\Psi_i[\phi(\mathbf{x})]\big|_{\phi\equiv\phi_{Ci}} = c_i\cdot\exp\left\{-\alpha\int d\mathbf{x}[\phi_{ci}(\mathbf{x})-\phi_0]^2\right\}\rightarrow c_1\cdot\exp\left(-\alpha_1\cdot\int d\tilde{x}[\phi_F]^2\right)\equiv\Psi_{initial}, \tag{6}$$

APPENDIX V: EXTRA DIMENSIONS AND THE BREAK DOWN OF THE SEMI - CLASSICAL APPROXIMATION.THIS IS AN ILLUSTRATION OF THIS CONCEPT, AND NOTHING MORE

Here, I used equation 4.7 of the main text. For the first potential system, if we set xb=1, xa= - 1, and b = 10. (a sharp slope) for the scalar field boundary we have.

$$\alpha := \frac{.373}{1} \tag{1}$$

This assumes a Gaussian wave functional of

$$\psi(x) := \exp(-\alpha\cdot\phi(x)) \tag{2}$$

As well as a power parameter of

$$\nu := 9 \tag{3}$$

Also, we are using, initially, a phase evolution parameter of

$$\phi(x) := \pi \cdot [\tanh[b \cdot (x - xa)] - \tanh[b \cdot (xb - x)]] \tag{4}$$

The first potential system is re scaled as

$$V1(x) := \frac{1}{2} \cdot (1 - \cos(\phi(x))) - \frac{1}{200} \cdot (\phi(x) - \pi)^2 \tag{5}$$

In addition, the following is used as a rescaling of the inner product

$$c1 := \frac{1}{\int_{-30}^{30} (\exp(-\alpha \cdot \phi(x)))^2 \cdot \frac{\pi^3}{3} \cdot x^5 \, dx} \tag{6}$$

$$c2 := \int_{-30}^{30} (\exp(-\alpha \cdot \phi(x)))^2 \cdot \frac{\pi^3}{3} \cdot x^5 \cdot (V1(x))^{\nu} \cdot |c1| \, dx \tag{7}$$

$$c3 := \left[\int_{-30}^{30} (\exp(-\alpha \cdot \phi(x)))^2 \cdot \frac{\pi^3}{3} \cdot x^5 \cdot V1(x) \cdot |c1| \, dx \right]^{\nu} \tag{8}$$

$$c3b := \frac{c2}{c3} \tag{9}$$

Here,

C3b = .999 (9a)

For the 2nd potential system, if we assume a sharp slope, i.e. b1 = b = 10, and

$$V2(x) := \frac{1}{2} \cdot \frac{(\phi a(x))^2}{1 + .000001 \cdot (\phi a(x))^3} \tag{10}$$

If

$$\phi a(x) := \pi \cdot [\tanh[b1 \cdot (x - xa)] - \tanh[b1 \cdot (xb - x)]] \tag{11}$$

and a modification of the 'Gaussian width' to be

$$\alpha 1 := \frac{.373}{30} \tag{12}$$

We do specify a denominator, due to a normalization contribution we write as

$$c1a := \frac{1}{\int_{-30}^{30} \left(\exp(-\alpha 1 \cdot \phi a(x))\right)^2 \cdot \frac{\pi^3}{3} \cdot x^5 \, dx} \tag{13}$$

$$c4 := \int_{-30}^{30} \left(\exp(-\alpha 1 \cdot \phi a(x))\right)^2 \cdot \frac{\pi^3}{3} \cdot x^5 \cdot (V2(x))^{\nu} \cdot |c1a| \, dx \tag{14}$$

In addition:

$$c5 := \left[\int_{-30}^{30} \left(\exp(-\alpha \cdot \phi a(x))\right)^2 \cdot \frac{\pi^3}{3} \cdot x^5 \cdot V2(x) \cdot |c1a| \, dx \right]^{\nu} \tag{15}$$

We then use a ratio of

$$c5b := \frac{c4}{c5} \tag{16}$$

Here, when one has the six dimensions, plus the thin wall approximation:

$$C5b = 2.926E\text{-}3 \tag{17}$$

When one has three dimensions, plus the thin wall approximation

$$c6 := \int_{-30}^{30} \left(\exp\left(-\alpha 1 \cdot \phi a(x)\right)\right)^2 \cdot \frac{\pi}{.25}^{1} \cdot x^2 \cdot (V2(x))^{\nu} \cdot |c1b| \, dx \tag{18}$$

$$c7 := \left[\int_{-30}^{30} \left(\exp\left(-\alpha \cdot \phi(x)\right)\right)^2 \cdot \frac{\pi}{.25}^{1} \cdot x^2 \cdot V2(x) \cdot |c1b| \, dx \right]^{\nu} \tag{19}$$

$$c7b := \frac{c6}{c7}. \tag{20}$$

This leads to

$$c7b = .019 \tag{21}$$

When one has the thin wall approximation removed, via b1 = 1.5, one does not see a difference in the ratios obtained.

For the 3rd potential system, which is intermediate between the 1st and 2nd potentials if the b1 = b = 10 value is used, one obtains for when we have six dimensions

$$\alpha 1 := \frac{.373}{6} \tag{22}$$

As well as

$$V2(x) := \frac{1}{2} \cdot \frac{\left(\phi a(x)\right)^2}{1 + .5 \cdot \left(\phi a(x)\right)^3} \tag{23}$$

(When we have six dimensions)

$$C5b = 0.024 \tag{24}$$

(When we have three dimensions)

C7b = .016 (25)

So, then one has C5b = .024, and C7b = .016 in the thin wall approximation

When b1 = 3 (non thin wall approximation)

C5b = .027 (26)

(**Six dimensions**)

C7b = .02 (27)

(**Three dimensions**)

Summarizing, if

$$V1(x) := \frac{1}{2}\cdot\left(1 - \cos\left(\phi(x)\right)\right) - \frac{1}{200}\cdot\left(\phi(x) - \pi\right)^2 = V1 \quad (28)$$

$$V2(x) := \frac{1}{2}\cdot\frac{\left(\phi a(x)\right)^2}{1 + .000001\cdot\left(\phi a(x)\right)^3} = V3 \quad (29)$$

$$V2(x) := \frac{1}{2}\cdot\frac{\left(\phi a(x)\right)^2}{1 + .5\cdot\left(\phi a(x)\right)^3} = V2 \quad (30)$$

One finally obtains the following results, as summarized below

	b=b1 = 10	b1 = 3	b1 = 1
V1 (6 dim)	C3b = .999	No data	No data
V3 (6 dim)	C5b = 2.926E-3	No data	C5b = same value
V3 (3 dim)	C7b = .019	No data	C7b = same value
V2(6 dim)	C5b = .027	C5b = .024	No data
V2 (3 dim)	C7b = .02	C7b = .016	No data

APPENDIX VI: **DECAY RATES, AND COSMIC NUCLEATION, I.E. PRESENTING A NEW WAY TO OBTAIN INITIAL EVOLUTION OF THE HUBBLE PARAMETER AND A RATE EQUATION**

Garriga [33], assuming a nearly flat De Sitter universe also came up with an expression for the number density of particles per unit length (time independent)

$$n \approx \frac{1}{2 \cdot \pi} \cdot \sqrt{M^2 + e \cdot \frac{E_0^2}{H^2}} \cdot \exp\left(-S_E\right) \tag{1}$$

where for our purposes we would set

$$M \leq M_P \to 1 \tag{2}$$

We prefer instead to use an estimation of a nucleation rate per Hubble volume per Hubble time[29]

$$\in (t) \equiv \lambda_0 \Big/ \left(H(t)^4\right) \approx 1 \tag{3}$$

to show the influence an evolving Hubble parameter would have , in early times, without the complexity of predicting the S_E (a Euclidian action integral) which would be in our example a D+1 dimensional space knocked down to being quasi 1 dimensional in 'character' . We assume, also, rescaling of Planckian length to be unity where $\hbar \equiv c \equiv G \equiv 1$.

This leads to, then

APPENDIX VII: PREDICTING HOW A SCALE FACTOR EVOLVES IN THE BEGINNING OF INFLATIONARY COSMOLOGY

I wish now to look at how the scale factor, a, changes in time, in a manner we view which will enable us to delineate Hubble parameter variations in the first few moments after creation. In doing this, we can note the typical value[34] (as given by Dodelson)

$$a(t) \cong a_B \cdot \exp\left(H_B\left(t - t_B\right)\right) \tag{1}$$

with a_B , H_B and t_B being scale factor, Hubble parameter, and time values at the end of an inflationary period of expansion. Needless to say, in doing this, we are not obtaining values of what the scale factor and Hubble parameter could be at the onset of inflation, which is a situation we wish to remedy. So we set

$$\widetilde{a}_0 \equiv a_B \exp\left(H_B\left(t_P - t_B\right)\right) \tag{2}$$

and afterwards approximate the evolution of phase after time t_P via use of

$$\phi \equiv \widetilde{\phi}_0 - \frac{m}{\sqrt{12 \cdot \pi \cdot G}} \cdot t \cong \widetilde{\phi}_i \cdot \left(\exp(-\widetilde{a}_0 \cdot t / \alpha) \approx 1 - \widetilde{a}_0 \cdot t / \alpha \right) \tag{3}$$

If we assume that $\widetilde{\phi}_0 \cong \widetilde{\phi}_i$,and that the time factors are small, we can state

$$\frac{m}{\sqrt{12 \cdot \pi \cdot G}} \cong \frac{\widetilde{a}_0}{\alpha} \tag{4}$$

as an order of magnitude estimate for the initial value of our scale factor at the beginning of inflation. So being the case, we move then to obtain a value for the initial evolution of the Hubble parameter via use of conformal time, with an Einstein equation

$$\ddot{\phi} + 2 \cdot a \cdot H \cdot \dot{\phi} + a^2 \cdot m^2 \left(\phi - \phi^*\right) = 0 \tag{5a}$$

where the conformal time we write as

$$\widetilde{t} \cong -\frac{1}{a(t) \cdot H} \tag{5b}$$

which may be re written using ordinary time as

$$\ddot{\phi} + 3 \cdot H \cdot \dot{\phi} + m^2 \left(\phi - \phi^*\right) = 0 \tag{5c}$$

which would lead to $\in(t) \equiv \lambda_0 \Big/ \left(H(t)^4\right) \approx 1$ [29] implying a nucleation rate evolution along the lines of

$$H \cong \frac{1}{3} \cdot \left(\frac{\tilde{a}_0}{\alpha}\right)^{-1} + \left(\frac{\tilde{a}_0}{\alpha}\right)\frac{m^2}{3} \cdot \left(1 - \frac{\phi^*}{\phi_0} \cdot \exp(\frac{\tilde{a}_0}{\alpha} \cdot \tilde{t})\right) \tag{6}$$

implying

$$\lambda_0\left(t_P + \delta \cdot t\right) \approx H^4\left(t_P + \delta \cdot t\right) \tag{7}$$

which for small times just past the initial value of $t \equiv t_P + \delta \cdot t$ leads to a nearly stable but increasing rate of the Hubble parameter right after a nucleation of a universe. This also leads to a phase change in behavior which I claim is motivated by the pre Planck time value of the Hubble parameter being set by (for times $t \le t_P$)

$$H^2 \equiv \frac{8 \cdot \pi}{3} \cdot G \cdot V(\phi) \to \frac{8 \cdot \pi}{3} \cdot V(\phi) \tag{8}$$

with the potential given by a washboard potential with a small driving potential proportional to $\left(\phi - \phi^*\right)^2$ which blends into Guths chaotic inflationary model for times $t_P + \delta \cdot t$.

BIBLOGRAPHY

[1] A.W. Beckwith, white paper (appropriately) submitted to the Dark Energy Task Force, accepted June 28, 2005 by Rocky Kolb and Dana Lehr

[2] Qin, U.Pen, and J. Silk: arXIV : astro-ph/0508572 v1 26 Aug 2005 : *Observational Evidence for Extra dimensions from Dark Matter*

[3] Precision of Inflaton Potential Reconstruction from CMB Using the General Slow-Roll Approximation by *K. Kadota*, *S. Dodelson*,W. *Hu*, and *E. D. Steward* arXIV:astro-ph/0505185 v1 9 May 2005

[4] 'Dark Matter as Dense Color Superconductor' By A.R. Zhitnitsky arXIV: astro-ph/0204218 v1 12 April 2002

[5] R.Buniy, S. Hsu: arXiv:hep-th/0504003 v3 8 Jun 2000

[6] *A.W. Beckwith* 'Making an analogy between a multi-chain interaction in Charge Density Wave transport and the use of wave functionals to form S-S' pairs' International Journal of Modern Physics B (Accepted in 7 28 05), in October 2005 edition of IJMPB

[7] A.W. Beckwith 'An open question: Are topological arguments helpful in setting initial conditions for transport problems in condensed matter physics?' Modern Physics Letters B (Accepted in 10-28, 05), to be published. Also as arXIV math-ph/0411031

[8] A. Guth . arXIV :astro-ph/0002156 v1 7 Feb 2000, A. Guth . arXIV :astro-ph/0002186 v1 8 Feb 2000, A. H. Guth, Phys. Rev. D 23, 347-356 (1981)

[9] A.W.Beckwith arXIV math-ph/0410060 'How false vacuum synthesis of a universe sets initial conditions which permit the onset of variations of a nucleation rate per Hubble volume per Hubble time'

[10] A.W. Beckwith ' How the alteration of a thin wall for S-S' di quark pairs signifies an Einstein constant dominated cosmology and the break down of semi classical approximations for Inflation' Will be included in PANIC 2005 conference proceedings, by the AIP. January 2006. Copywrite form for this already signed

[11] R. Aloisio, A. Galante, A. Grillo, S. Liberati, E. Luzio, F. Mendez " Deformed special relativity as an effective theory of measurements on quantum gravitational backgrounds' arXIV:gr-qc/0511031 v1 Nov 6 , 2005

[12] G. Veneziano : arXIV : hep-th/0002094 v1 11 Feb 2000

[13] Edward (Rocky) Kolb in presentation at SSI 2005, Stanford Linear accelerator cosmology school. Also a datum which was given to me at 2005 CTEQ Summer school of QCD phenomenology, La Puebla, Mexico.

[14] Private communications with Joseph Lykken, in FNAL, 2004

[15] E. Volt, and G.H. Wannier, Phys. Rev 95, 1190(1954)

[16] R.J. Scherrer, arXIV astro-ph/0402316 v3 , May 6, 2004

[17] A. Guth. arXIV: astro-ph/0002156 v1 7 Feb 2000, A. Guth. arXIV :astro-ph/0002186 v1 8 Feb 2000, A. H. Guth, Phys. Rev. D 23, 347-356 (1981)

[18] S. Coleman ; 'The fathe of the false vacuum ' *Phys.Rev*.**D 15**, 2929 (1977)

[19] 'How false vacuum synthesis of a universe sets initial conditions which permit the onset of variations of a nucleation rate per Hubble volume per Hubble time' By A.W.Beckwith, arXIV math-ph/0410060

[20] J. Garriga and V.F. Mukhanov, *Phys. Lett*. B **4 58**, 219 (1999)

[21] A.W. Beckwith, white paper (appropriately) submitted to the Dark Energy Task Force, accepted June 28, 2005 by Rocky Kolb and Dana Lehr

[22] A.W. Beckwith , arXIV math-ph/0412002

[23] V.F. Cardone, A. Troisi, and S. Capozziello, astro-ph/0402228.

[24] Kolb E. W. and Turner M.S. , *The early universe*, Addison-Wesley , Redwood City, CA , 1990 ; Linde A.D. , *Particle Physics and Inflationary Cosmology*, Hardwood, New York, 1990.

[25] Edward (Rocky) Kolb in presentation at SSI 2005, Stanford Linear accelerator cosmology school. Also a datum which was given to me at 2005 CTEQ Summer school of QCD phenomenology, La Puebla, Mexico

[26] Kolb E. W. and Turner M.S. , *The early universe*, Addison-Wesley , Redwood City, CA , 1990 ; Linde A.D. , *Particle Physics and Inflationary Cosmology*, Hardwood, New York, 1990.

[27] L. P. Chimento, arXIV astro-ph/0311613

[28] M. Trodden : arXIV hep-th/9901062 v1 15 Jan 1999 ; M. Trodden, VF. Mukhanov, R.H. Brandenburger hep-th/9305111 v1 22 May 1993, pp 5-6

[29] Y. Gong, arXIV : gr-qc/ 9809015 v2 3 sep 1999, formula 30, p 7

[30] K. Kadota, in talk in parallel session of early universe models given at Pheno 2005, a conference organized by the Phenomenology institute of the physics department of the University of Wisconsin, Madison

[31] On the reliability of inflaton potential reconstruction By *Edmund J. Copeland*, *Ian J. Grivell*, and *Edward W. Kolb* arXIV : astro-ph/9802209 v1 15 Feb 1998

[32] O. Dias, J. Lemos ; arxiv :hep-th/0310068 v1 7 Oct 2003

[33] J. Garriga ; Phys.Rev.D 49, 6343 (1994) ; J. Garriga ; Phys.Rev.D 57, 2230 (1998) ; J. Garriga and V.F. Mukhanov, Phys. Lett. B 4 58, 219 (1999)

[34] S. Dodelson , ' Modern Cosmology' ; Academic press, 2003 ; Burlington, Mass

MAASTRO lab has a vacancy for a Senior scientist, Head of Laboratory Research in molecular oncology (M/F)

Vac.nr. 2007.009/KC

MAASTRO, Maastricht Radiation Oncology, is a co-operation between MAASTRO clinic, the University of Maastricht (UM) and the University Hospital Maastricht (azM) (see www.maastro.nl). MAASTRO consists of several division, including Maastro Clinic, which offers state-of-the-art radiotherapy to more than 3500 cancer patients each year from the Mid and South Limburg area in the Netherlands. MAASTRO clinic is also world-wide reference centre for Siemens Medical. In addition, research and training at Maastro is carried out in Maastro Physics, Maastro Trials, Maastro School, and Maastro Lab.

MAASTRO Lab is a basic and translational research laboratory embedded within the GROW research institute of the Faculty of Health, Medicine and Life Sciences at Maastricht University. Research carried out in the past has been focused on the tumour microenvironment and EGFR signalling pathways, both of relevance to radiation oncology. MAASTRO Lab has made several important discoveries in these fields, including demonstration that EGFR is up regulated by radiation and that hypoxia inhibits the initiation step of mRNA translation. In addition, we have initiated translational and clinical studies based on these results including both phase I novel treatment and molecular imaging trials as well as a Biobank project with more then 1500 patients included.

The lab has 4 permanent scientists, 5 technicians, more then 5 PhD students and is fully equipped for cell culture, molecular biology, flow cytometry, hypoxia, gene expression, proteomics and microscopy. Maastro lab has set up the necessary infrastructure for controlled exposures to hypoxia and hypoxia/reoxygenation, including development of novel equipment that allows rapid and precise changes in oxygenation. Access to expertise, equipment and resources within the much larger GROW research institute and other facilities in the University are also readily available, including the genome centre, advanced microscopy, and the animal facility with its imaging facility (Optical imager, MRI 7Tesla and micro CTPET to come). MAASTRO has a structural collaboration with the VU in Amsterdam on molecular PET biomarkers, with the TU/Eindhoven on Systems Biology and is initiating a new collaboration with the University of Toronto on research related to the Unfolded Protein Response and tumour hypoxia.

MAASTRO lab has a vacancy for a

Senior scientist, Head of Laboratory Research in molecular oncology (M/F)

Vac.nr. 2007.009/KC

In this position you will be responsible for carrying out basic and translational research that is of relevance to radiation oncology in the broadest possible scope. You will initiate an independent research program based on demonstrated skills and expertise in fundamental aspects of biology. In addition, you will be chiefly responsible for the scientific research and training within the lab of experimental Radiation Oncology (MAASTRO lab). As head of research you will manage the laboratory scientific research, direct the research policy, and participate actively in ongoing and newly initiated research lines and projects. Successful grant applications to prestigious (inter)national organizations to support expansion of research activities will constitute an important part of your work.

Depending on experience, the process to appoint you as professor or associate professor at the faculty of Health, Medicine and Life Sciences from Maastricht University will be started. You will participate in research and educational activities within the faculty. The emphasis in this faculty appointment is on *microenvironment of solid tumours and cell signalling (EGFR)* but there is room for your specific area of expertise.

We are looking for a senior scientist with training and experience in basic molecular biology, biochemistry, cell biology or related area. Candidates should have a proven track record or demonstrate a strong potential to function as a principal investigator, with high impact scientific publications and several large operating scientific grants. Candidates should have experience and knowledge of molecular oncology and have a recognized expertise within a specific research area relevant to radiation oncology. Experience in radiation biology, collaboration with clinicians and ability to speak Dutch is a plus but is *not* a prerequisite. Preferably candidates will have experience in research group management. In addition, candidates should be capable of formulating strategic goals for their research program in line with the organisational strategy.

Conditions of Employment and salary are based on the Dutch Collective Labour Agreement for Hospitals (CAO-Ziekenhuizen). You will receive a permanent contract on a fulltime basis (36 hours/week), depending on your relevant experience.

Further information will be gladly given by Prof. Philippe Lambin, head of the Dpt of Radiation Oncology azM (e-mail: philippe.lambin@maastro.nl) or telephone number: +31-(0)88-4455666. Please also visit www.maastro.nl and www.grow-um.nl.

Your application letter, Curriculum Vitae and listing of publications can be sent before to the department of Personell to the attention of mrs. M.T.V. Vaessens, pbox 5800, 6202 AZ Maastricht, the Netherlands.

New York Science Journal

ISSN: 1554-0200

The international academic journal, "New York Science Journal" (ISSN: 1554-0200), is registered in the New York of the United States, and invites you to publish your papers.

Any valuable papers that describe natural phenomena and existence or any reports that convey scientific research and pursuit are welcome, including both natural and social sciences. Papers submitted could be reviews, objective descriptions, research reports, opinions/debates, news, letters, and other types of writings that are nature and science related. There is no charge for the manuscript submissions.

The Journal is published in the both printed version and online version. The abstracts of all the articles in this journal are free accessed publicly online, and the full text will be charged to the readers for US$10/article. The authors will get 30% of the article selling and the other 70% of the article selling will be used to cover the publication cost.

If the authors (or others) need hard copy of the journal, it will be charged for US$60/issue to cover the printing and mailing fee.

Here is a new avenue to publish your outstanding reports and ideas. Please also help spread this to your colleagues and friends and invite them to contribute papers to the journal. Let's work together to disseminate our research results and our opinions.

Papers in all fields are welcome, including articles of natural science and social science.

Please send your manuscript to editor@sciencepub.net; sciencepub@gmail.com

For more information, please visit http://www.sciencepub.org/newyork

New York Science Journal
525 Rockaway PKWY, #B44, Brooklyn, NY 11212, The United States,
Telephone: 347-321-7172
Email: editor@sciencepub.net; sciencepub@gmail.com
Website: http://www.sciencepub.org/newyork

New York Science Journal

ISSN 1545-0200

Volume 1 - Number 1 (Cumulated No. 1), January 1, 2008

Marsland Press

Brooklyn, New York, the United States

ISSN 1554-0200

9 771554 020011